Engineering Knowledge Transfer Units to Increase
Student´s Employability and Regional Development

Module 3: Vehicle Design + Dynamics

PhD, Assoc. prof., Sanjarbek Ruzimov
sanjarbek.ruzimov@polito.it

Co-funded by the
Erasmus+ Programme
of the European Union

Agenda

- Slot 3: Vehicle dynamics simulation
  - Longitudinal dynamics and fuel consumption simulation in Matlab/Simulink
  - Braking dynamics simulation
- Slot 4 and 5: Vertical dynamics
  - Vertical dynamics of the vehicle
  - State of Art of Passive, Semi active and Active damping systems
  - Roll motion
- Slot 6: Control systems
  - Height adjustment system control
  - Regenerative Suspension control
  - Active roll control

Co-funded by the Erasmus+ Programme of the European Union

Vehicle dynamics simulation

- Longitudinal dynamics and fuel consumption simulation in Matlab/Simulink
- Braking dynamics simulation

Co-funded by the Erasmus+ Programme of the European Union

Motor Vehicle Design

- 8 ECST (Lectures + Practice + Projects)
  - Part 1 : Forces and moments at the tire-road contact
  - Part 2: Longitudinal dynamics of the vehicle
  - Part 3: Suspensions
  - Part 4: Lateral dynamics of the vehicle
  - Part 5: Brake system
  - Part 6: Transmission system
- Prerequisites
  - Physics: rigid body equilibrium, vector analysis.
  - Applied mechanics: kinematics, vibration analysis
  - Engineering drawing.

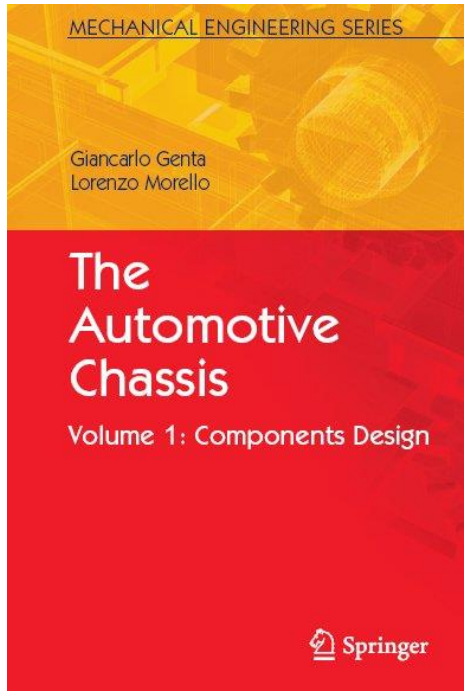

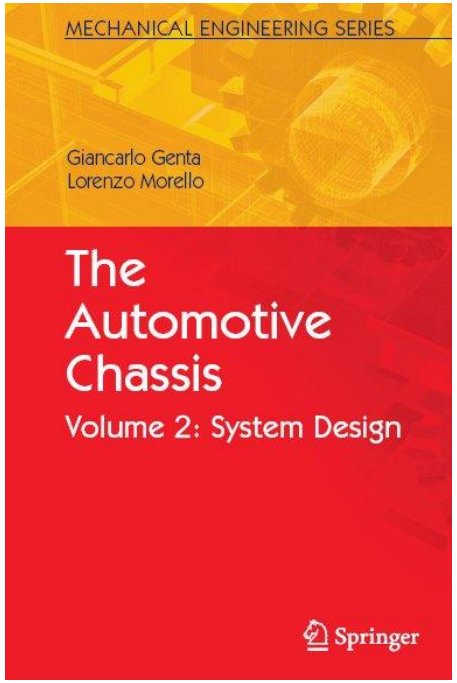

Co-funded by the Erasmus+ Programme of the European Union

Longitudinal dynamics and fuel consumption simulation in Matlab/Simulink

Co-funded by the
Erasmus+ Programme
of the European Union

Modelling approaches

Forward model

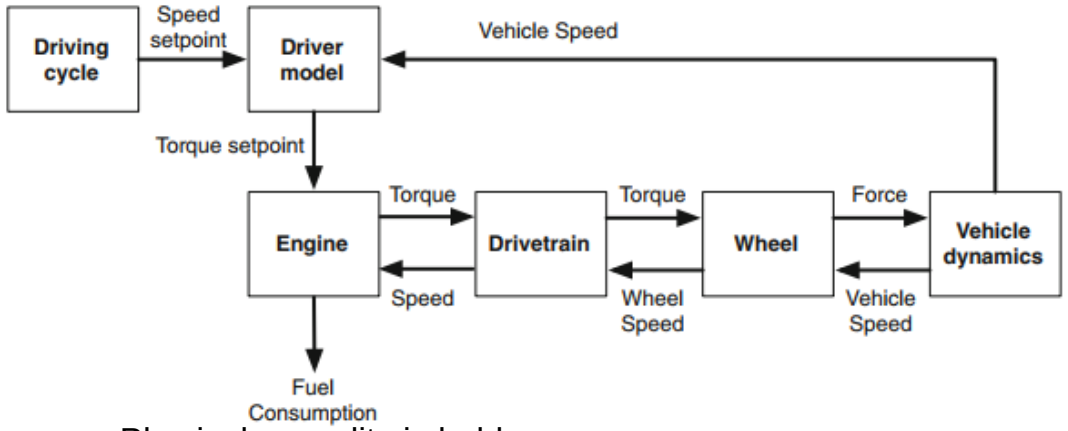

- Physical causality is held;
- Driving cycle speed is compared with the actual vehicle speed;
- Driver model (e.g. PID controller) generates braking and throttle commands;
- Commands are sent to the supervisor block responsible to generate the actuators set points.
- Deviation from speed set point;
- Powertrain limitations are taken into consideration;
- Useful to develop online control strategy;
- Drivability model can be included.

Source: Onori

Backward model

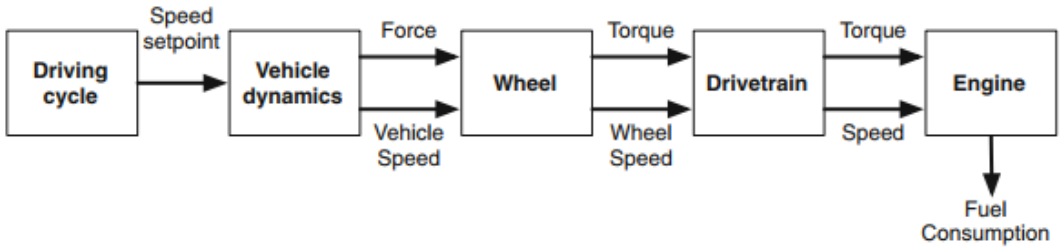

- Desired speed is used to compute accelerations, power at the ground level, forces and torques;
- Driver model is not necessary;
- Torque/speed characteristics of the different powertrain components are considered in order to determine the engine operating conditions and its fuel consumptions;
- Powertrain limitations are not considered;
- Actual speed is exactly the same as speed set point;
- Preliminary analysis of different EMS.

Co-funded by the Erasmus+ Programme of the European Union

Homologation Drive Cycle

Worldwide harmonized Light vehicles Test Procedure (WLTP)

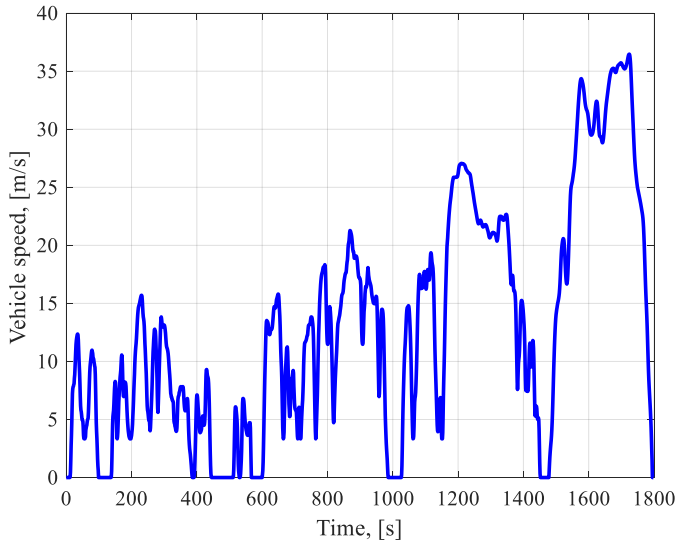

New European Driving Cycle

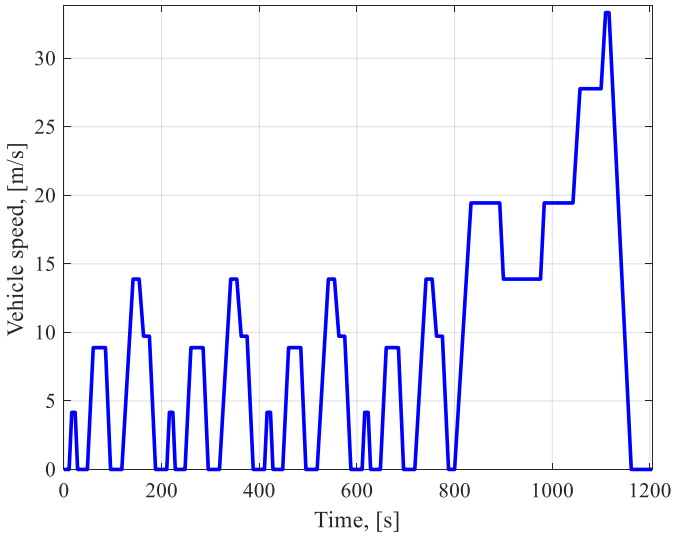

Co-funded by the
Erasmus+ Programme
of the European Union

Vehicle longitudinal dynamics model

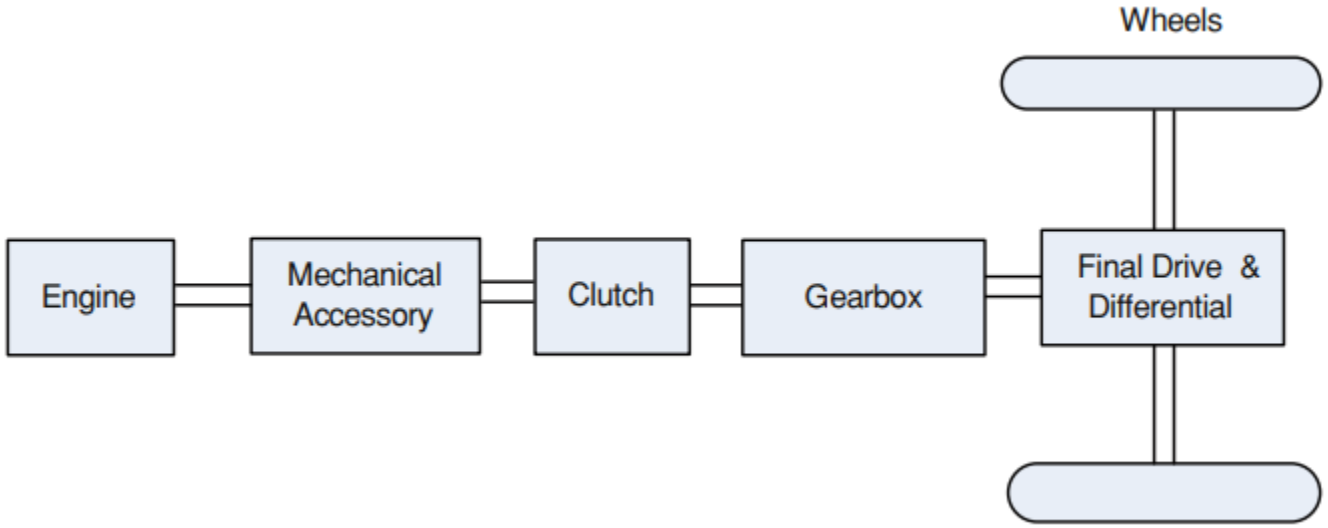

Co-funded by the Erasmus+ Programme of the European Union

Simulink model of the vehicle (Backward)

The QSS-toolbox 2.0.1 (Mozilla Public License, v. 2.0.)

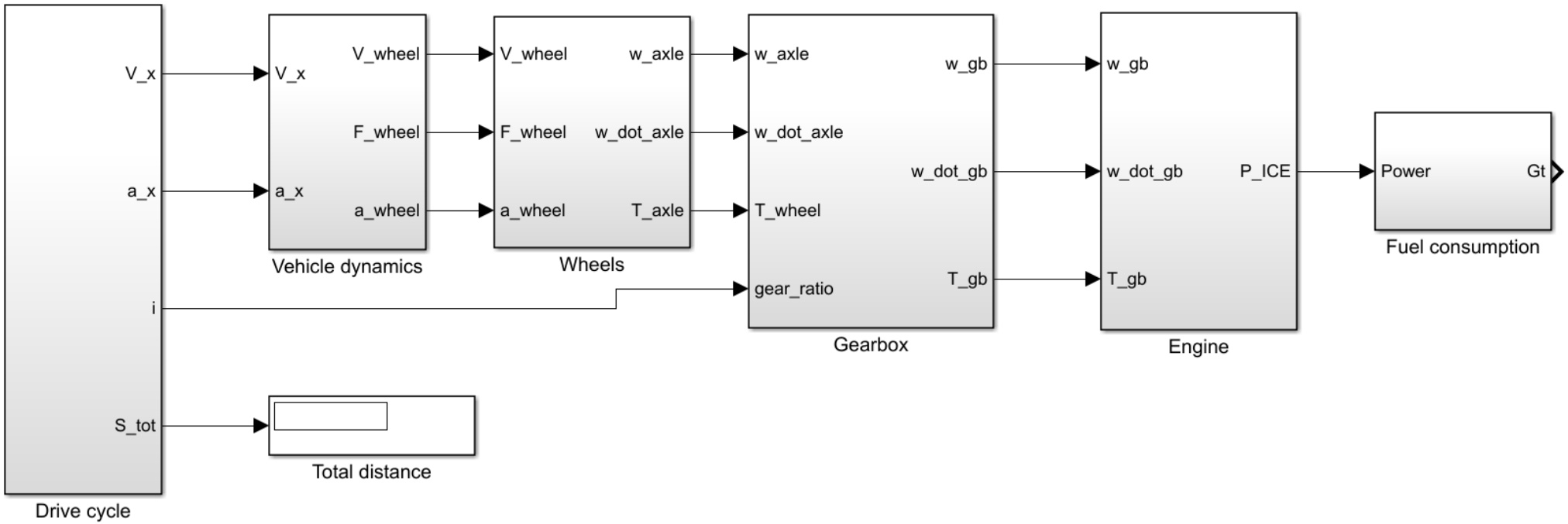

Source: https://ethz.ch/content/dam/ethz/special-interest/mavt/dynamic-systems-n-control/idsc-dam/Research_Onder/Downloads/qss.zip

Source: Guzella

Co-funded by the Erasmus+ Programme of the European Union

Drive cycle

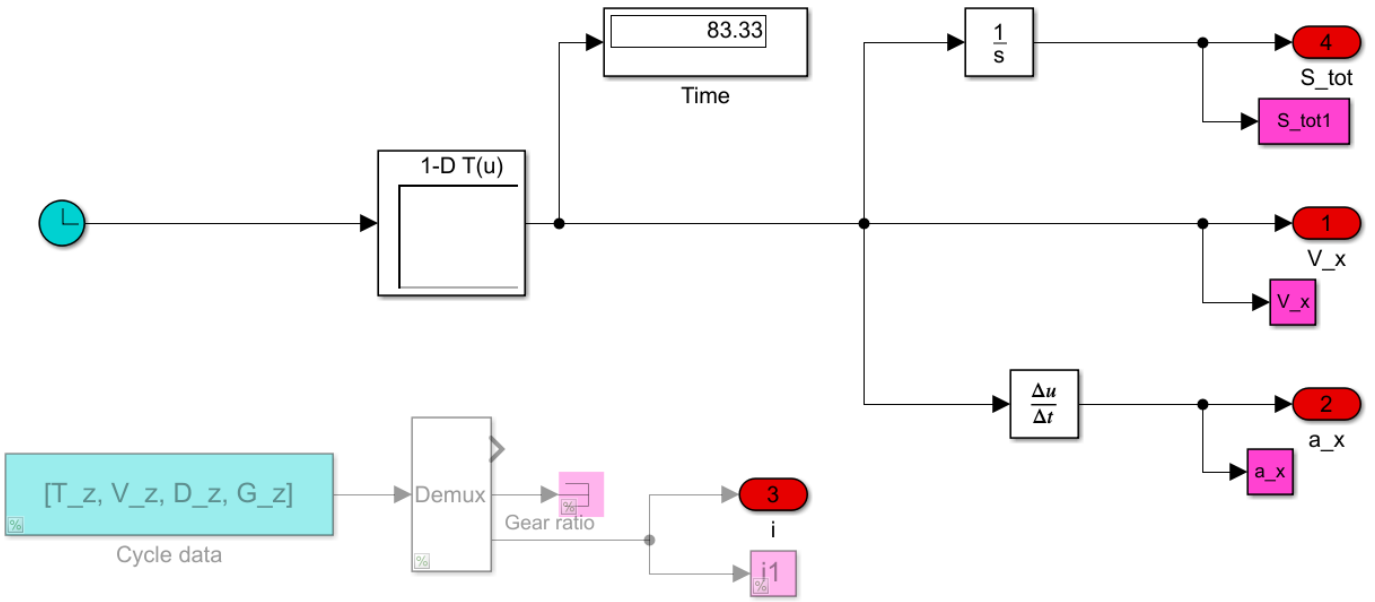

$$a_x(t) = dV_x/dt \qquad S_x(t) = \int V_x dt$$

Co-funded by the
Erasmus+ Programme
of the European Union

Vehicle longitudinal dynamics

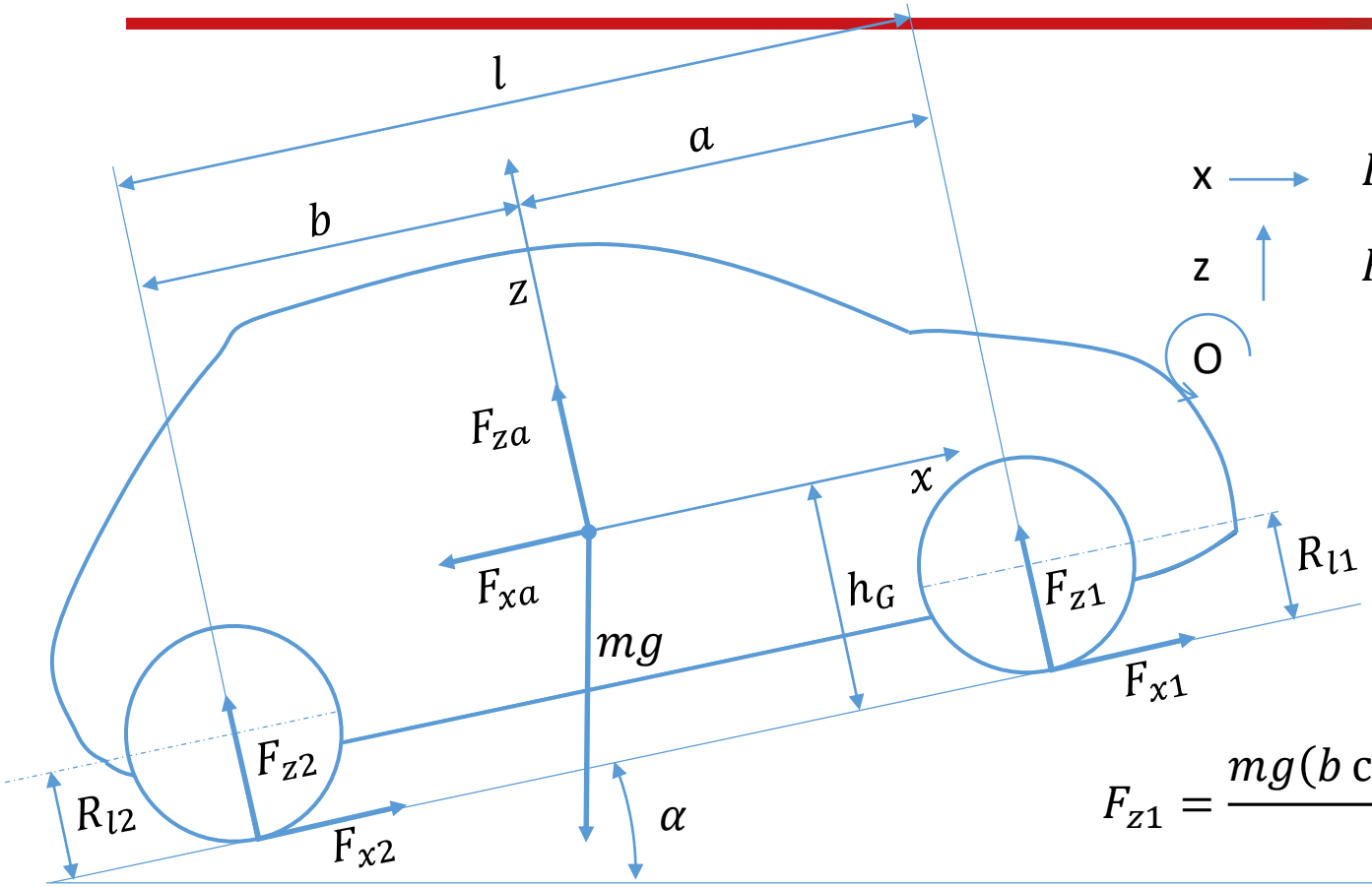

x → $F_{x1} + F_{x2} - F_{xa} - mg\sin\alpha = m\dot{V}$

z ↑ $F_{z1} + F_{z2} + F_{za} - mg\cos\alpha = 0$

$F_{z1}a - F_{z2}b + mg\sin\alpha\, h_G + F_{xa}h_G - M_{ya} = -mh_G\dot{V}$

$$F_{z1} = \frac{mg(b\cos\alpha - h_G\sin\alpha) - bF_{za} - h_GF_{xa} + M_{ya} - mh_G\dot{V}}{l}$$

$$F_{z2} = \frac{mg(a\cos\alpha + h_G\sin\alpha) - aF_{za} + h_GF_{xa} - M_{ya} + mh_G\dot{V}}{l}$$

Co-funded by the Erasmus+ Programme of the European Union

Vehicle dynamics block

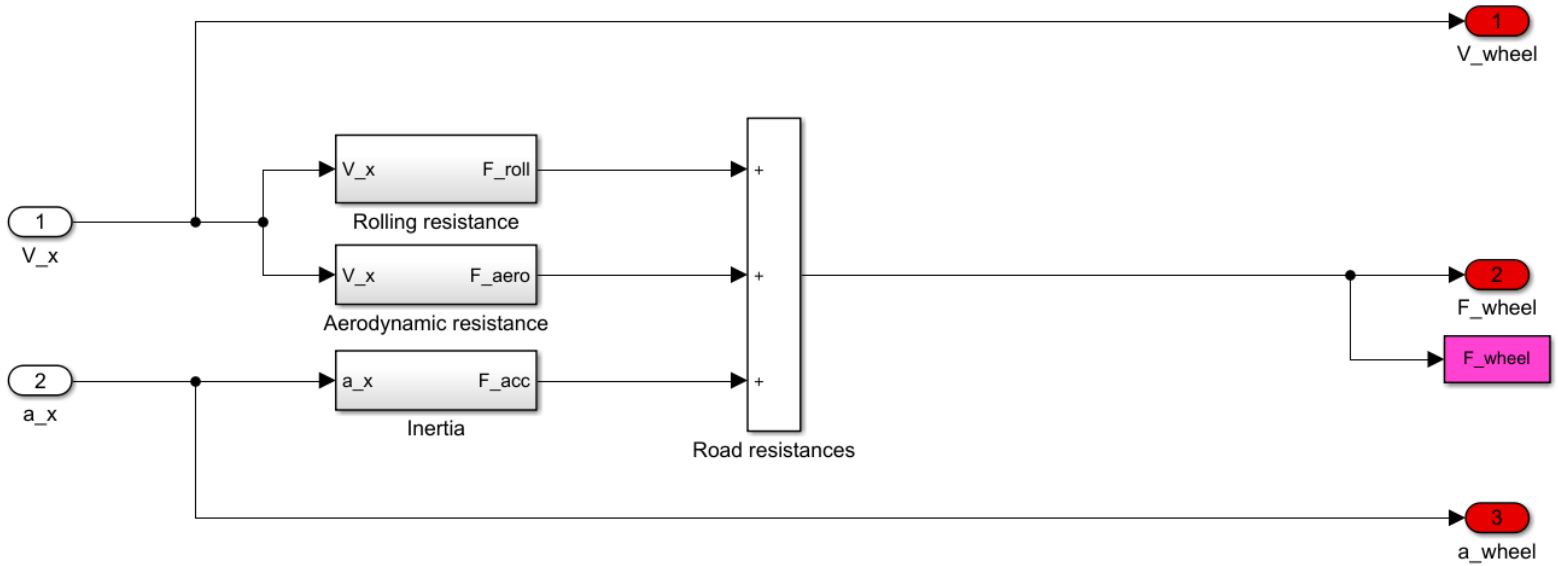

$$F_{\text{roll}} = M \cdot g \cdot f_{\text{r}}$$

$$F_{\text{acc}} = M \cdot a_{\text{x}}$$

$$F_{\text{aero}} = 0.5 \cdot \rho \cdot C_{\text{x}} \cdot A_{\text{f}} \cdot V_{\text{x}}^2$$

$$F_{\text{res}} = F_{\text{roll}} + F_{\text{aero}} + F_{\text{acc}}$$

Co
Erasmus+ Programme
of the European Union

Wheel (Tire) block

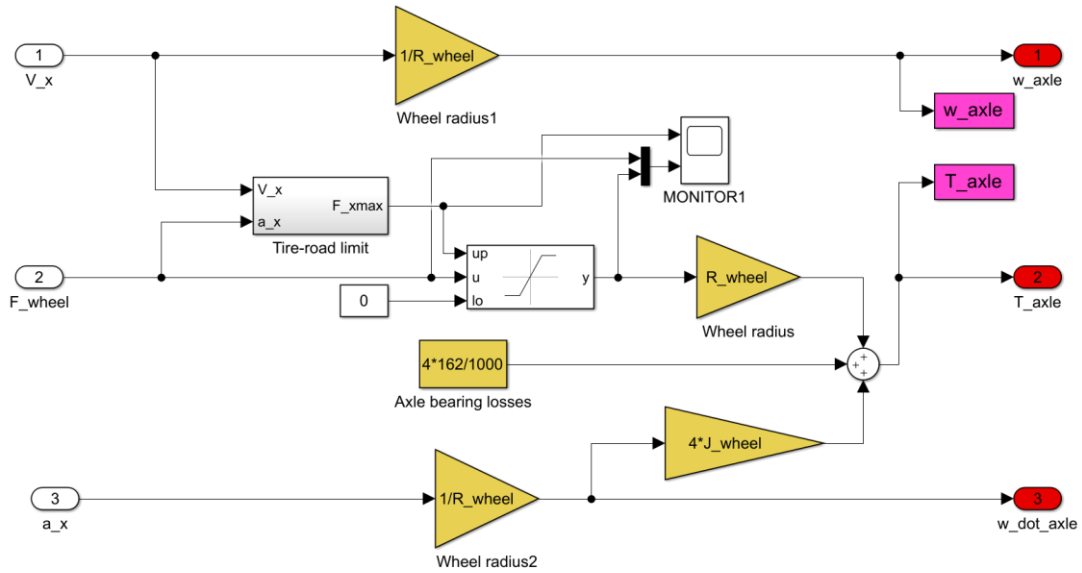

$$\omega_{\text{wheel}} = \frac{V_x}{R_{\text{wheel}}}$$

$$\dot{\omega}_{\text{wheel}} = \frac{a_x}{R_{\text{wheel}}}$$

$$T_{\text{wheel}} = F_{\text{wheel}} \cdot R_{\text{wheel}}$$

Wheel inertia

$$T_{\text{axle}} = 4 \cdot J_{\text{wheel}} \cdot \dot{\omega}_{\text{wheel}} + T_{\text{wheel}}$$

Road –tire Limitations:

$$F_{z.\text{front}} = (M \cdot g \cdot b - M \cdot a_x \cdot h_G - 0.5 \cdot \rho \cdot A_f \cdot V_x^2 \cdot (h_G \cdot C_x - L \cdot C_{My} + b \cdot C_z))/L$$

$$F_x = F_z \cdot \mu_x$$

$$F_{z.\text{rear}} = (M \cdot g \cdot a + M \cdot a_x \cdot h_G - 0.5 \cdot \rho \cdot A_f \cdot V_x^2 \cdot (-h_G \cdot C_x + L \cdot C_{My} + a \cdot C_z))/L$$

Co-funded by the Erasmus+ Programme of the European Union

Gearbox (transmission) block

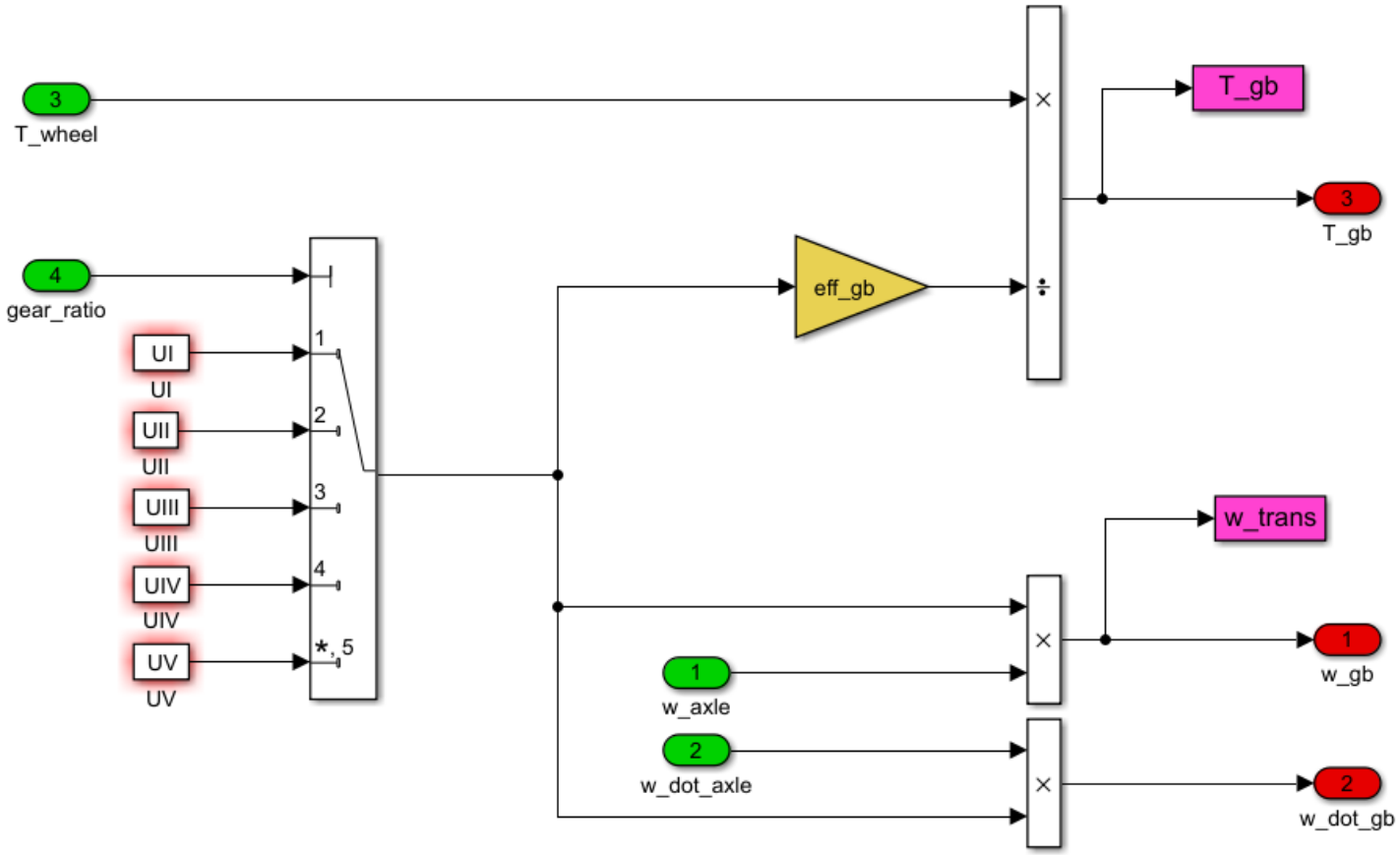

$$T_{\mathrm{gb}} = \frac{T_{\mathrm{axle}}}{i_{\mathrm{gb}} \cdot \eta_{\mathrm{gb}}}$$

$$\omega_{\mathrm{gb}} = \omega_{\mathrm{axle}} \cdot i_{\mathrm{gb}}$$

$$\dot{\omega}_{\mathrm{gb}} = \dot{\omega}_{\mathrm{axle}} \cdot i_{\mathrm{gb}}$$

Co-funded by the Erasmus+ Programme of the European Union

Engine characteristics: Efficiency contour lines

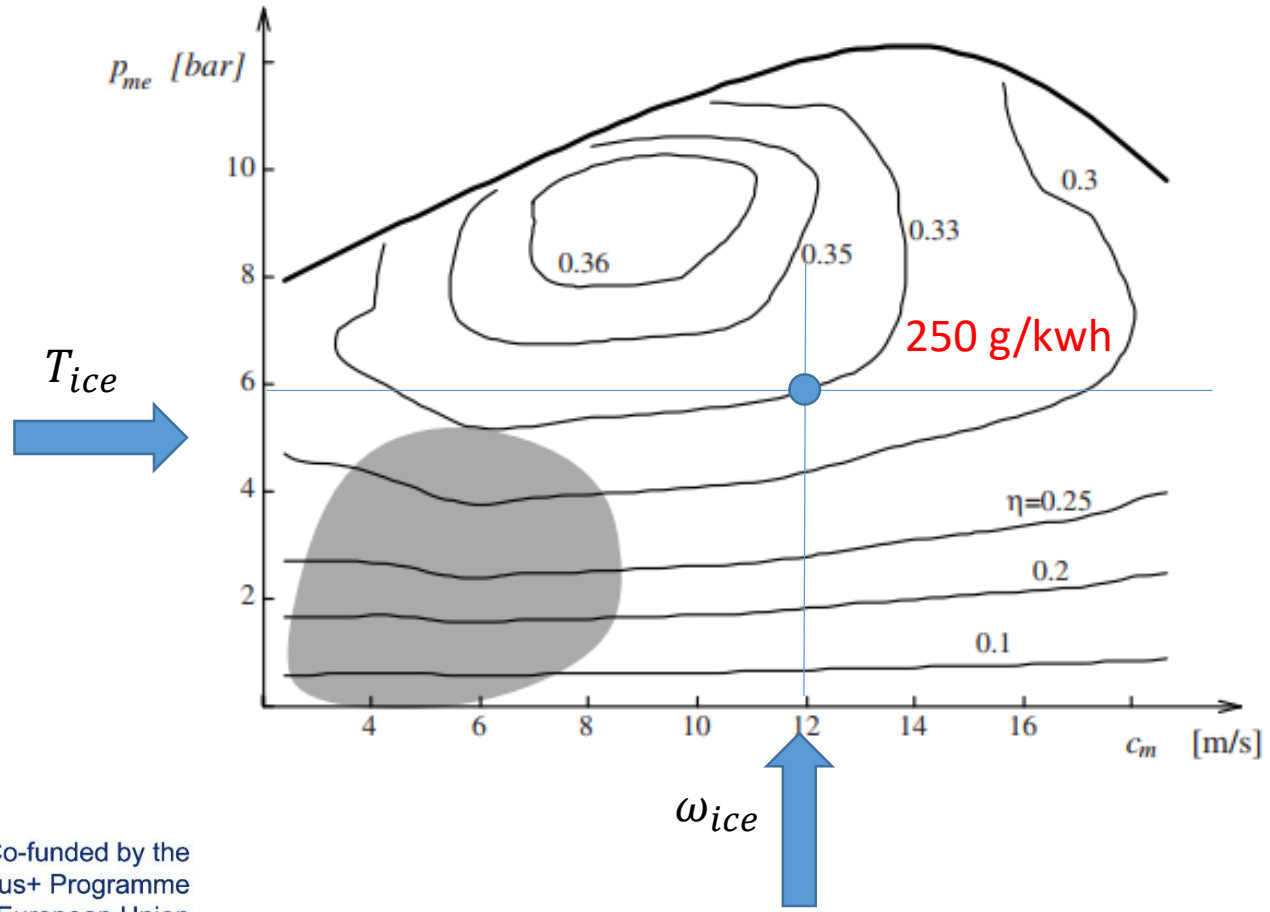

$$p_{me} = \frac{T_{ice}\, 4\pi}{V_d}$$ ICE mean effective pressure

$$p_{fuel} = \frac{m_f\, H_u}{V_d}$$ Fuel mean effective pressure

$$\eta_{ice} = \frac{p_{me}}{p_{fuel}}$$

H – lower heating value of the fuel, [J/kg]

$$m_f = \frac{4\,\pi\, T_{ice}}{H_u\, \eta_{ice}}$$

fuel consumption per engine cycle

$$q = P_{ice}\, g_{ice}\ , \text{[g/s]}$$

$$Q = \int q\, dt\ , \text{[g]}$$

$$g_{ice} = f(T_{ice}, \omega_{ice}), \text{[g/kwh]}$$

Co-funded by the Erasmus+ Programme of the European Union

Braking dynamics simulation

Co-funded by the
Erasmus+ Programme
of the European Union

Braking – ideal case

$$\frac{dV}{dt} = \frac{F_{x1} + F_{x2} - F_{xa} - mg\sin\alpha}{m}$$

$$\mu_{x1} = \mu_{x2} = \mu_{xmax}$$

$$\frac{dV}{dt} = \frac{\mu_x\left(mg - \frac{1}{2}\rho C_z S V^2\right) - \frac{1}{2}\rho C_x S V^2}{m} - g\sin\alpha$$

If $V \cong 0$ and $\alpha = 0$ $\quad \boxed{\dot{V} = -|\mu_x|g}$ (Already found in study of longitudinal dynamics)

$$t_{V1\to V2} = \frac{V_1 - V_2}{|\mu_x|g} \qquad s_{V1\to V2} = \frac{V_1^2 - V_2^2}{2|\mu_x|g}$$

$$t_{stop} = \frac{V_1}{|\mu_x|g} \qquad s_{stop} = \frac{V_1^2}{2|\mu_x|g}$$

Time and distance to reduce the speed from V_1 to V_2 or to stop the vehicle from V_1. ($V_1 > V_2$)

Co-funded by the Erasmus+ Programme of the European Union

Source: Genta

Ideal braking - tire longitudinal forces

If $V \cong 0$ and $\boxed{\dot{V} = \mu_x \mathrm{g}}$

$$F_{z1} = \frac{mg(b\cos\alpha - h_G \sin\alpha) - mh_G\dot{V}}{l}$$

$$F_{z2} = \frac{mg(a\cos\alpha + h_G \sin\alpha) + mh_G\dot{V}}{l}$$

$$F_{z1} = \frac{mg}{l}[(b\cos\alpha - h_G \sin\alpha) - h_G\mu_x]$$

$$F_{z2} = \frac{mg}{l}[(a\cos\alpha + h_G \sin\alpha) + h_G\mu_x]$$

Small compared to other terms

$$F_{x1} = \mu_x F_{z1} = \mu_x \frac{mg}{l}[b\cos\alpha - h_G\mu_x]$$

$$F_{x2} = \mu_x F_{z2} = \mu_x \frac{mg}{l}[a\cos\alpha + h_G\mu_x]$$

Co-funded by the Erasmus+ Programme of the European Union

Ideal braking – tire forces

$$F_{x1} = \mu_x F_{z1} = \mu_x \frac{mg}{l}[b\cos\alpha - h_G\mu_x]$$

$$F_{x2} = \mu_x F_{z2} = \mu_x \frac{mg}{l}[a\cos\alpha + h_G\mu_x]$$

$$(F_{x1} + F_{x2})^2 + mg\cos^2\alpha\left(F_{x1}\frac{a}{h_G} - F_{x2}\frac{b}{h_G}\right) = 0$$

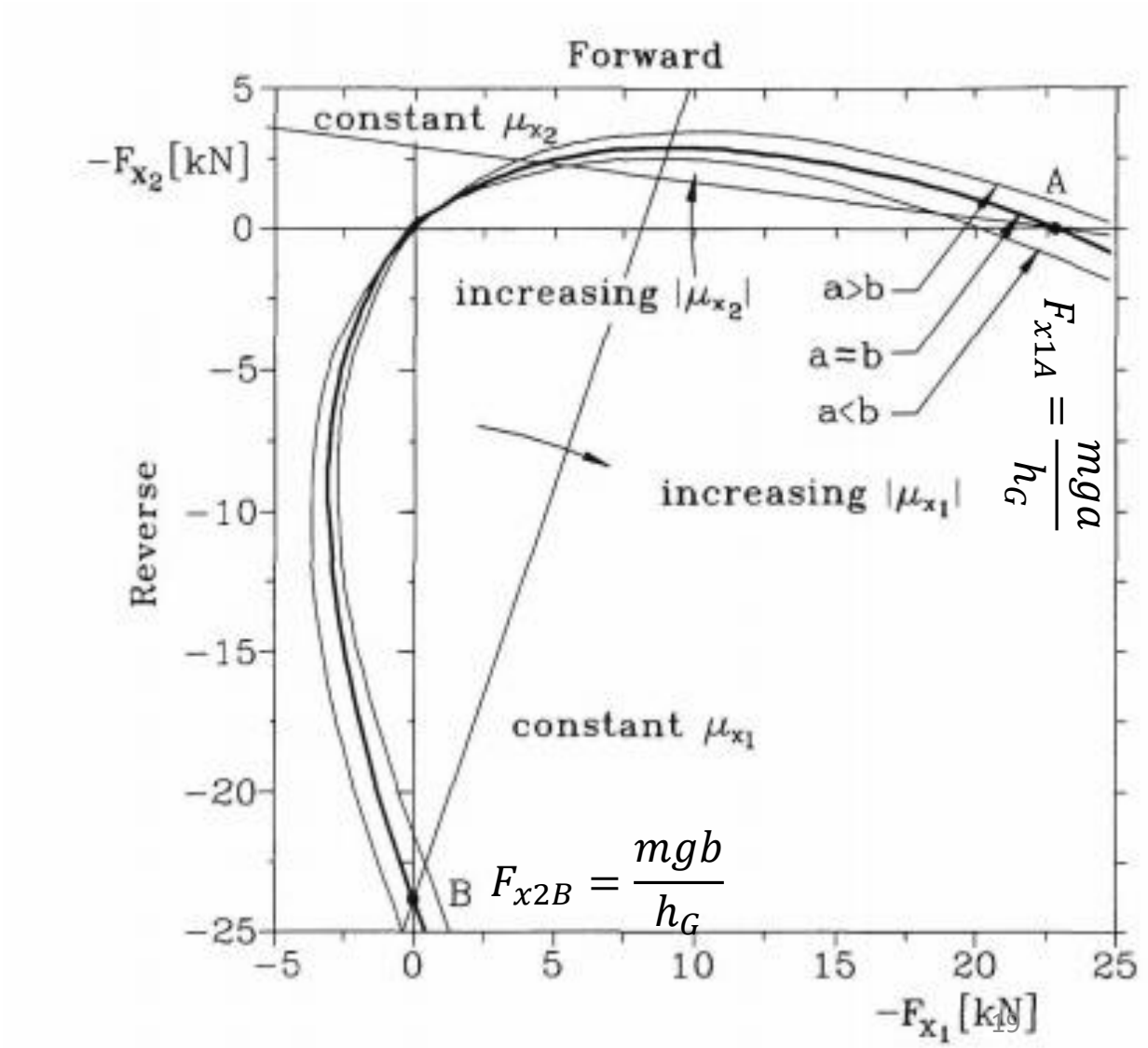

Ideal braking

$$\alpha = 0 \qquad \frac{dV}{dt} = \frac{F_{x1} + F_{x2}}{m} \qquad \frac{dV}{dt} = \frac{F_{x1} + F_{x2} - F_{xa} - mg\sin\alpha}{m}$$

$$F_{x1} = \mu_{x1}\frac{mg(b\cos\alpha - h_G\sin\alpha) - h_G(F_{x1} + F_{x2})}{l}$$

$$F_{x1} = \mu_{x1}\frac{mgb - h_G(F_{x1} + F_{x2})}{l}$$

$$F_{x1} = \mu_{x1}\frac{mgb - h_G F_{x2}}{\left(1 + \mu_{x1}\frac{h_G}{l}\right)l}$$

$F_{x1} = 0$ if $F_{x2} = \frac{mgb}{h_G}$ **Capsize limit during braking in reverse**

$$F_{x2} = \mu_{x2}\frac{mg(a\cos\alpha + h_G\sin\alpha) + h_G(F_{x1} + F_{x2})}{l}$$

$$F_{x2} = \mu_{x2}\frac{mga - h_G(F_{x1} + F_{x2})}{l}$$

$$F_{x2} = \mu_{x2}\frac{mga - h_G F_{x1}}{\left(1 + \mu_{x2}\frac{h_G}{l}\right)l}$$

$F_{x2} = 0$ if $F_{x1} = \frac{mga}{h_G}$ **Capsize limit during braking in forward**

Co-funded by the Erasmus+ Programme of the European Union

Ideal braking – capsize limits

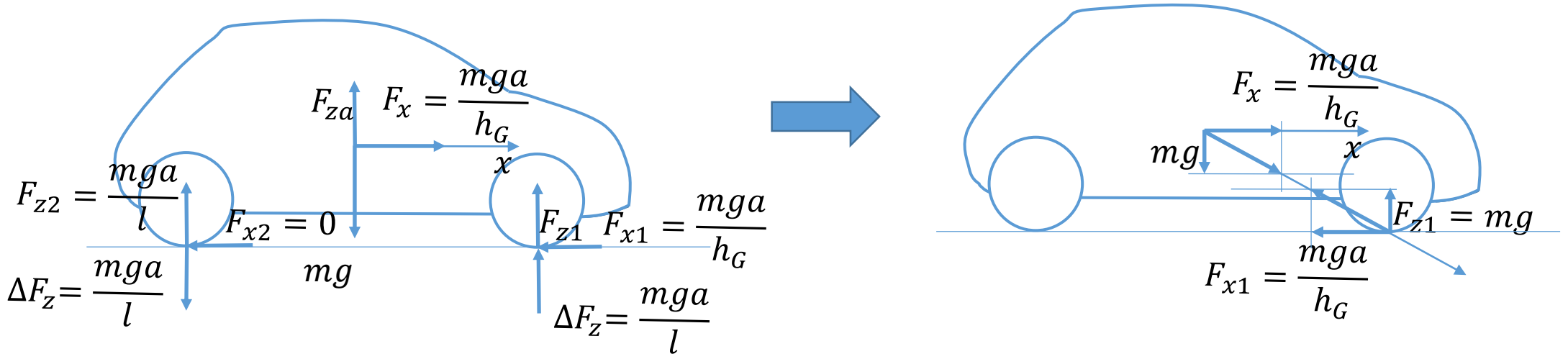

$F_{x1} = 0$ if $F_{x2} = \frac{mgb}{h_G}$ Capsize limit during braking in reverse

$F_{x2} = 0$ if $F_{x1} = \frac{mga}{h_G}$ Capsize limit during braking in forward

Co-funded by the Erasmus+ Programme of the European Union

Ideal braking

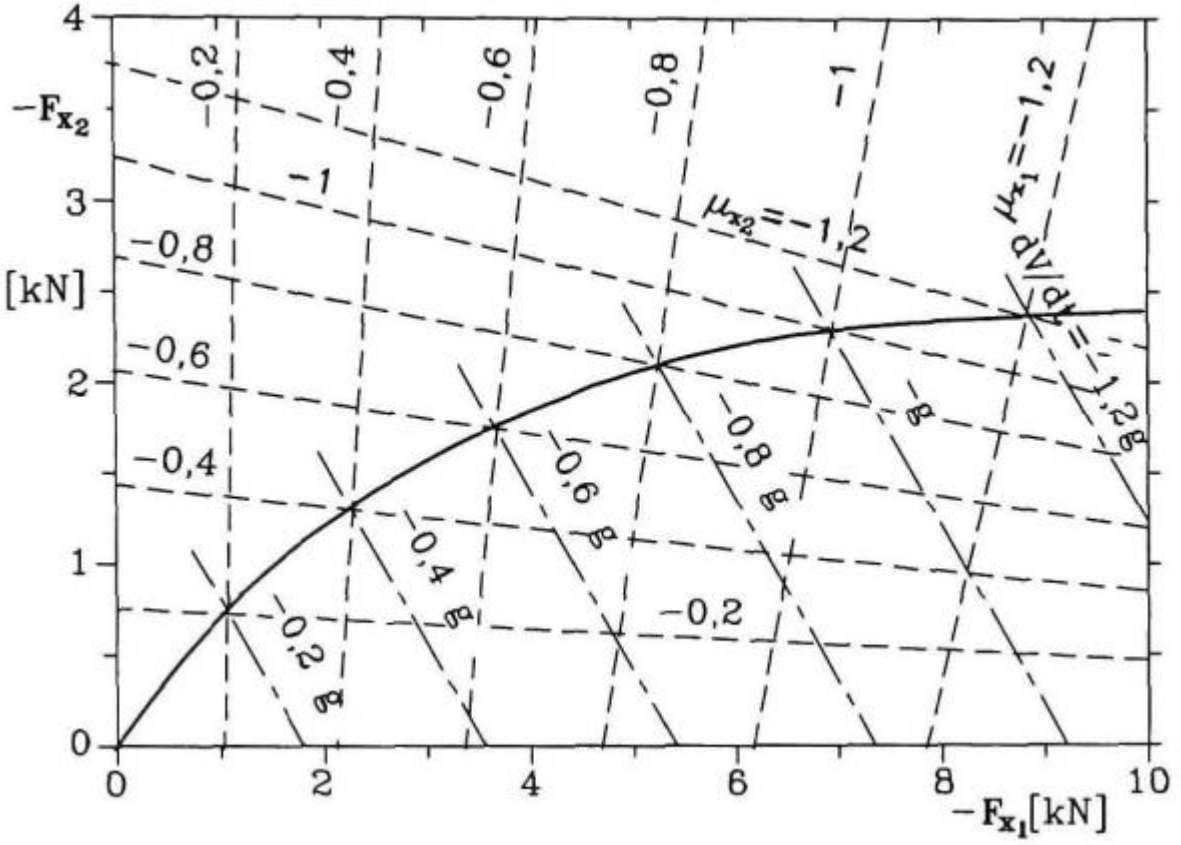

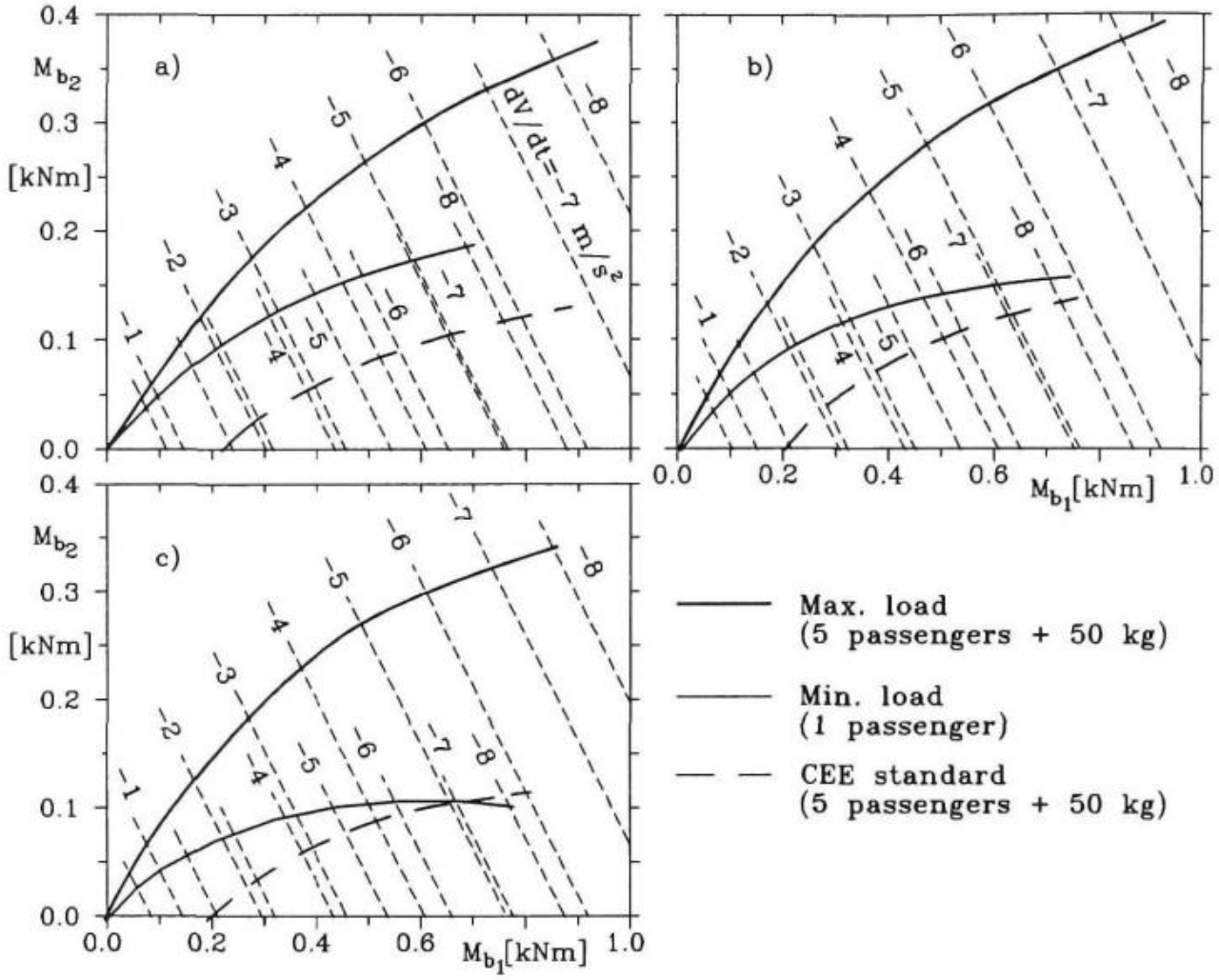

Fig. 4.29 Plots $M_{b_2}(M_{b_1})$ for ideal braking. (a) typical plot for a rear drive car with low ratio h_G/l; (b) typical plot for a front drive saloon car with higher ratio h_G/l; (c) plot for a small front drive car, sensitive to the load conditions and with high value of ratio h_G/l.

Source: Genta

Co-funded by the Erasmus+ Programme of the European Union

Real vs. ideal braking

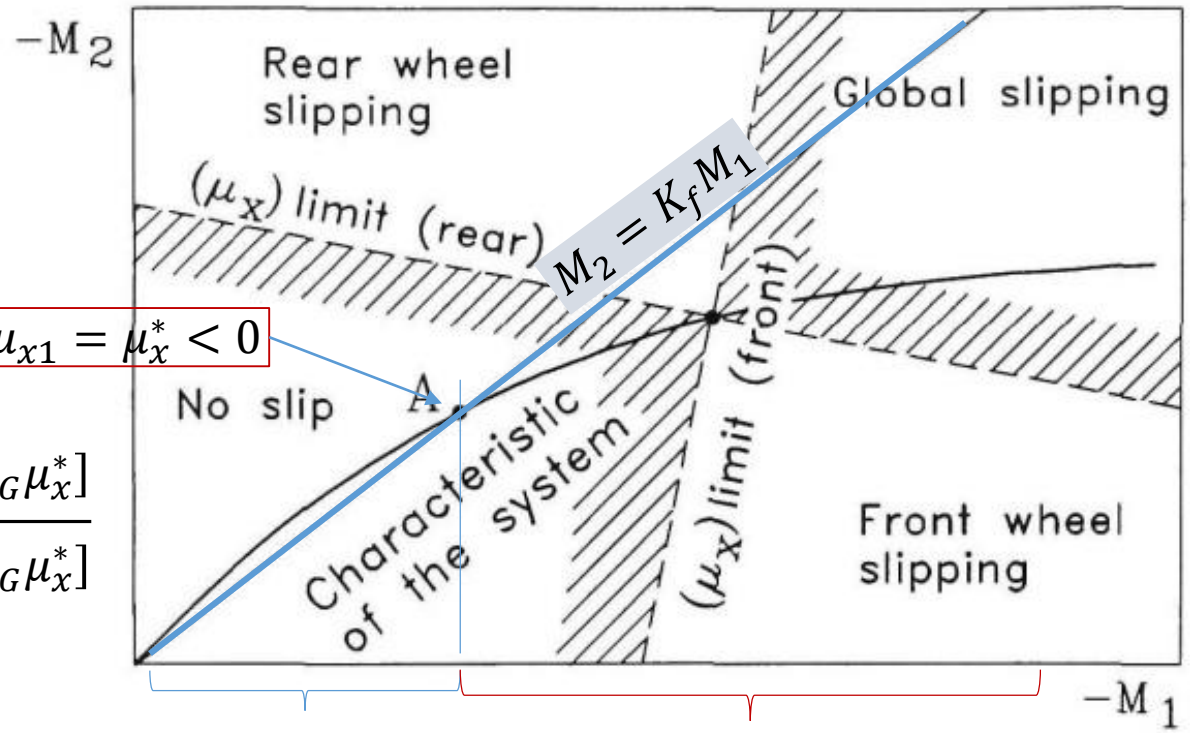

$$\eta_f = \frac{\dot{V}_{actual}}{\dot{V}_{ideal}} = \frac{\dot{V}_{actual}}{\mu_x g}$$

$$K_f \cong \frac{F_{x1}}{F_{x2}} = \frac{\mu_x^* \frac{mg}{l}[b + h_G \mu_x^*]}{\mu_x^* \frac{mg}{l}[a - h_G \mu_x^*]}$$

$$K_f \cong \frac{[b + h_G \mu_x^*]}{[a - h_G \mu_x^*]}$$

$\mu_{x2} < \mu_{x1}$

Front wheels lock earlier (safer)

$\mu_{x2} > \mu_{x1}$

Rear wheels lock earlier (unsafe)

Co-funded by the Erasmus+ Programme of the European Union

Rear braking controlled by valve

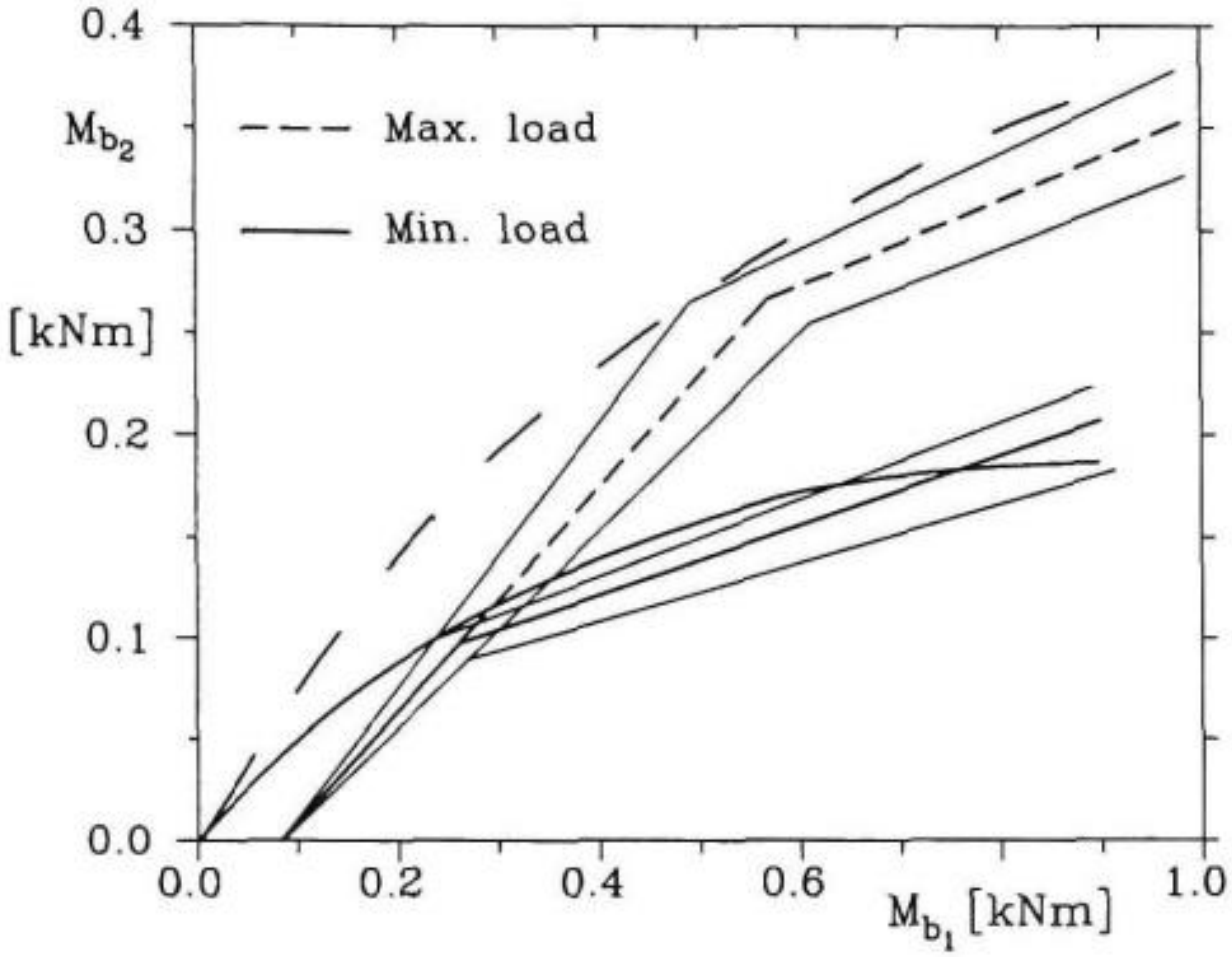

Co-funded by the
Erasmus+ Programme
of the European Union

Brake circuit

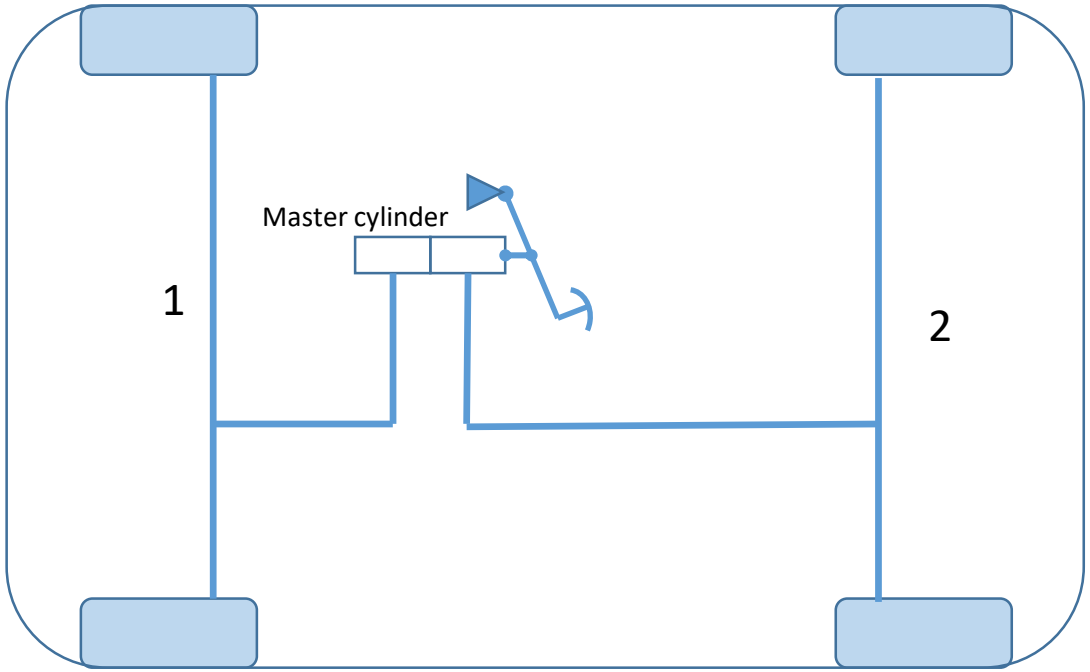

Front/rear split

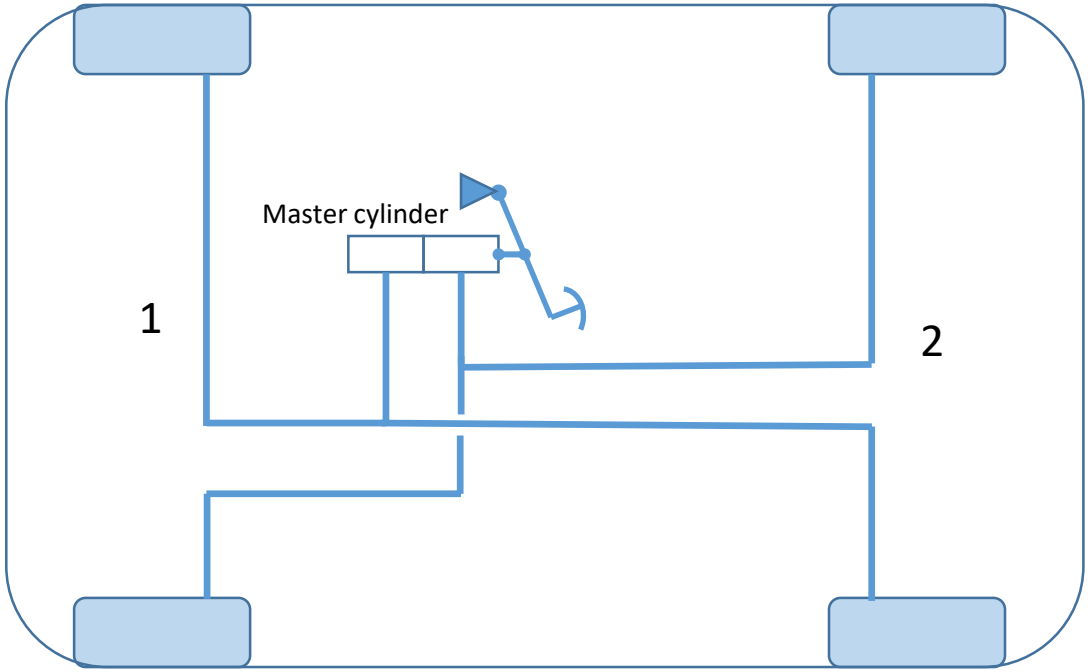

Diagonal split

Co-funded by the
Erasmus+ Programme
of the European Union

Brake circuit

Front/rear split

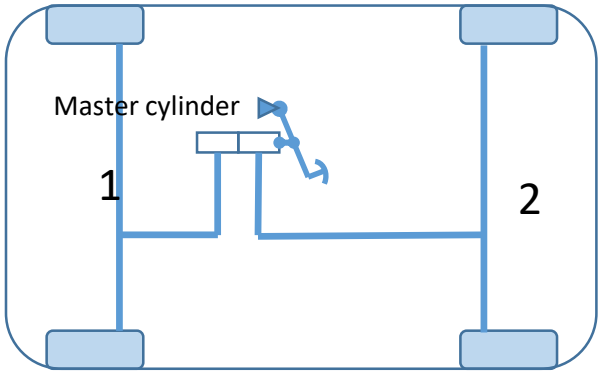

Pros
- Simple front/rear brake torque split
- Simpler hydraulic connections

Cons
- Potential loss of vehicle stability if front circuit has a failure

Diagonal split

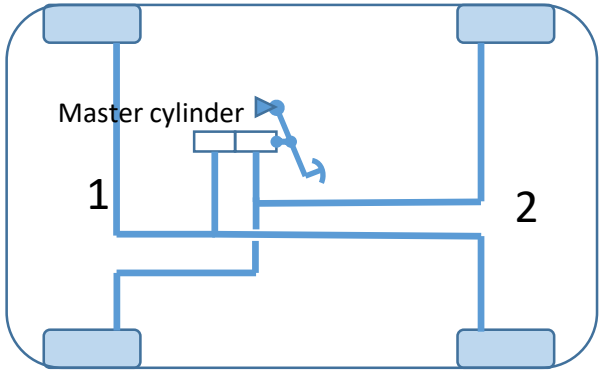

Pros
- Better stability in case of failure of one circuit

Cons
- More complicated hydraulic circuit
- Brake torque split managed by brake design.

Co-funded by the Erasmus+ Programme of the European Union

Master cylinder

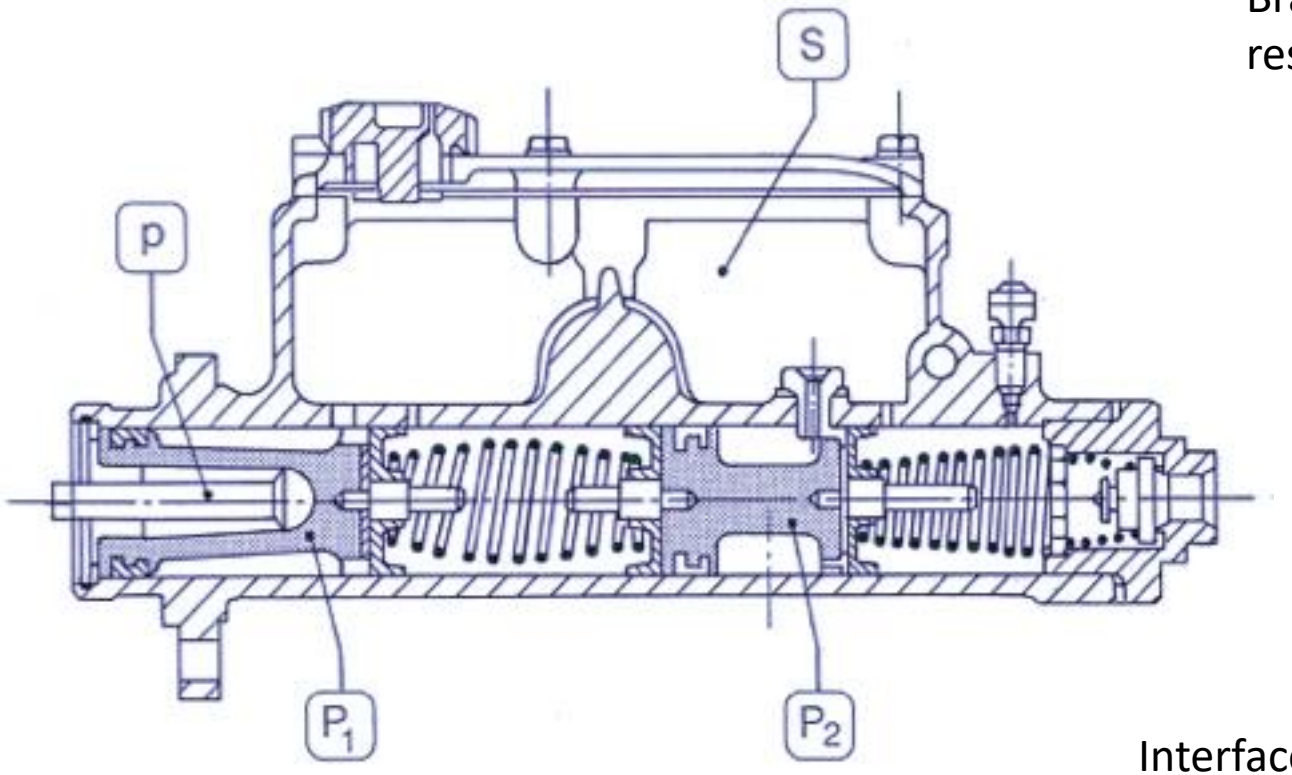

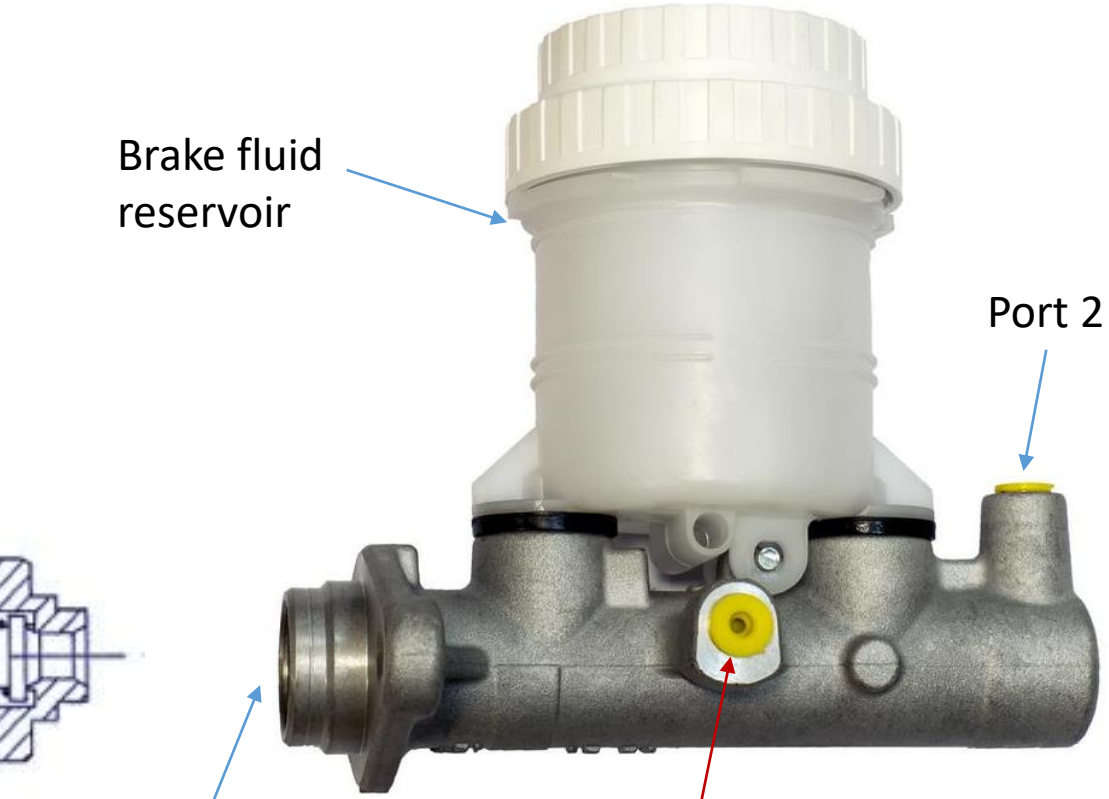

Co-funded by the Erasmus+ Programme of the European Union

Power brake - schematic

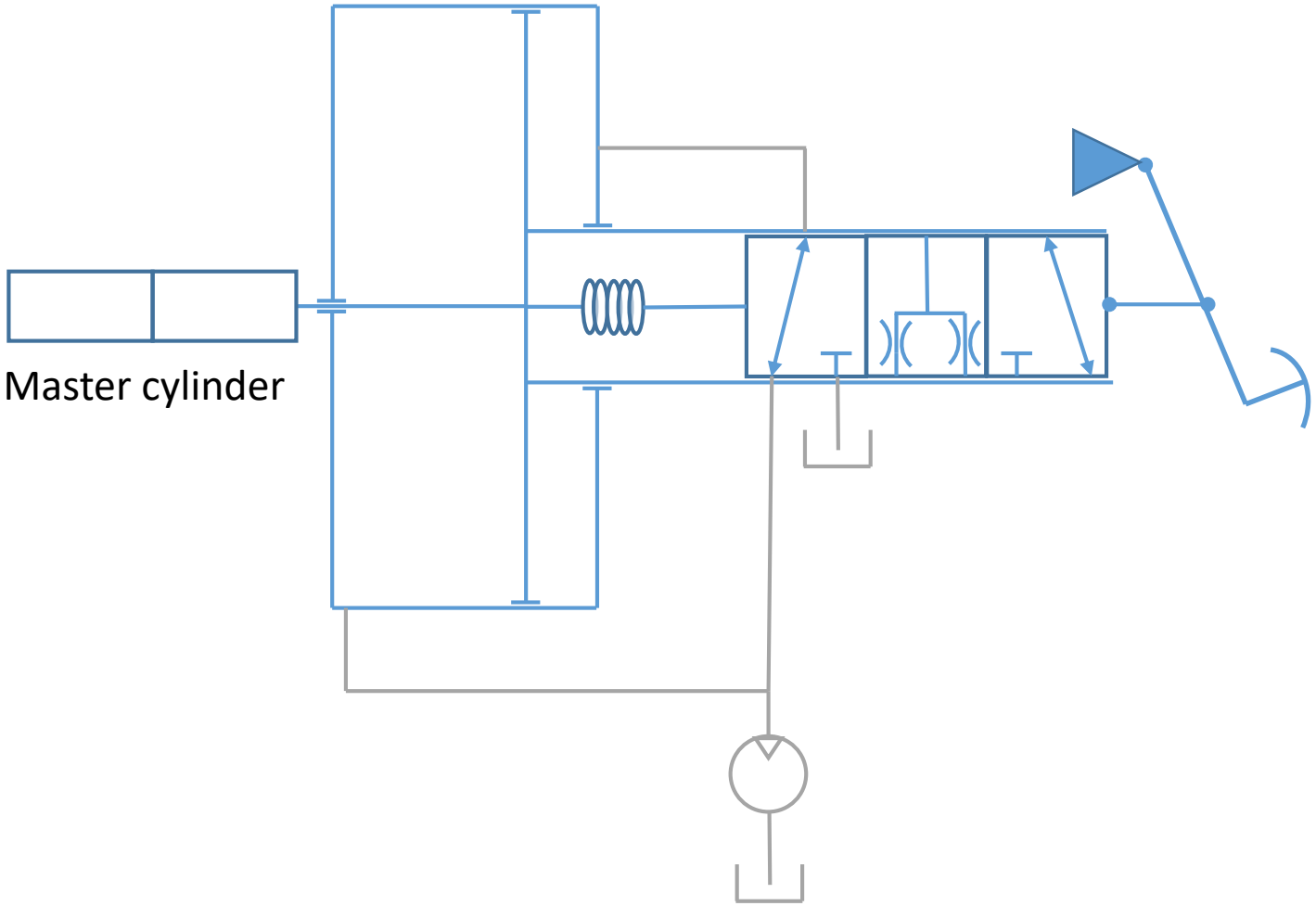

Co-funded by the
Erasmus+ Programme
of the European Union

Anti-locking braking system (ABS)

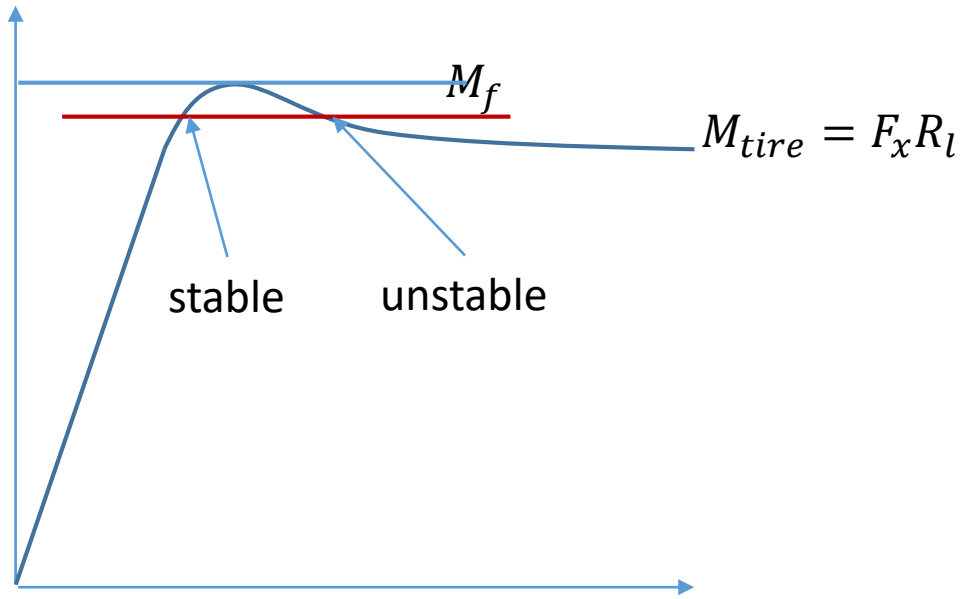

$\mu_{xmax} = 1.2$
$\sigma = 0.2$
$R_0 \cong R_l = 0.3\ m$
$F_z = 4\ kN$
$I_{wheel} = 1\ kg\ m^2$

Stable region: max wheel angular acceleration is according to vehicle

$$\dot{V} = \mu_{xmax} g$$

$$\dot{V} = R\dot{\omega}$$

$$\dot{V} = \frac{R_0 \dot{\omega}}{1+\sigma}$$

$$\dot{\omega} = \frac{\mu_{xmax} g (1+\sigma)}{R_0}$$

$$\dot{\omega} = 47 \frac{rad}{s^2}$$

Unstable region: wheel angular acceleration comes from dynamic equilibrium

$$I_{wheel}\dot{\omega} = M_f - M_{tire}$$

If, for example

$$M_f = \mu_{xmax} F_z R_l$$
$$M_{tire} = 0.8\ \mu_{xmax} F_z R_l$$

$$\dot{\omega} = \frac{0.2\ \mu_{xmax} F_z R_l}{I_{wheel}}$$

$$\dot{\omega} = 288 \frac{rad}{s^2}$$

Co-funded by the Erasmus+ Programme of the European Union

ABS

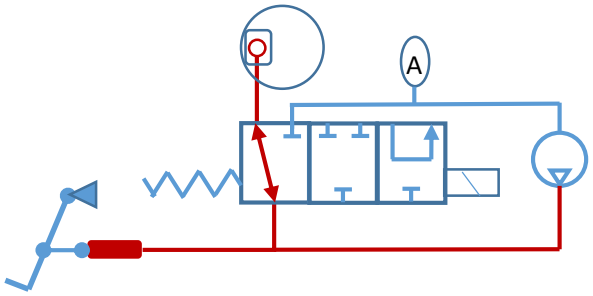

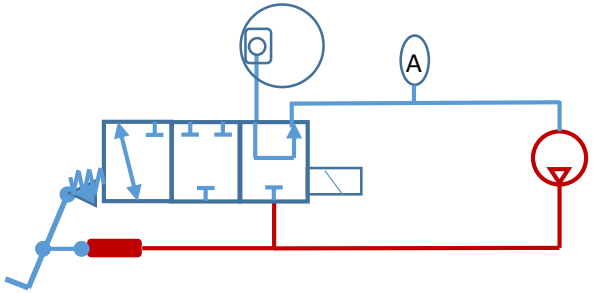

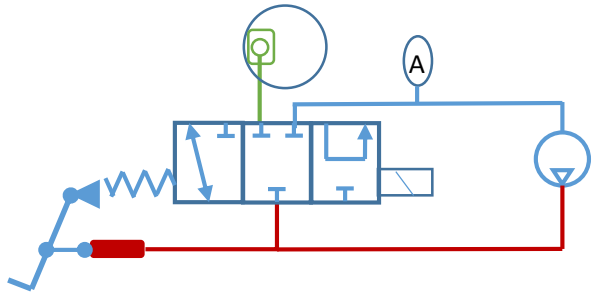

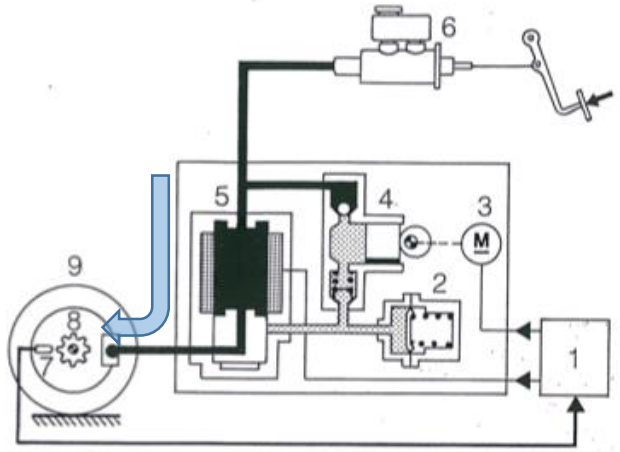

Off

Master cylinder pressure propagates to the brakes.

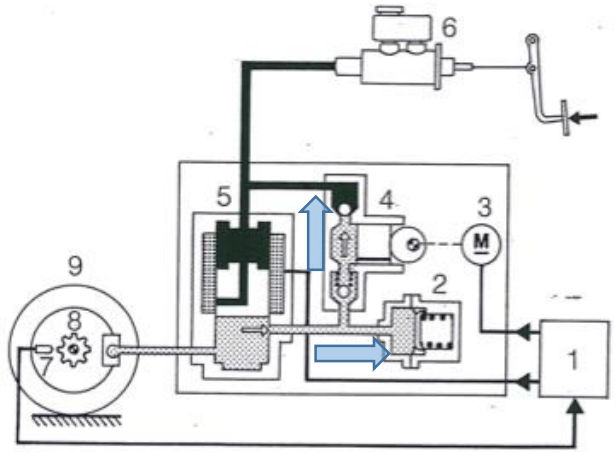

Reduce

Master cylinder is isolated from brakes.
Brake is connected to the accumulator (2).
Brake fluid is pumped (4) to the high pressure side to restore lost volume.

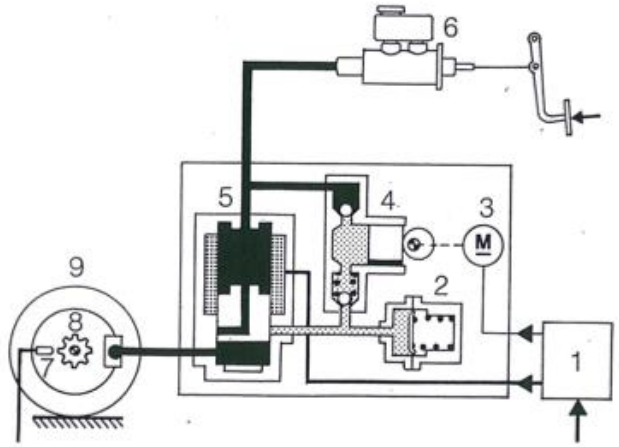

Hold

Master cylinder is isolated from brakes.
Accumulator is isolated (2).
Pump is off (4)

Source: Bosch

CarSim brake Simulation

CarSim window to choose the generation of the force during the brake maneuver

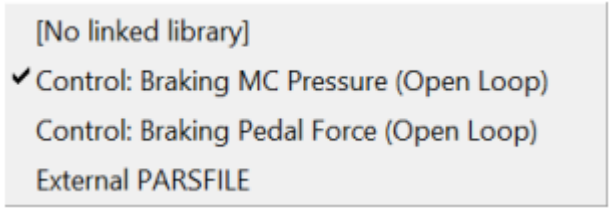

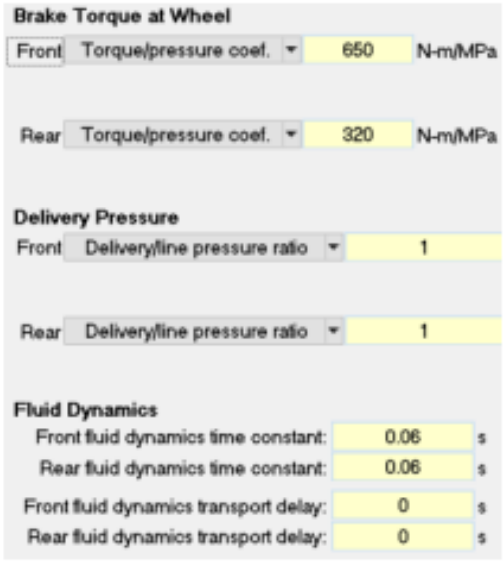

Constant brake torque application

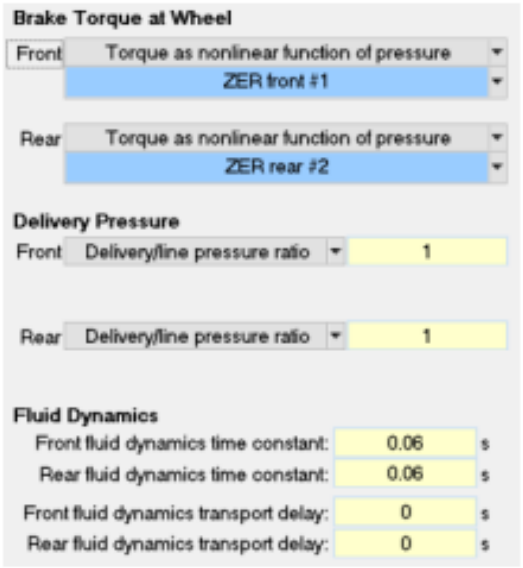

Variable brake torque application

M1[Nm]	M2[Nm]
0	0
-45,481935	-30,9950967
-93,07931	-63,4318258
-142,94323	-97,4131611
-195,23953	-133,052122
-246,52527	-147,49692
-302,40433	-163,23544
-360,82335	-179,689348
-421,95954	-196,908554
-486,00697	-214,947721
-553,17866	-233,866849

Braking torque values on front and rear axis

Co-funded by the Erasmus+ Programme of the European Union

CarSim brake Simulation

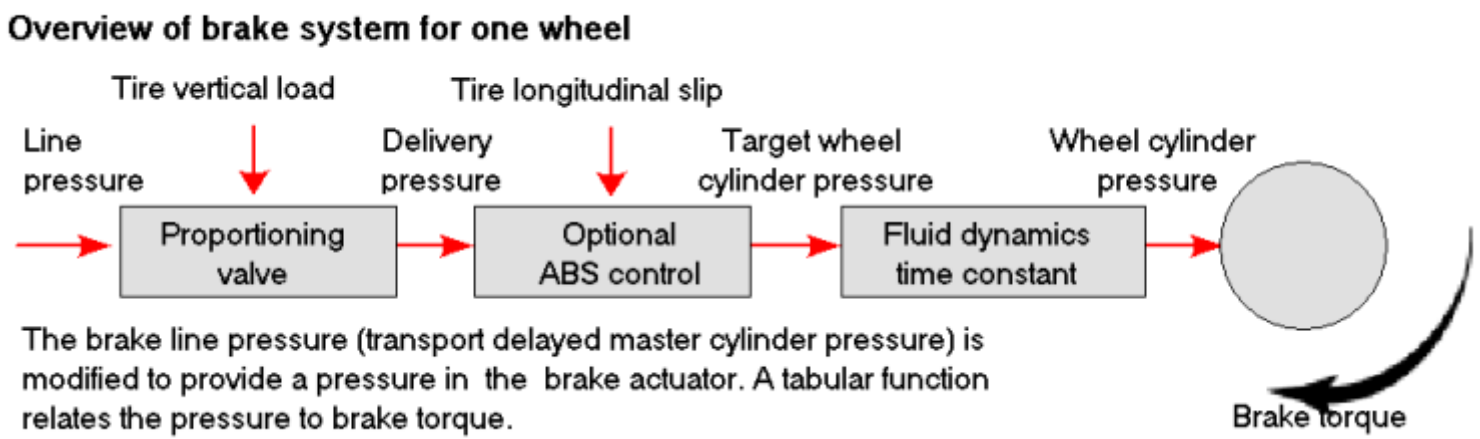

CarSim working principle relatively to the brake system

Co-funded by the Erasmus+ Programme of the European Union

CarSim brake Simulation

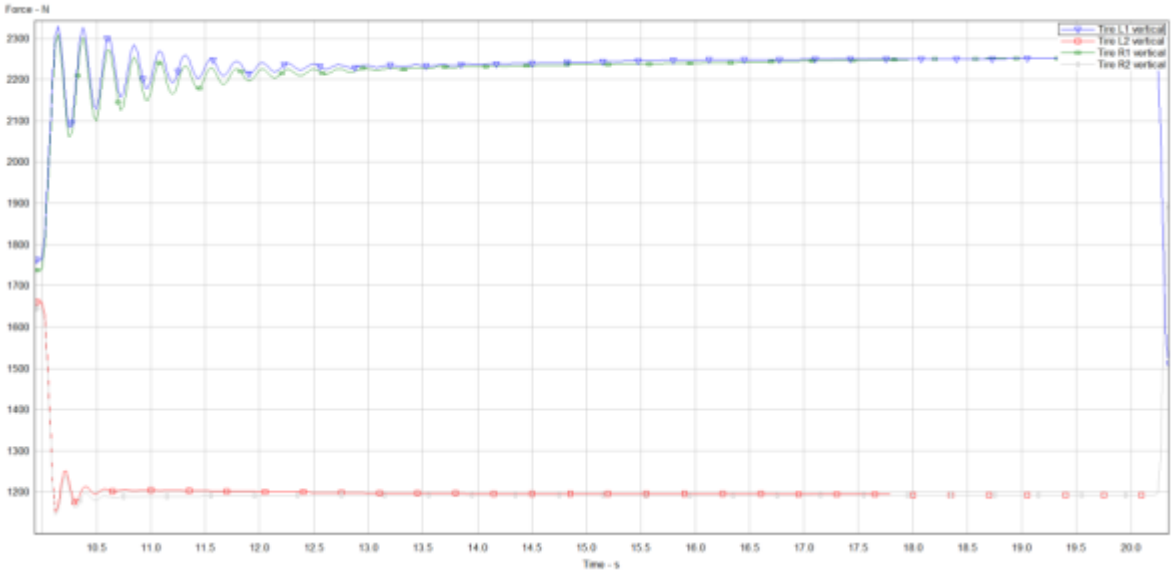

longitudinal force on the tires

result of straight braking maneuver (time)

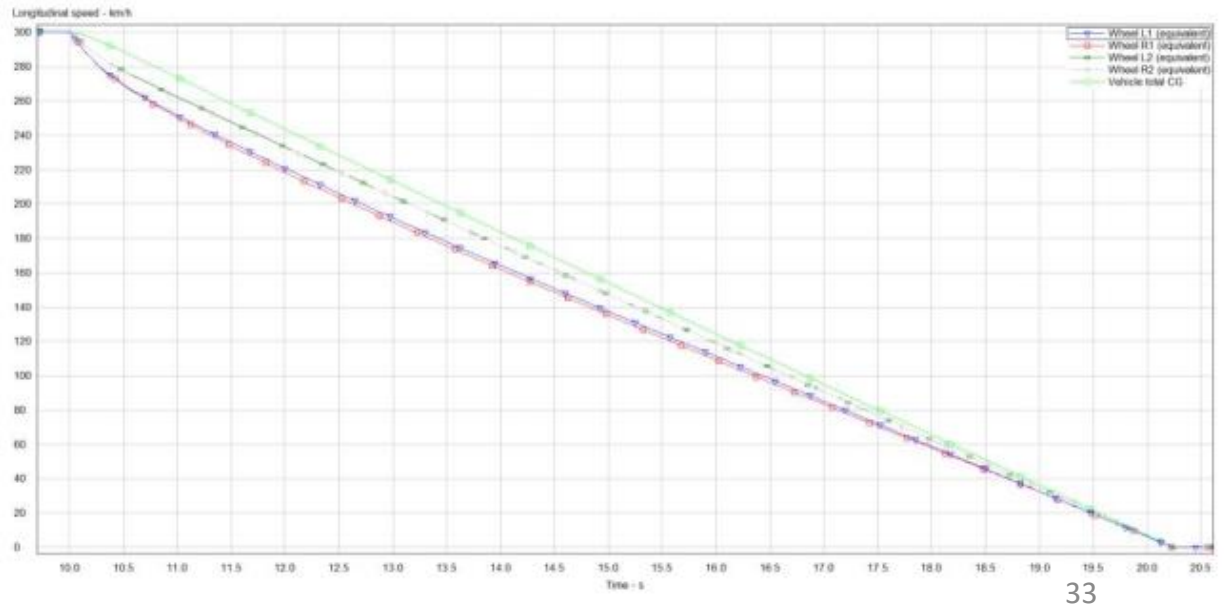

Co-funded by the
Erasmus+ Programme
of the European Union

Video simulation of the braking maneuver

Vehicle brakes from 300 km/h to full stop at Nardo test track

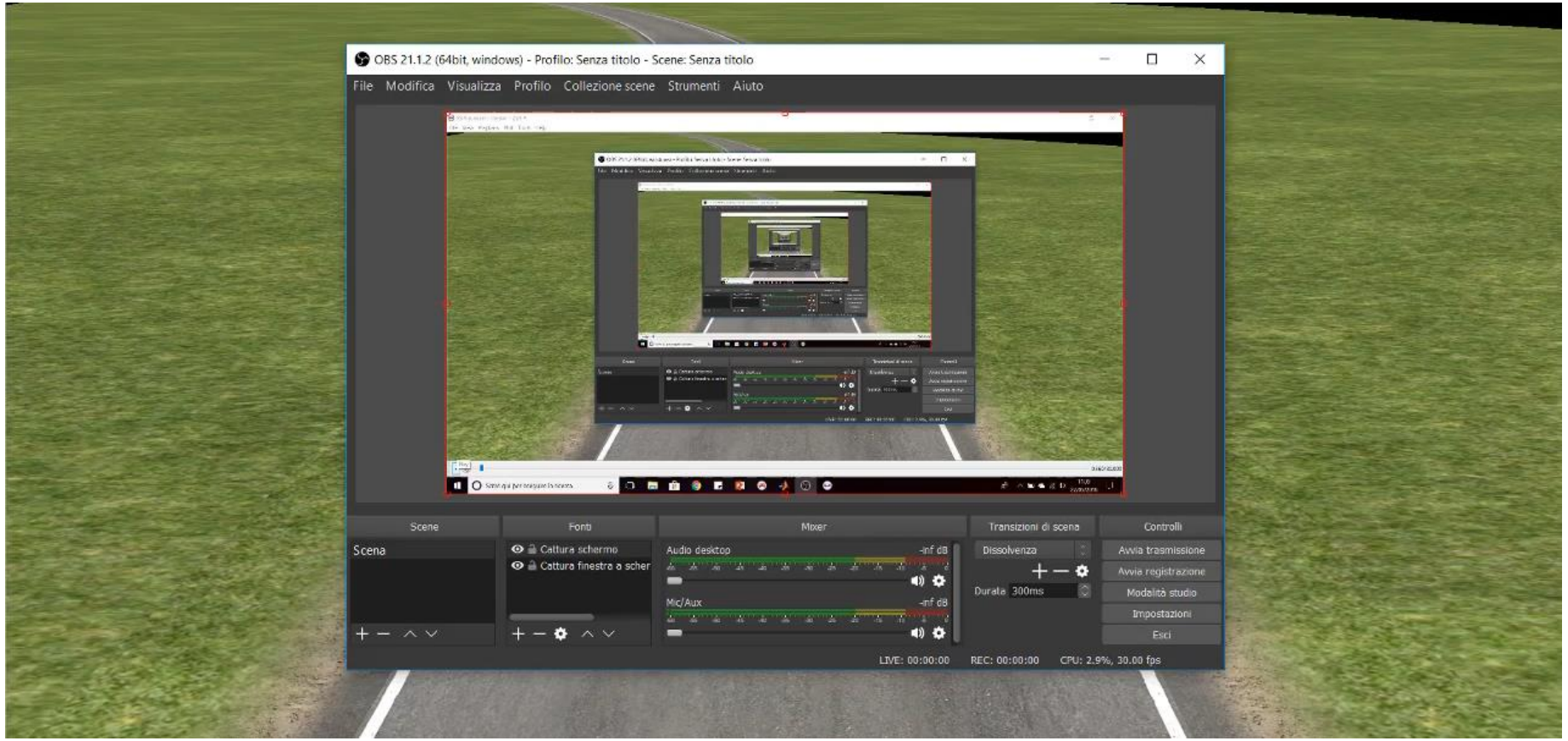

vehicle starts to brake after 10 seconds

Co-funded by the Erasmus+ Programme of the European Union

Slot 4 and 5: Vertical dynamics

- Vertical dynamics of the vehicle
- State of Art of Passive, Semi active and Active damping systems
- Roll motion

Co-funded by the
Erasmus+ Programme
of the European Union

Vertical dynamics of the vehicle

Co-funded by the
Erasmus+ Programme
of the European Union

ISO 2631 vibration comfort

- The human body reacts differently to vibrations depending on the frequency.
- The range between 4 and 8 Hz shows the largest sensitivity.
- ISO 2631 indicates a vibration sensitivity function that allows to take this into account

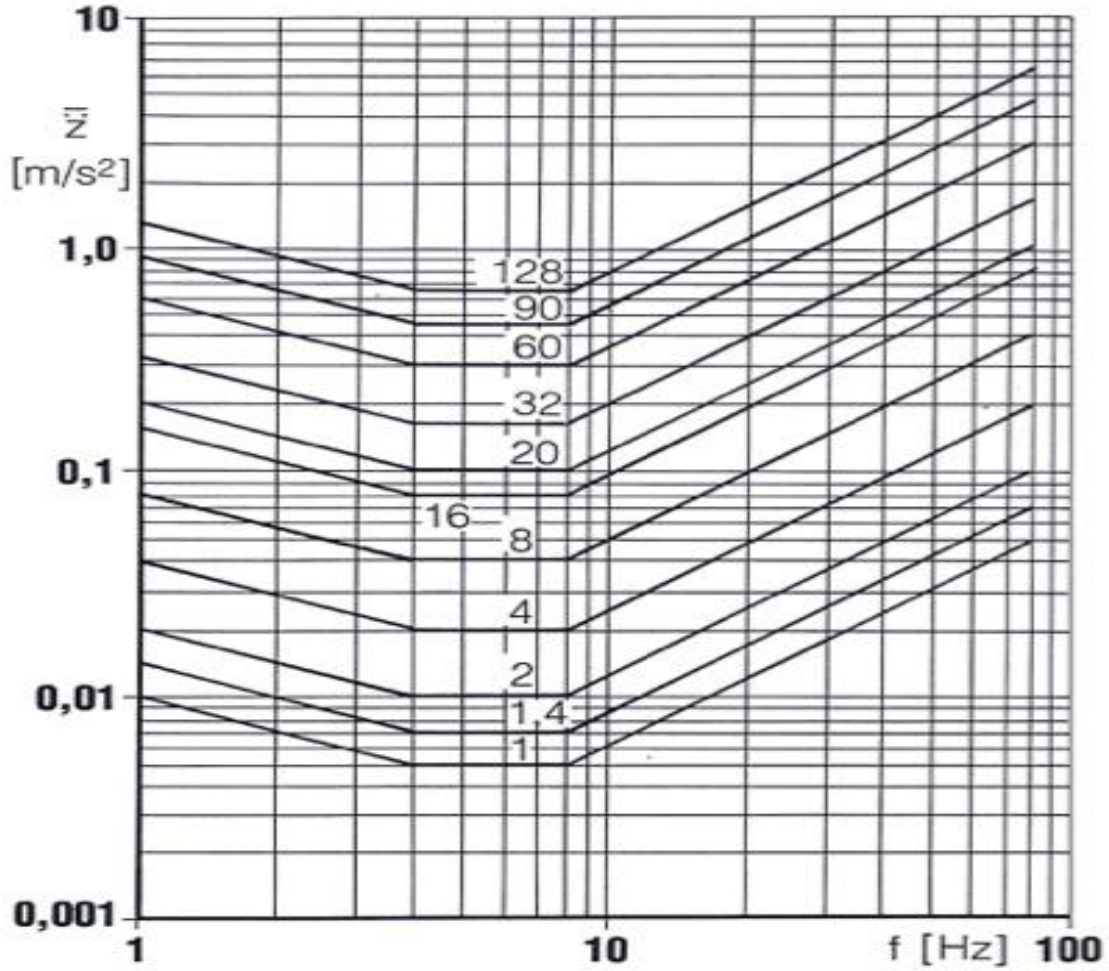

Source: Genta

Co-funded by the Erasmus+ Programme of the European Union

ISO 2631 vibration comfort

$$H_{2631}(s) = \frac{80.03s^2 + 989s + 0.02108}{s^3 + 78.92s^2 + 2412s + 5614},$$

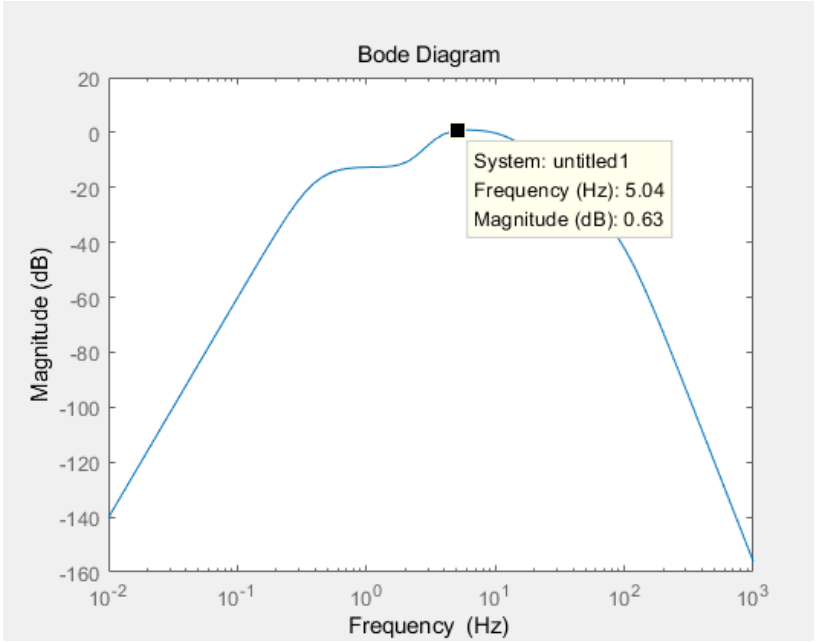

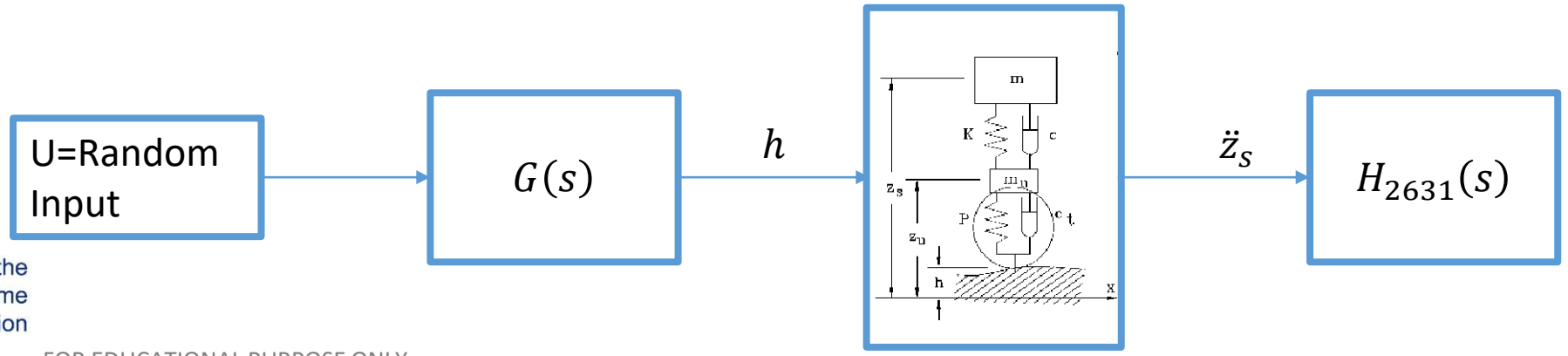

Co-funded by the Erasmus+ Programme of the European Union

Quarter car models

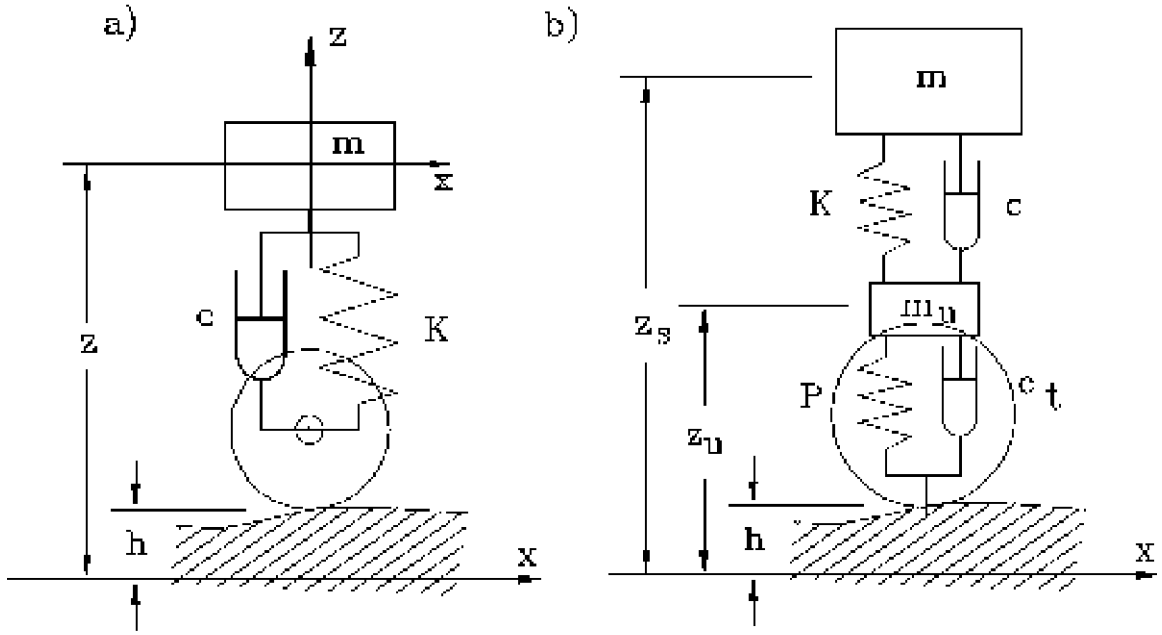

1DOF 2DOF

Co-funded by the
Erasmus+ Programme
of the European Union

1DOF quarter car model response

$$m\ddot{z} + c\dot{z} + Kz = c\dot{h} + Kh \ ,$$

$$\begin{cases} \dfrac{|z_0|}{|h_0|} = \sqrt{\dfrac{K^2 + c^2\omega^2}{(K - m\omega^2)^2 + c^2\omega^2}} \\ \Phi = \arctan\left(\dfrac{-cm\omega^3}{K\,(K - m\omega^2) + c^2\omega^2}\right) \end{cases} .$$

$$c_{opt} = \sqrt{\frac{Km}{2}} = c_{cr}\frac{1}{2\sqrt{2}} \ ,$$

$$c_{cr} = 2\sqrt{Km}$$

$$F_z = c\left(\dot{z} - \dot{h}\right) + K(z - h) - m\ddot{z}$$

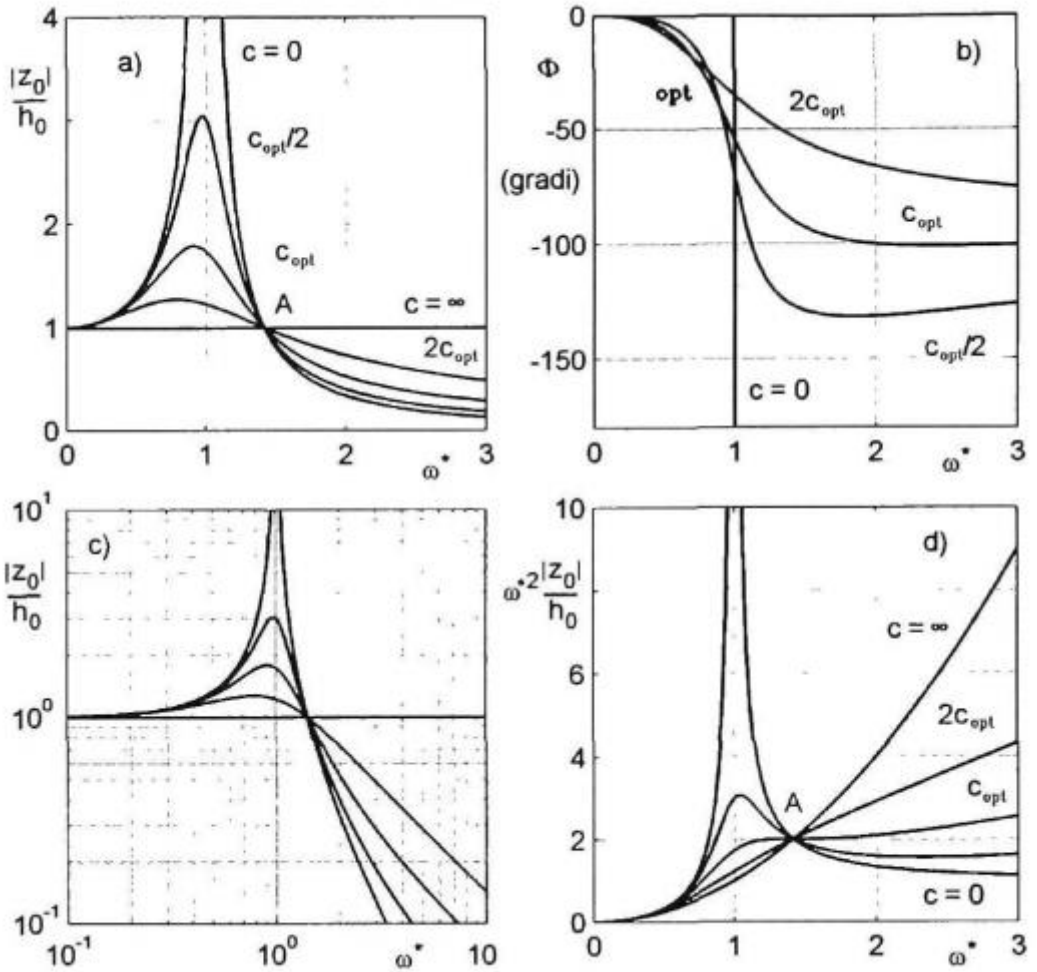

Co-funded by the Erasmus+ Programme of the European Union

2 DOF quarter car model response

$$\begin{bmatrix} m_s & 0 \\ 0 & m_u \end{bmatrix} \begin{Bmatrix} \ddot{z}_s \\ \ddot{z}_u \end{Bmatrix} + \begin{bmatrix} c & -c \\ -c & c+c_t \end{bmatrix} \begin{Bmatrix} \dot{z}_s \\ \dot{z}_u \end{Bmatrix} + \\ + \begin{bmatrix} K & -K \\ -K & K+P \end{bmatrix} \begin{Bmatrix} z_s \\ z_u \end{Bmatrix} = \begin{Bmatrix} 0 \\ c_t\dot{h} + Ph \end{Bmatrix},$$

$$\begin{cases} \dfrac{|z_{s_0}|}{|h_0|} = P\sqrt{\dfrac{K^2 + c^2\omega^2}{f^2(\omega) + c^2\omega^2 g^2(\omega)}} \\ \dfrac{|z_{n_0}|}{|h_0|} = P\sqrt{\dfrac{(K - m\omega^2)^2 + c^2\omega^2}{f^2(\omega) + c^2\omega^2 g^2(\omega)}} \end{cases},$$

$$c_{opt} = \sqrt{\frac{Km}{2}}\sqrt{\frac{P+2K}{P}}$$

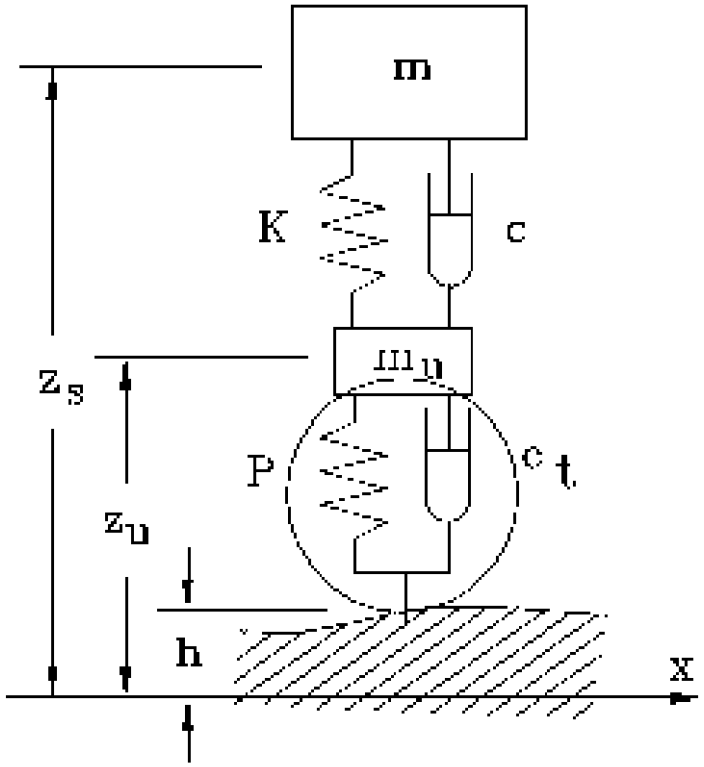

$$\begin{cases} f(\omega) = m_s m_u \omega^4 - [Pm_s + K(m_s + m_u)]\,\omega^2 + KP \\ \\ g(\omega) = (m_s + m_u)\omega^2 - P\,. \end{cases}$$

$$\frac{|F_{z_0}|}{|h_0|} = P\omega^2\sqrt{\frac{[K(m_s+m_u) - m_s m_u\omega^2]^2 + c^2(m_s+m_u)\omega^2}{f^2(\omega) + c^2\omega^2 g^2(\omega)}}\,.$$

Co-funded by the Erasmus+ Programme of the European Union

2 DOF quarter car model response

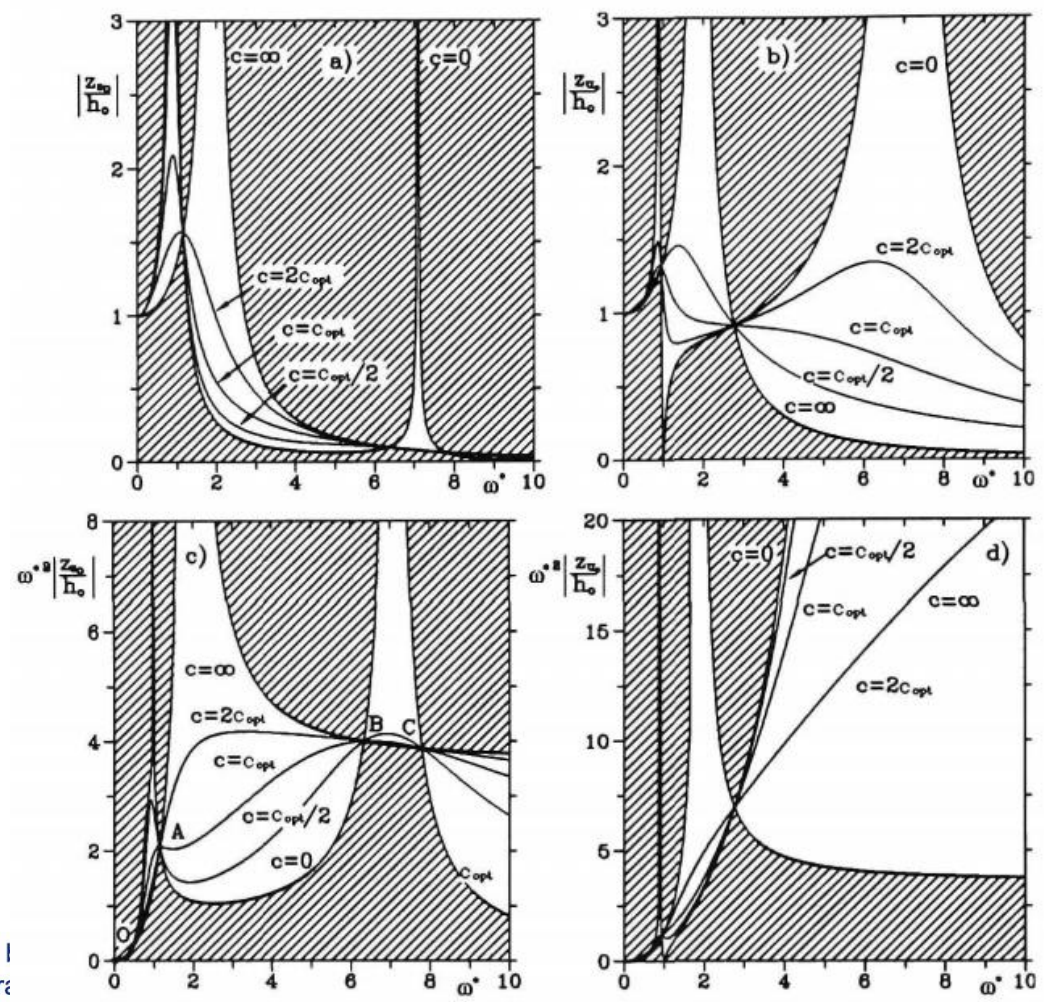

Sprung mass

Unsprung

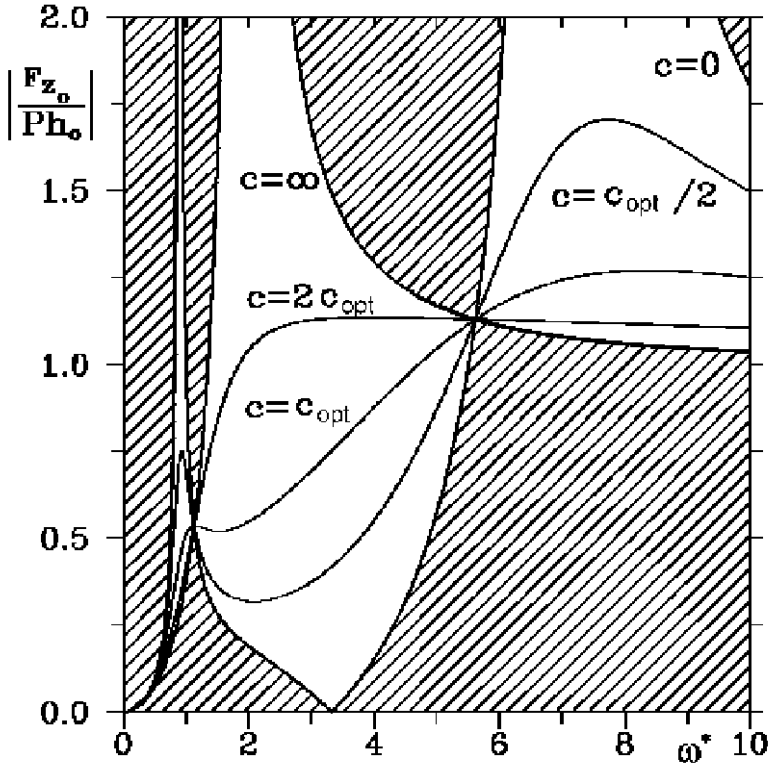

Tire force

Dampers

Twin tube

gas

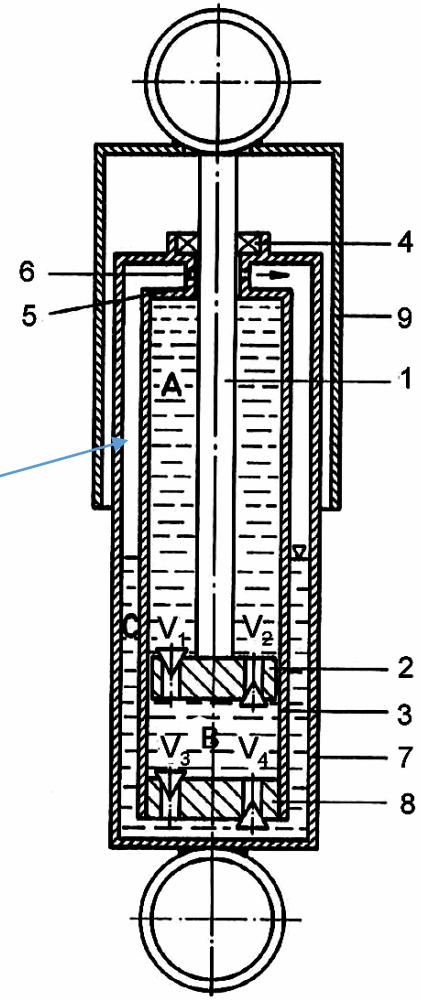

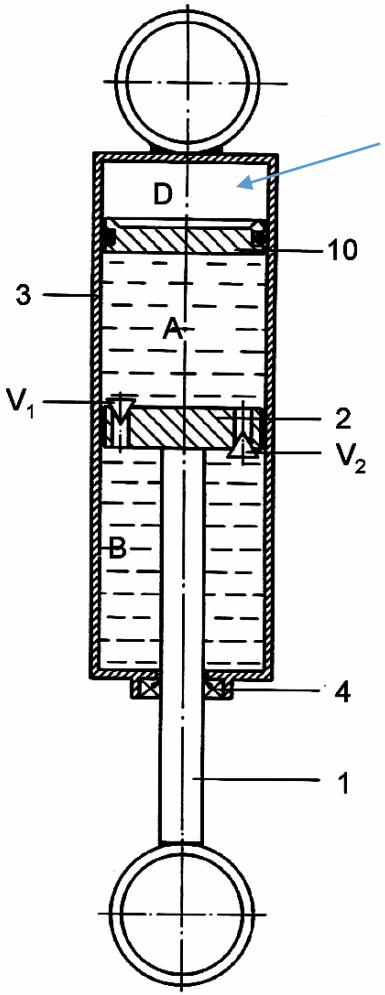

Monotube

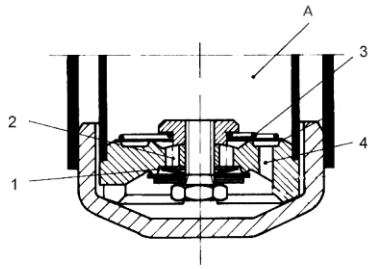

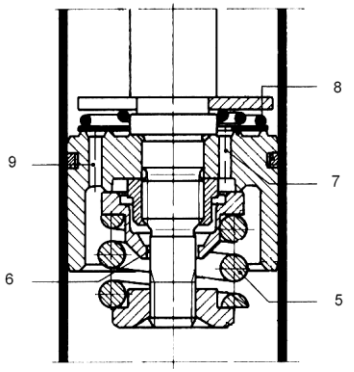

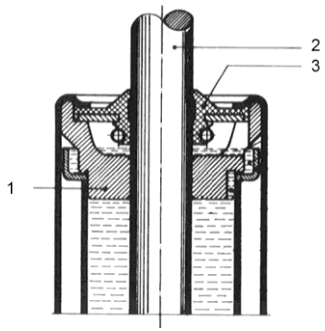

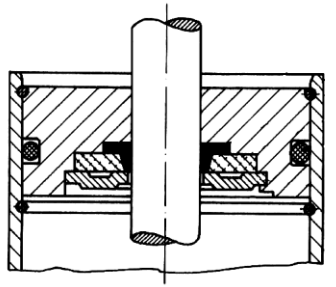

Co-fun
Erasmus+ F
of the European Union

Damper characterization

Force – travel diagram

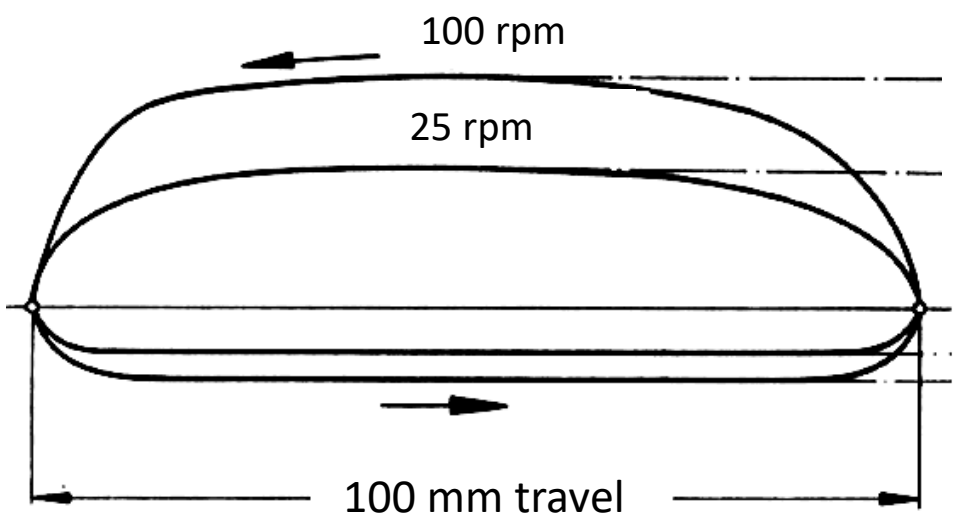

Force-speed diagram

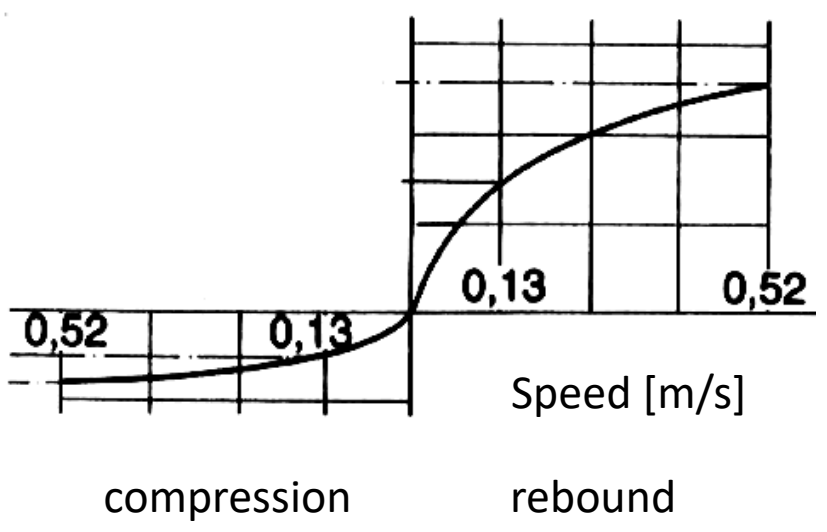

Co-funded by the
Erasmus+ Programme
of the European Union

Three tube – continuous damping control

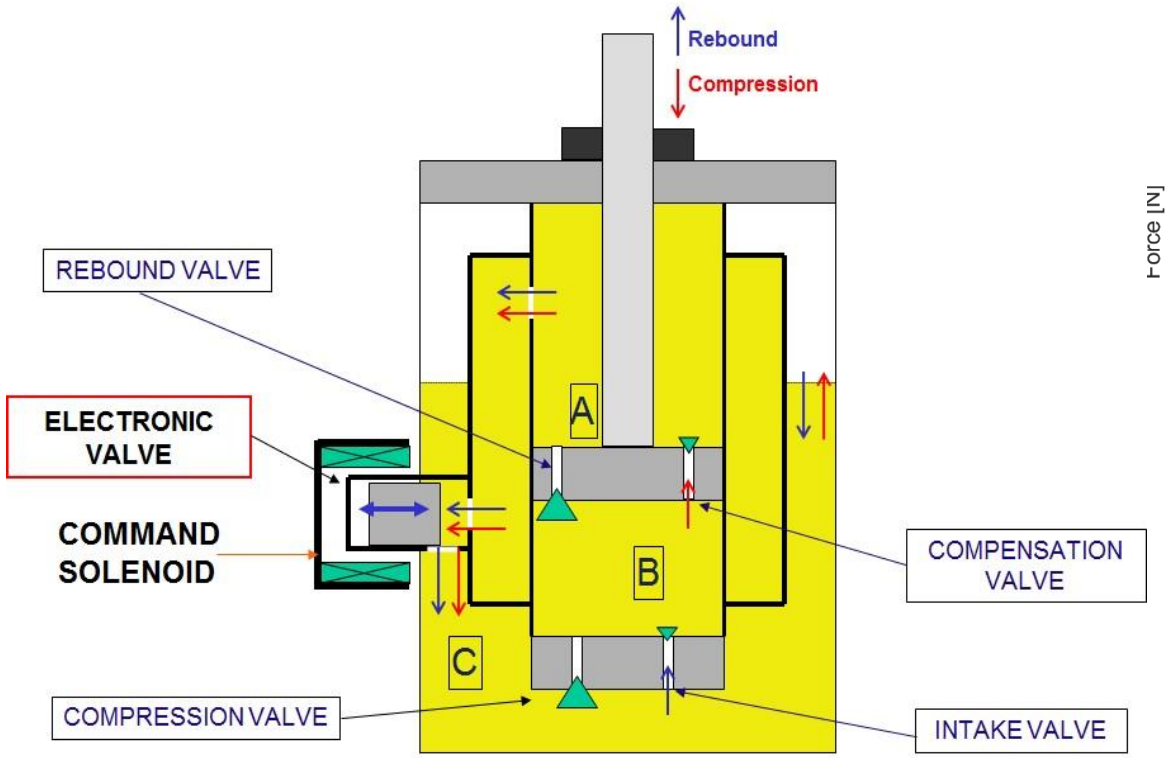

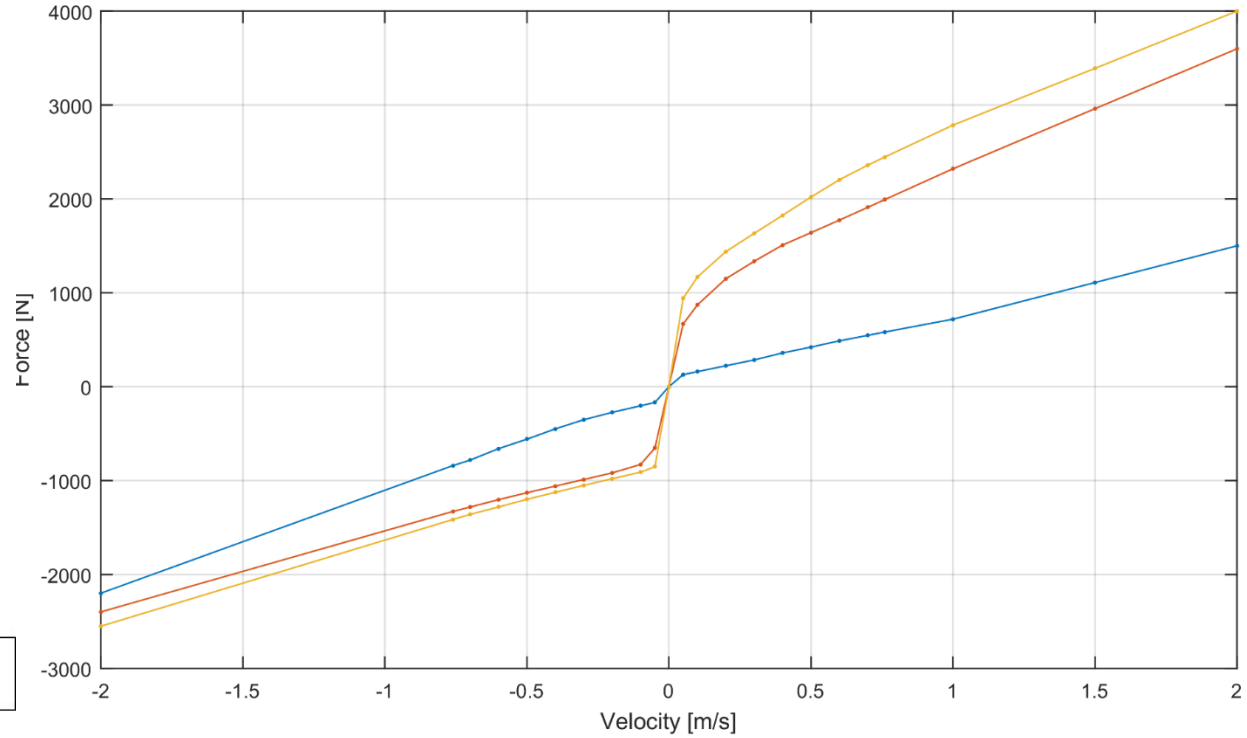

compression rebound

Source: Marelli

Co-funded by the Erasmus+ Programme of the European Union

Suspension kinematics – Instant center

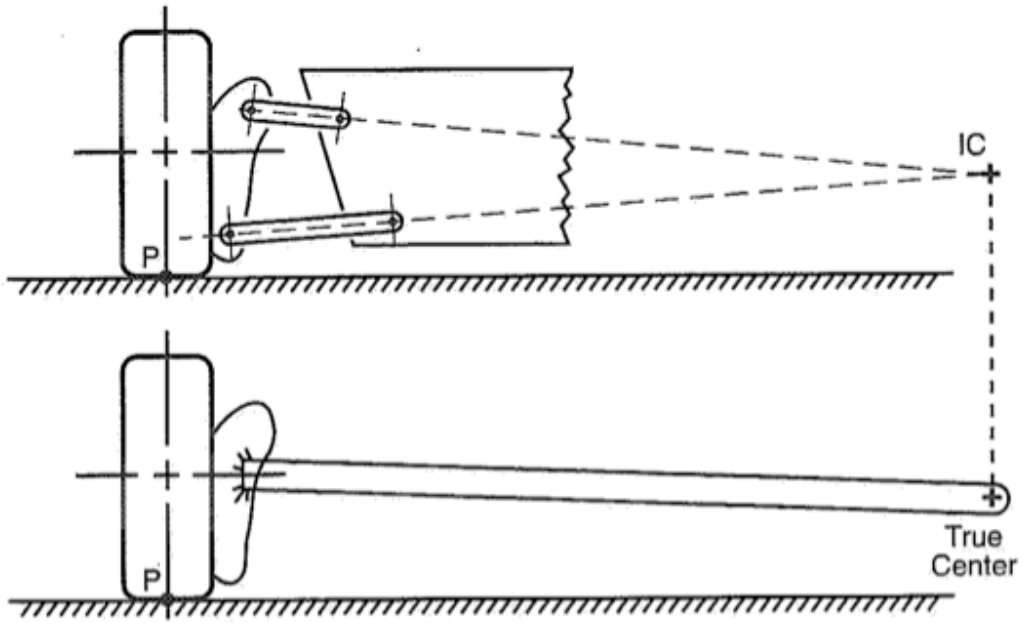

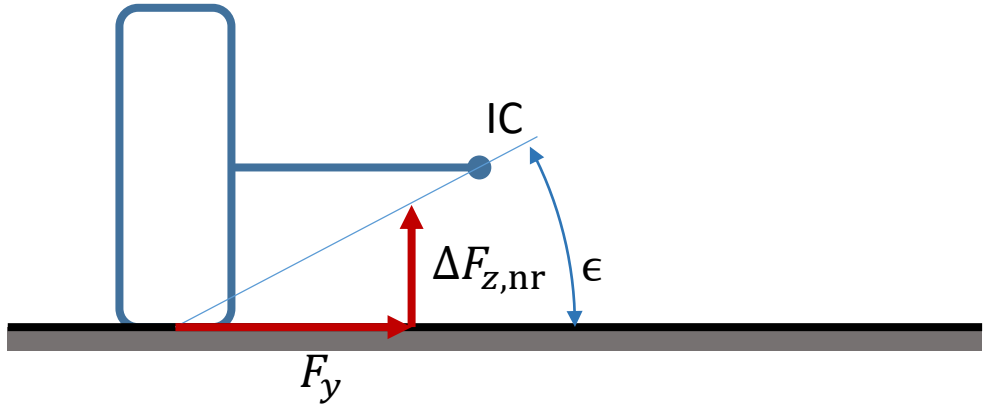

Jacking force effect

If the resultant change of the tire force (F_y, $\Delta F_{z,\mathrm{nr}}$) passes through IC, the suspension does not deflect. The load transfer $\Delta F_{z,\mathrm{nr}}$ is called "non rolling" load transfer.

$$\Delta F_{z,\mathrm{nr}} = F_y \tan \epsilon$$

Co-funded by the Erasmus+ Programme of the European Union

Roll center height

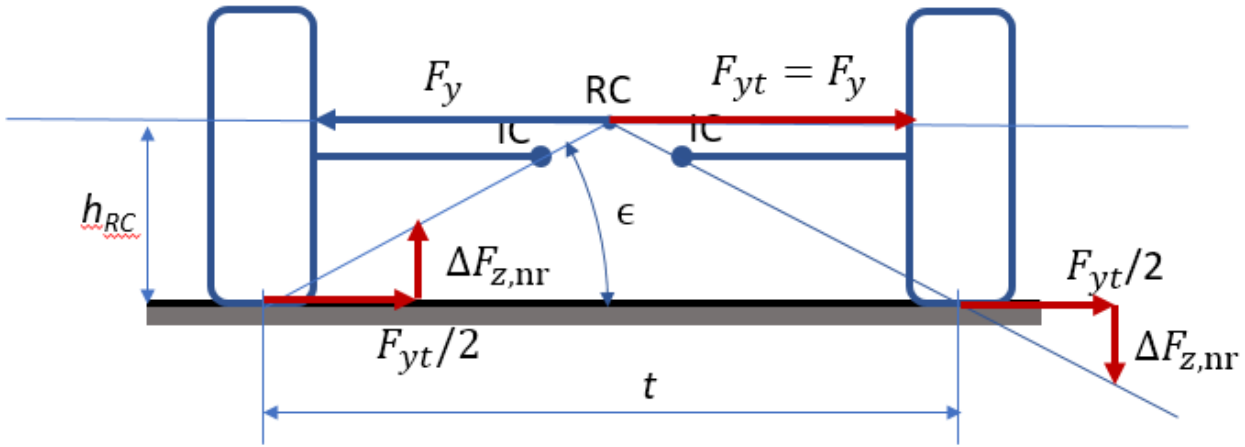

Due to roll torque balance

$$F_y\, h_{RC} = \Delta F_{z,nr}\, t$$

Therefore

$$\frac{\Delta F_{z,nr}}{F_y} = \frac{h_{RC}}{t}$$

And

$$\tan\epsilon = \frac{h_{RC}}{t/2} = \frac{\Delta F_{z,nr}}{F_y/2}$$

If the lateral force acts on RC the tire forces pass through the IC. The suspensions do not deform. The load transfer is indicated as non rolling.

Co-funded by the Erasmus+ Programme of the European Union

Roll center height

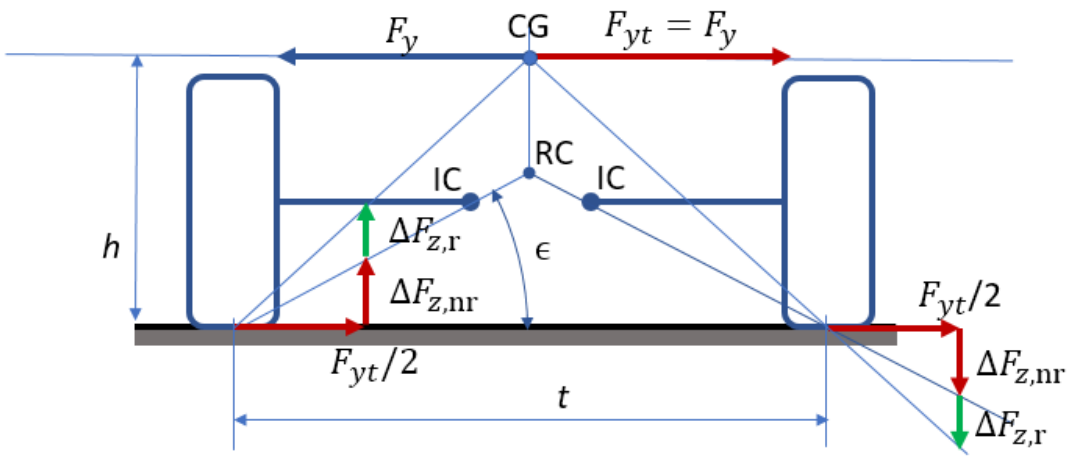

In general the lateral force acts on the CG that is not located in the RC. Due to roll torque balance

$$F_y\, h = (\Delta F_{z,r} + \Delta F_{z,nr})\, t$$

Therefore

$$\frac{(\Delta F_{z,r} + \Delta F_{z,nr})}{F_y} = \frac{h}{t}$$

And

$$\Delta F_{z,r} = F_y \frac{h}{t} - \Delta F_{z,nr} = F_y \frac{h}{t} - \frac{F_y}{2} \tan\epsilon = \frac{F_y}{t}(h - h_{RC})$$

The deformation of the suspension is just related to the rolling contribution to the load transfer. $\Delta F_{z,r}$

We can then define a "anti-roll" factor as the ratio between the non rolling to the total load transfer

$$A_r = \frac{\Delta F_{znr}}{\Delta F_z} = \frac{F_y/2 \tan\epsilon}{F_y h/t} = \frac{h_{RC}}{h}$$

Co-funded by the Erasmus+ Programme of the European Union

Camber gain

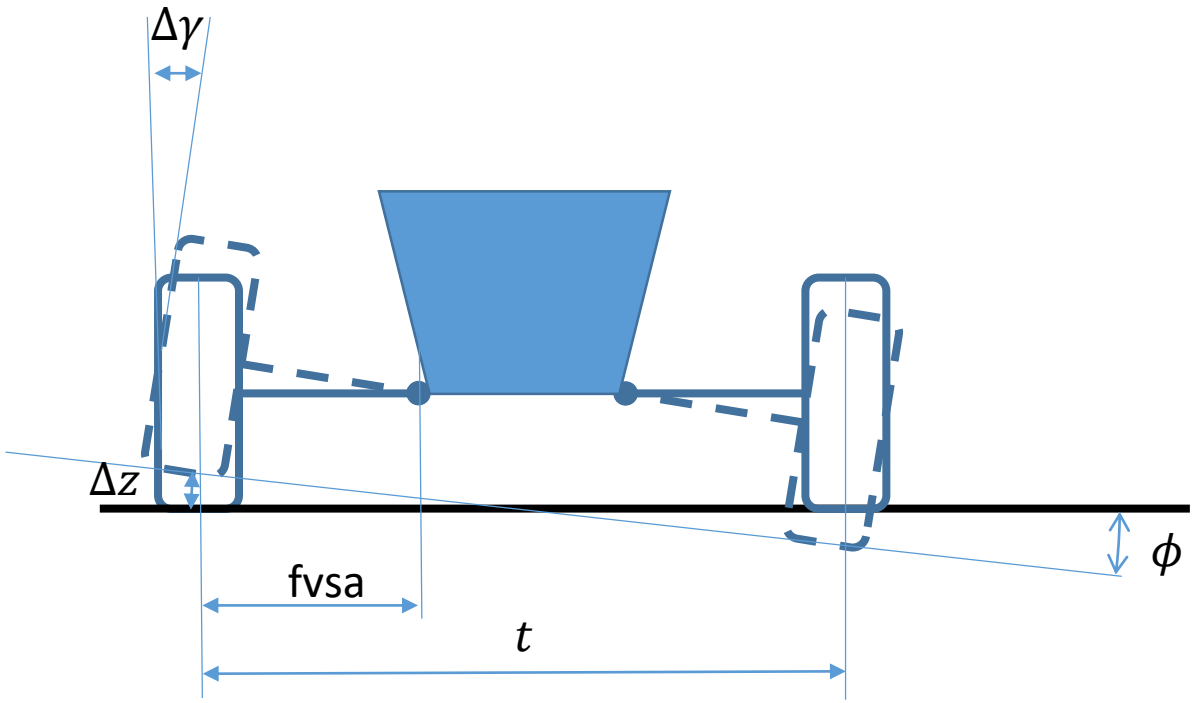

Considering small displacements, the opposite wheel travel induces a body roll angle

$$\phi = \frac{\Delta z}{t/2}$$

The same wheel travel corresponds to a change in the camber angle (camber recovery)

$$\Delta\gamma = \frac{\Delta z}{\text{fvsa}}$$

The roll camber gain is the ratio between the camber recovery and the roll

$$\frac{\Delta\gamma}{\phi} = \frac{t/2}{\text{fvsa}}$$

If the roll camber $\frac{\Delta\gamma}{\phi} \approx 1$ the suspensions recover the camber loss due to roll.

Co-funded by the Erasmus+ Programme of the European Union

Trailing arm

- Front view
  - Pure vertical motion. IC at ∞ along bushing axis and RC on ground.
  - No camber change with wheel travel
  - Body roll translates in the same change in camber (no camber recovery)
  - No toe change
- Side view
  - IC is the bushing axis. Vertical position of IC must leave appropriate ground clearance.
  - For front suspension the wheel moves against obstacle.
- Top view
  - No toe change due to wheel travel
  - Side force induces toe out of out-the-bend wheel (destabilizing for rear suspensions)

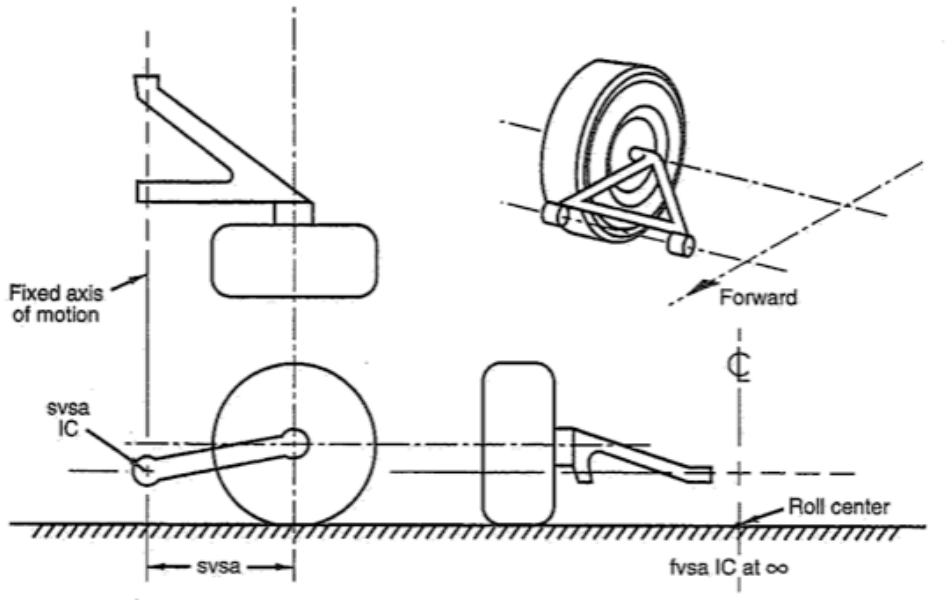

Co-funded by the Erasmus+ Programme of the European Union

Trailing arm – construction

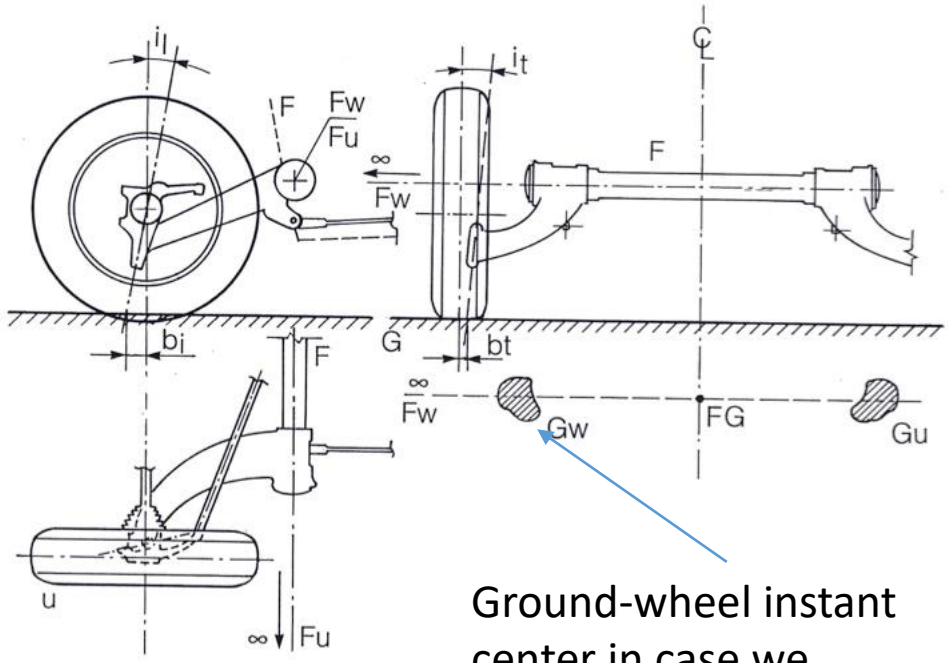

Ground-wheel instant center in case we consider the tire deformation

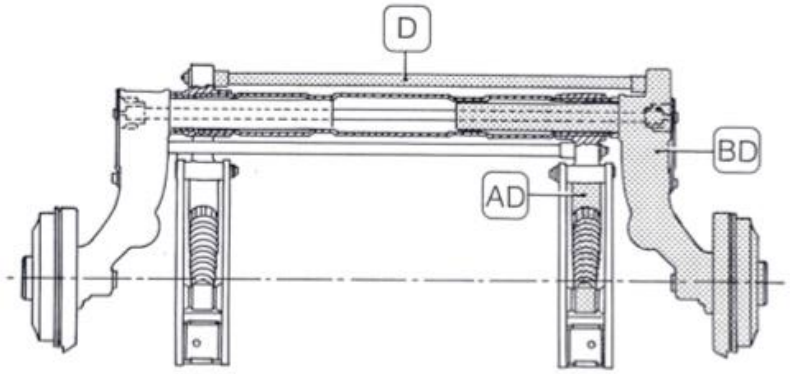

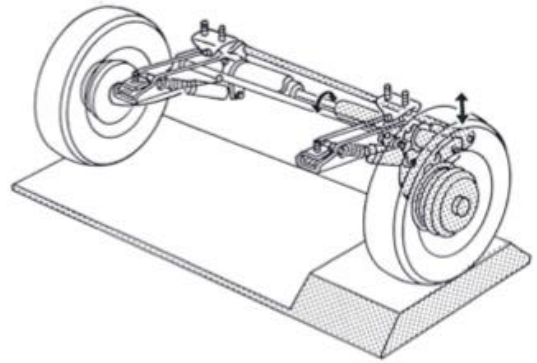

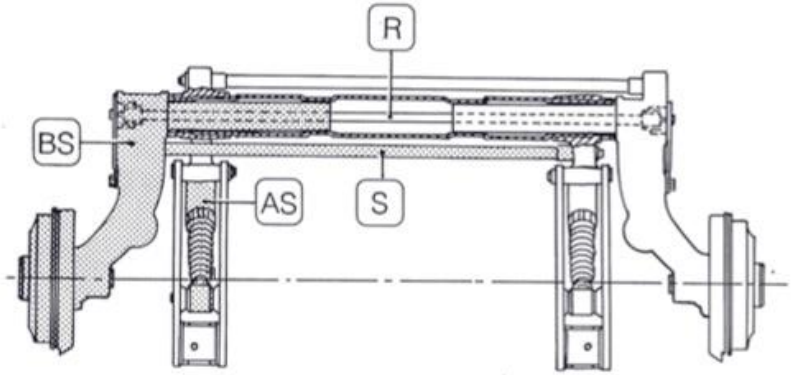

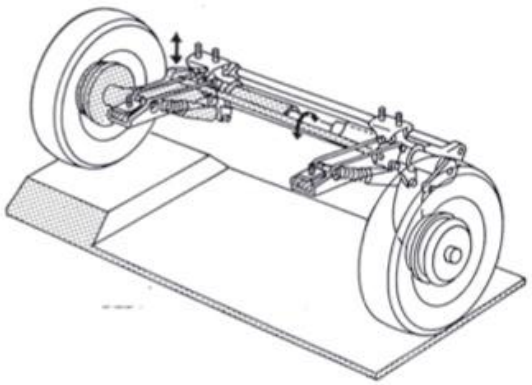

Source: Genta

Co-funded by the Erasmus+ Programme of the European Union

Twisted beam axle

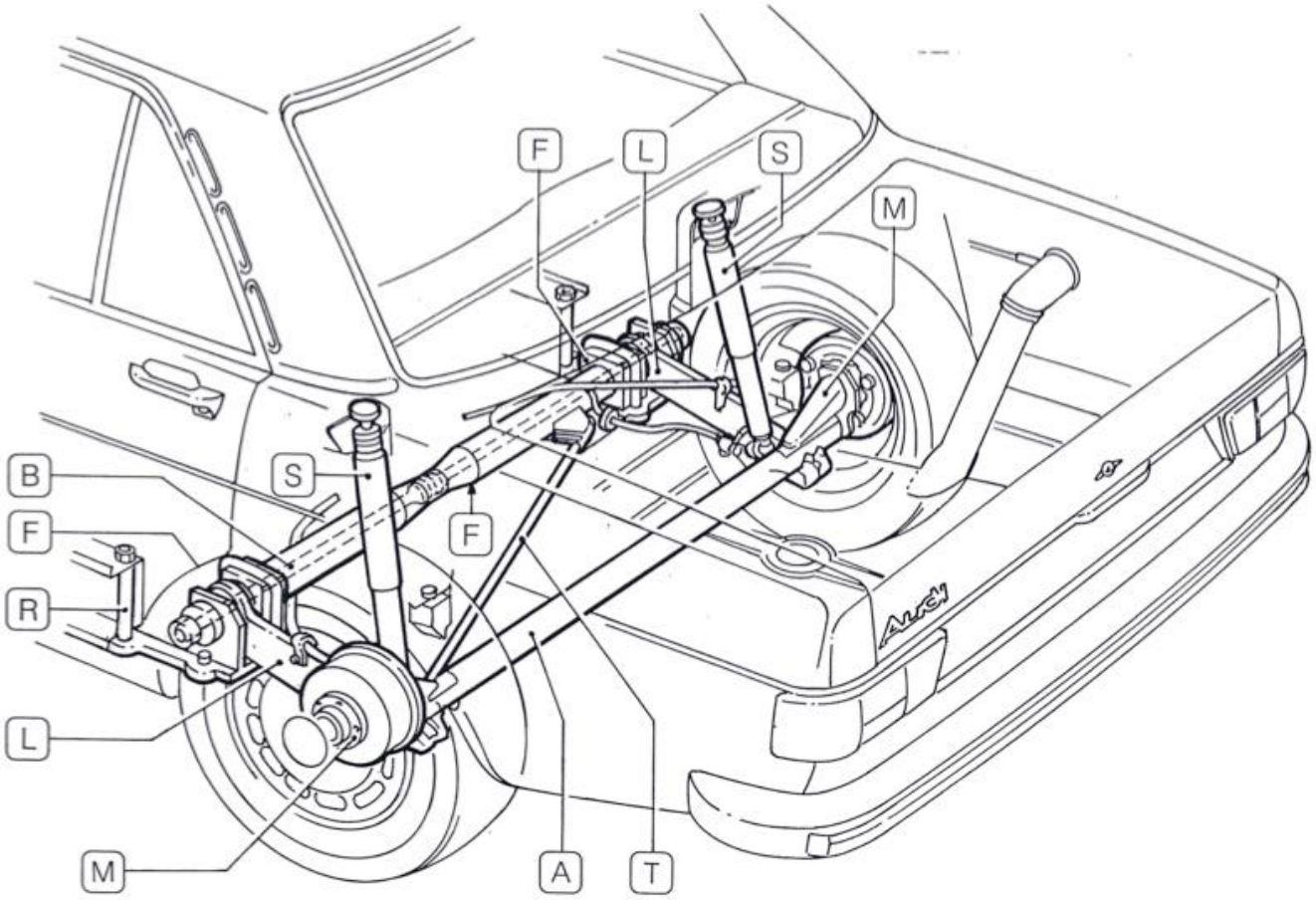

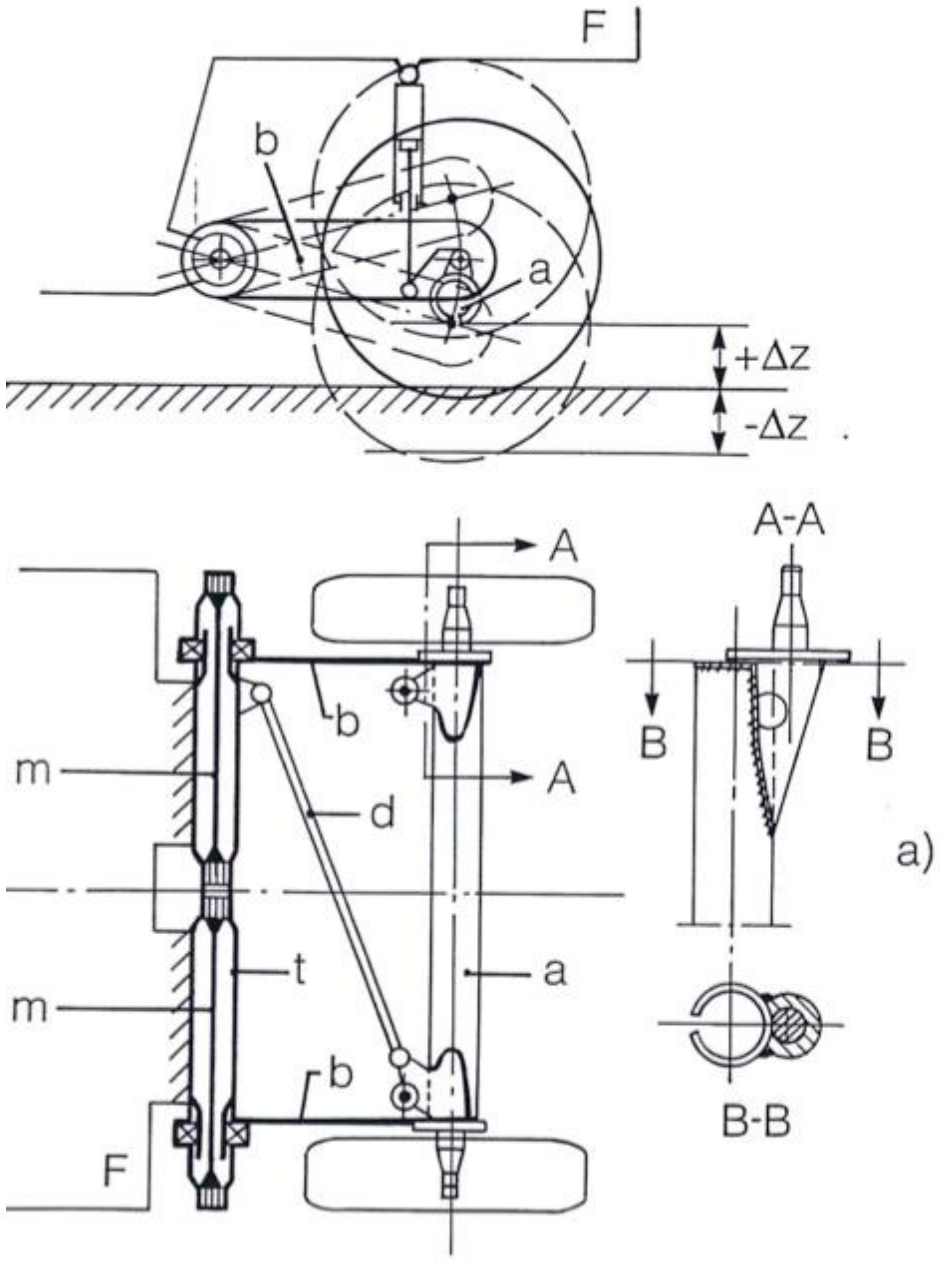

Co-funded by the
Erasmus+ Programme
of the European Union

Twisted beam suspension

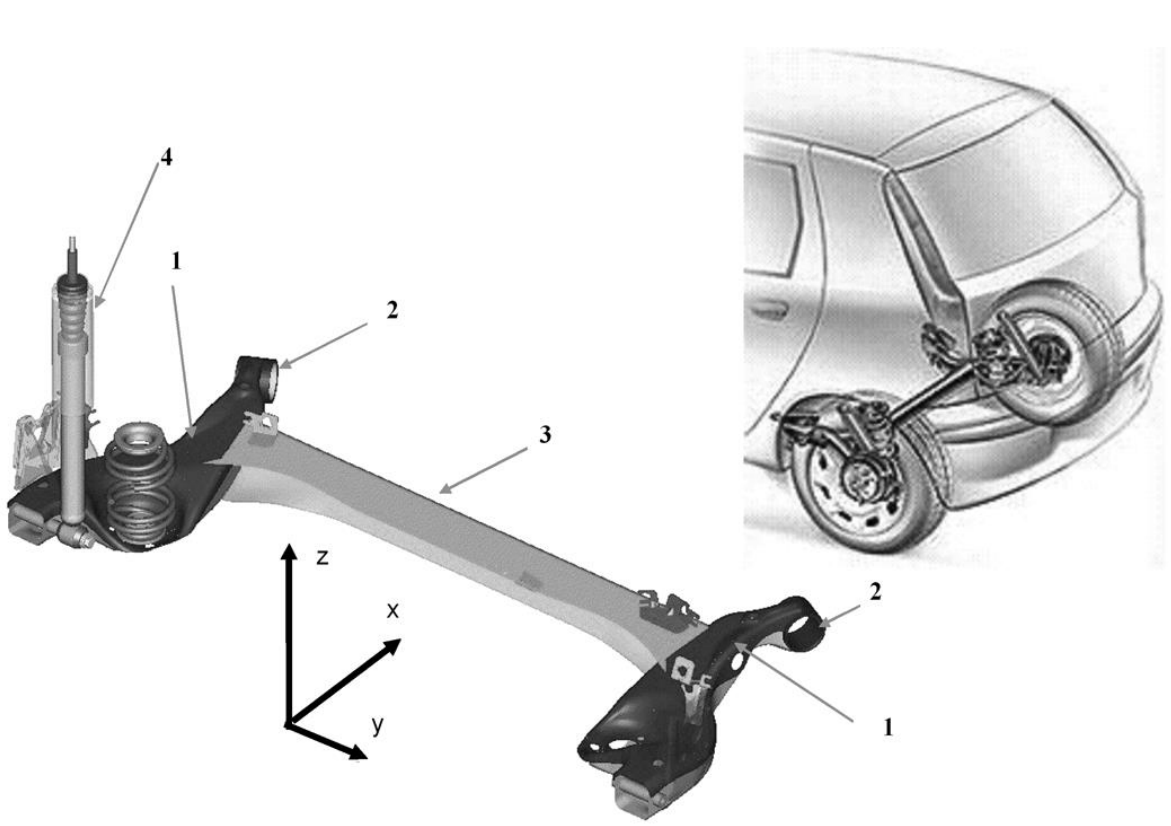

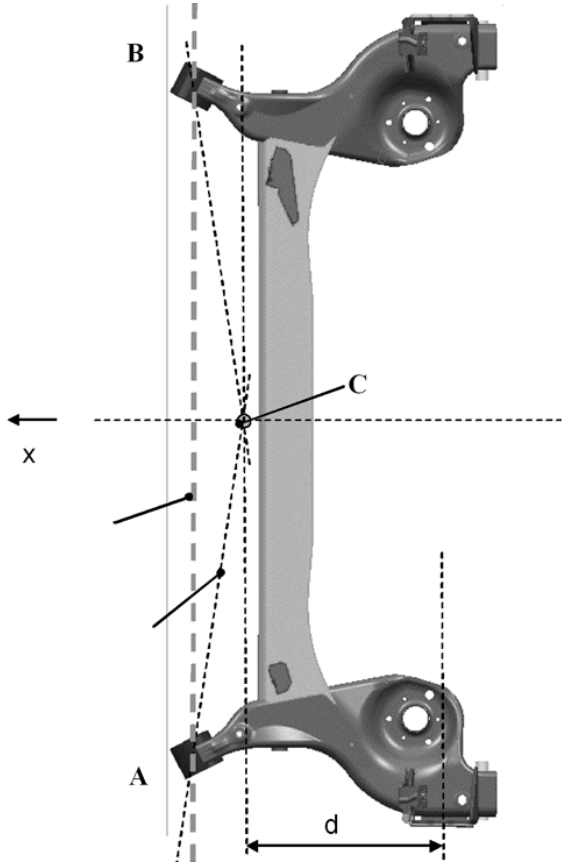

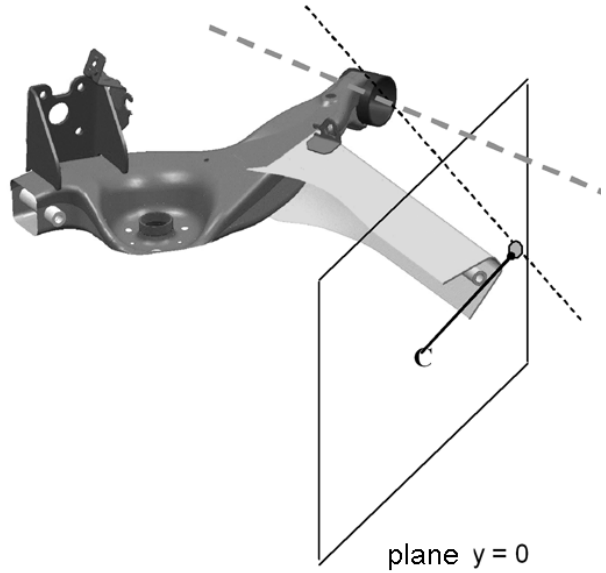

Co-funded by the
Erasmus+ Programme
of the European Union

Twisted beam suspension

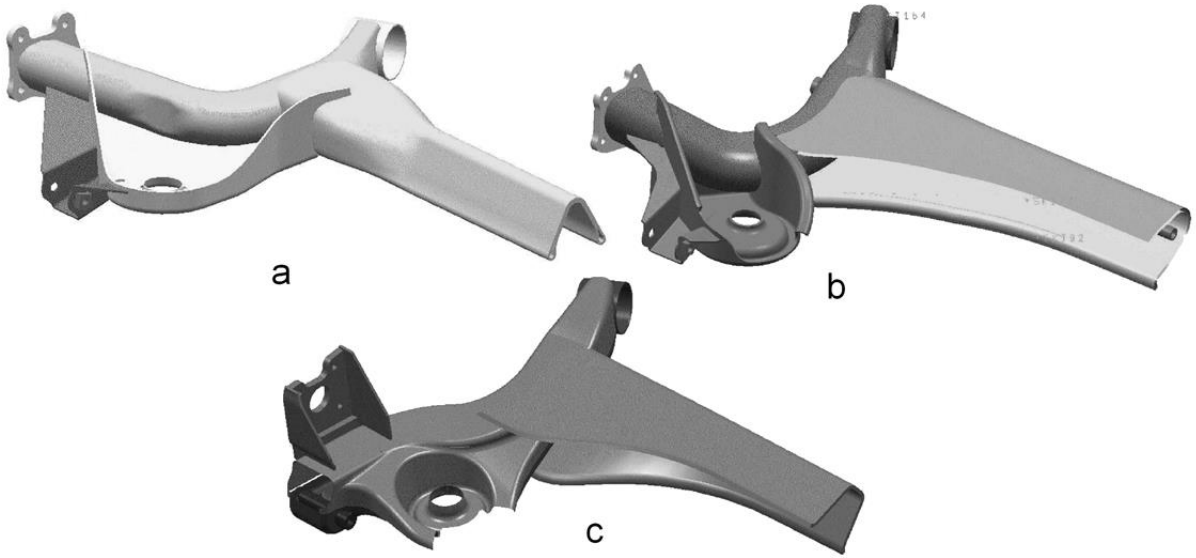

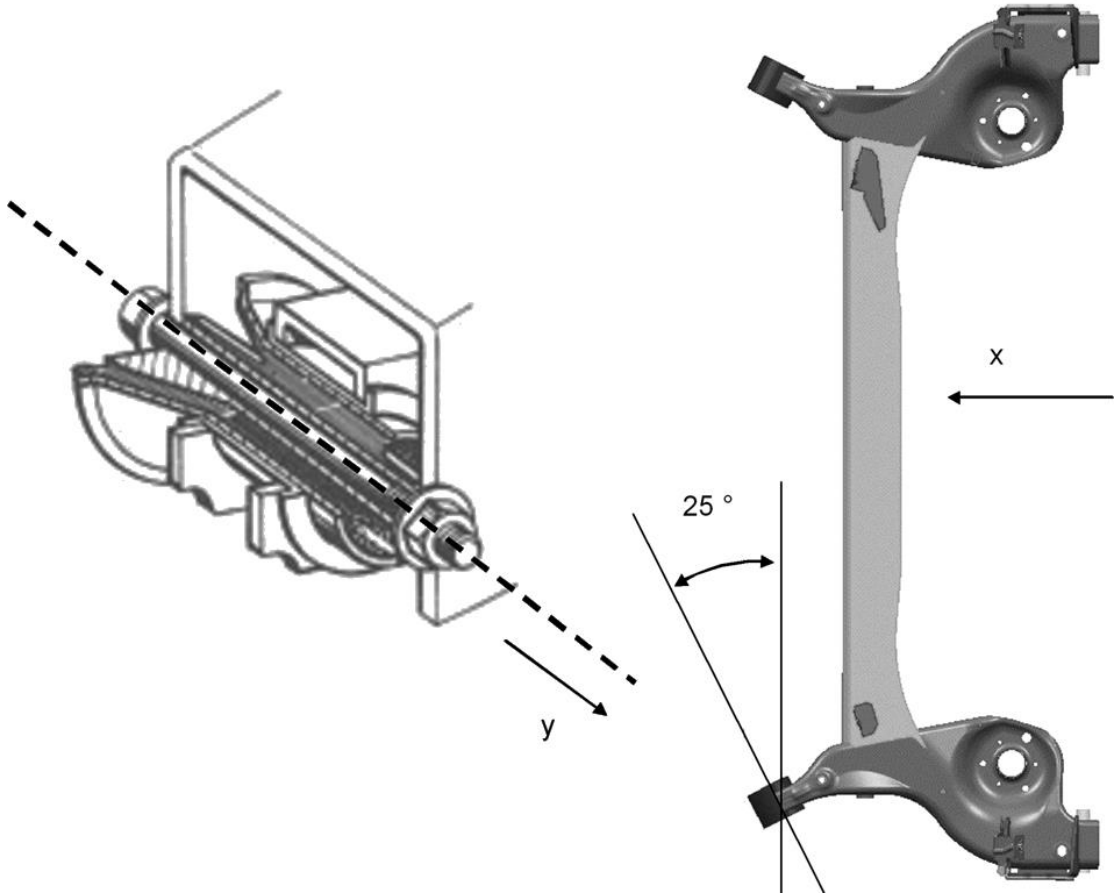

Source: Genta

Co-funded by the Erasmus+ Programme of the European Union

Double whishbone

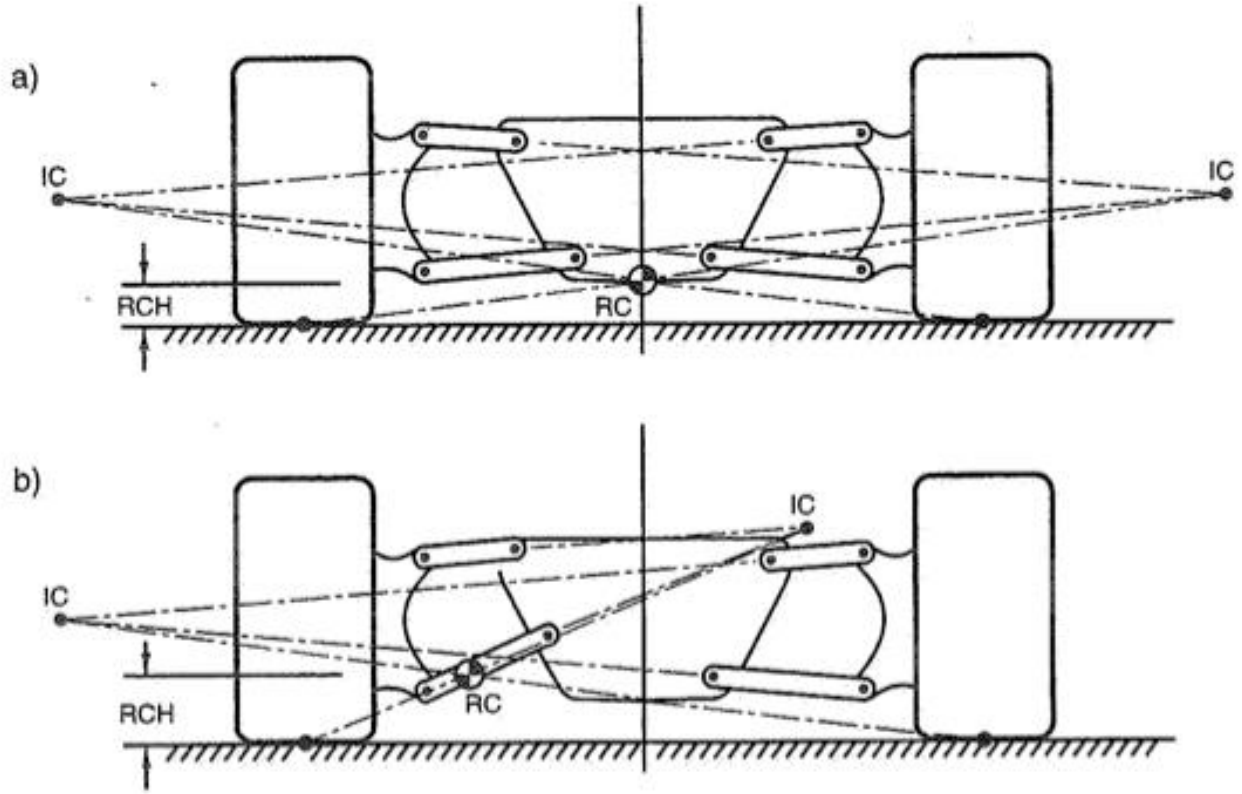

Co-funded by the
Erasmus+ Programme
of the European Union

Double whishbone IC migration

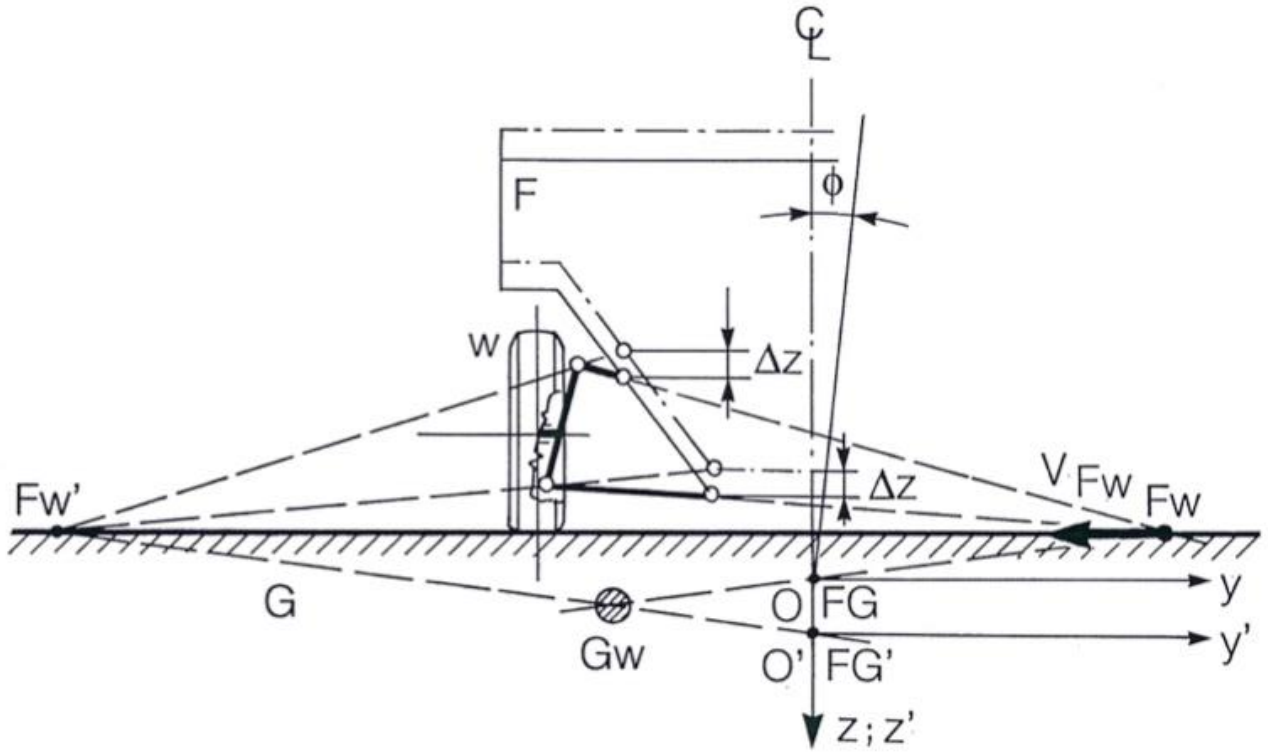

Co-funded by the
Erasmus+ Programme
of the European Union

Double whishbone – IC migration

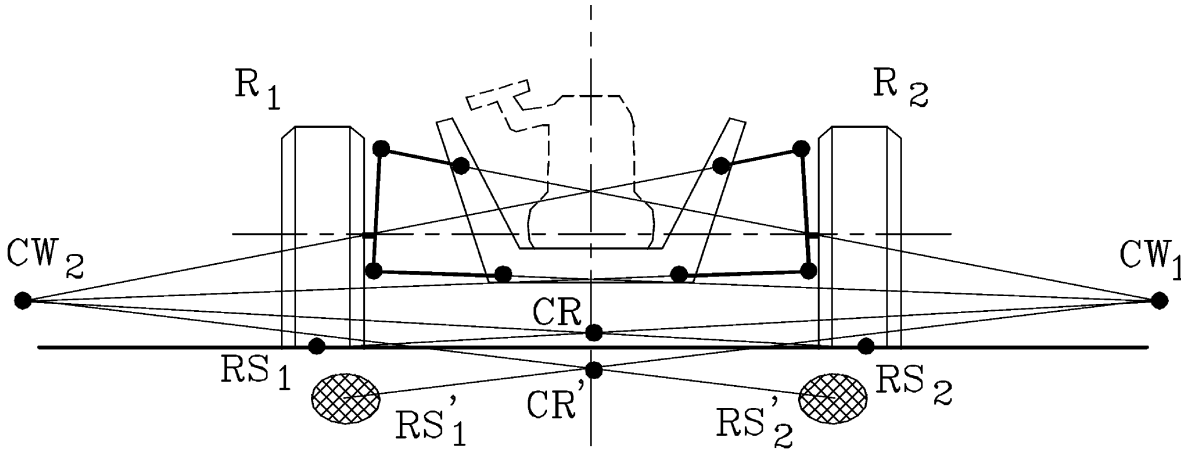

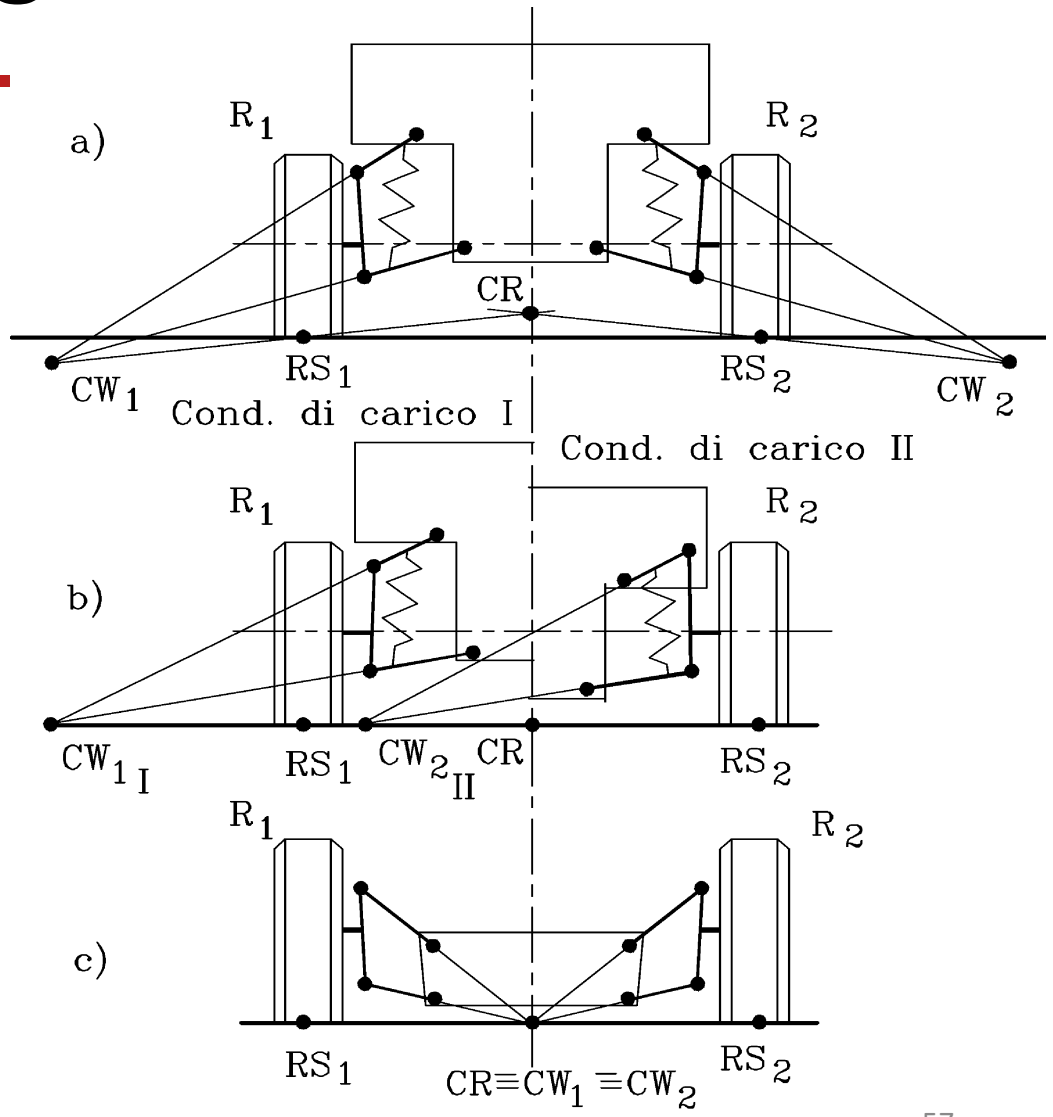

Co-funded by the Erasmus+ Programme of the European Union

Double whishbone

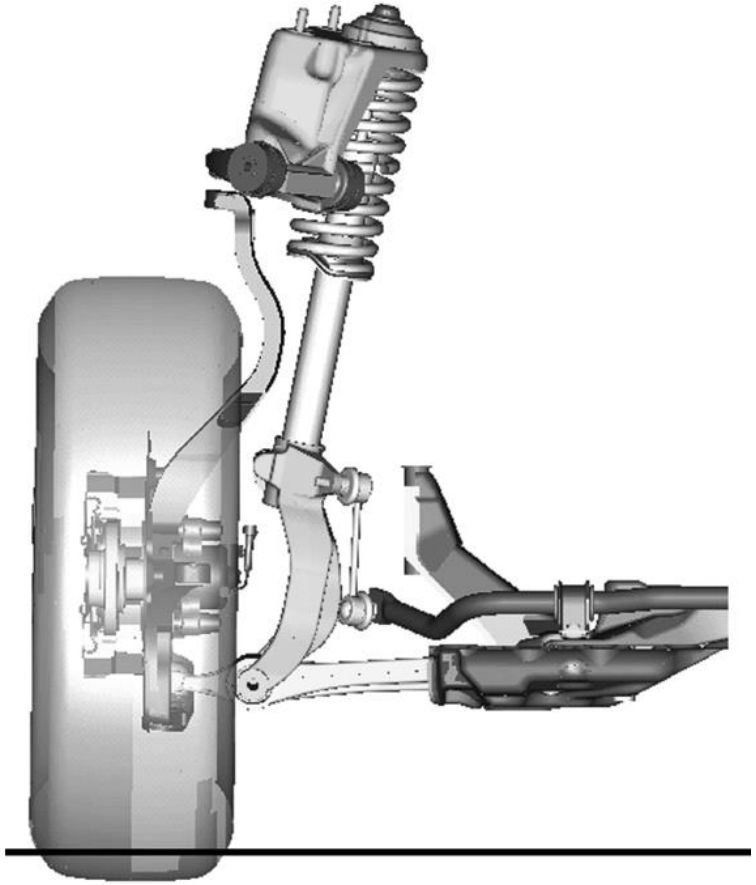

Long strut

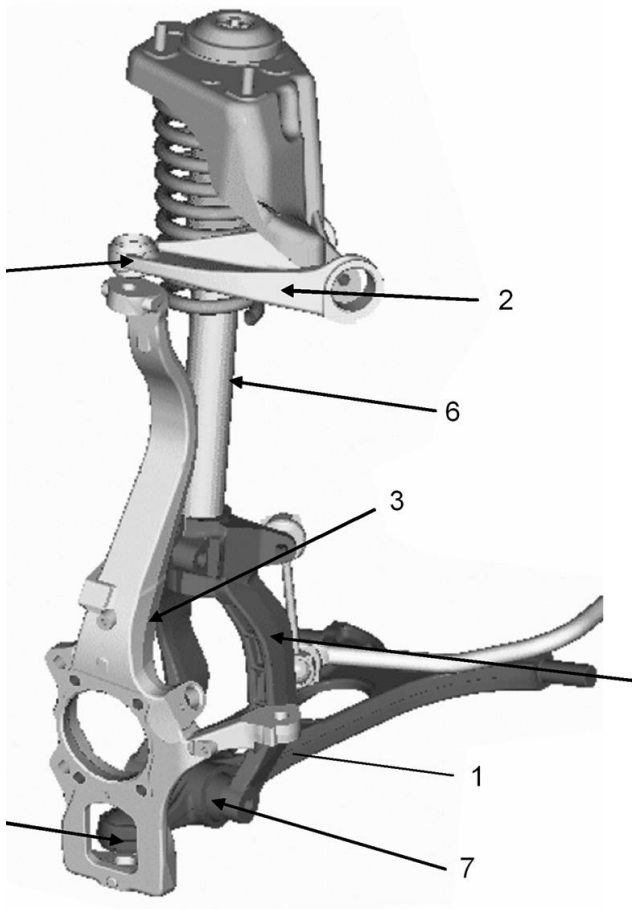

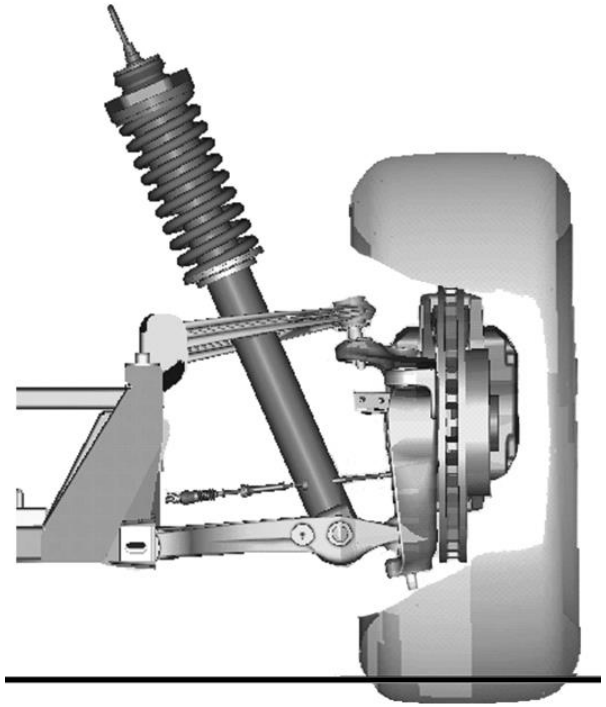

Short strut

Co-funded by the Erasmus+ Programme of the European Union

Mc Pherson IC and RC

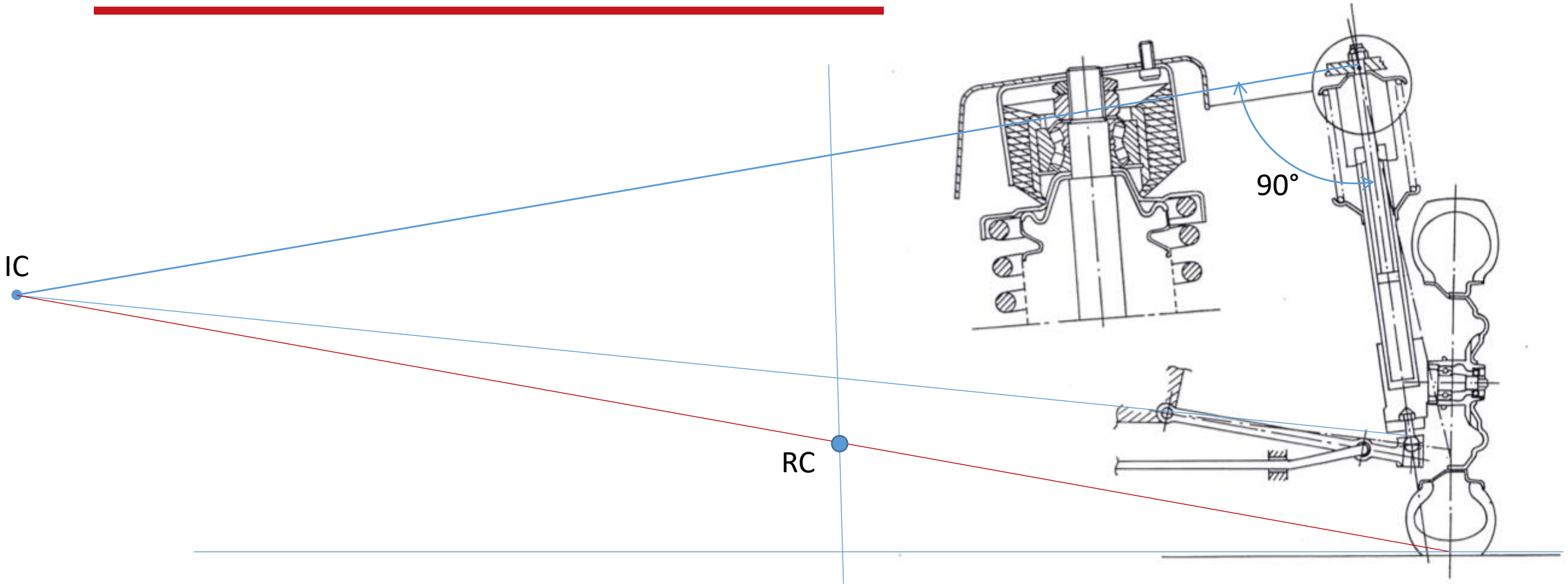

Co-funded by the
Erasmus+ Programme
of the European Union

Mc Pherson – steering angles

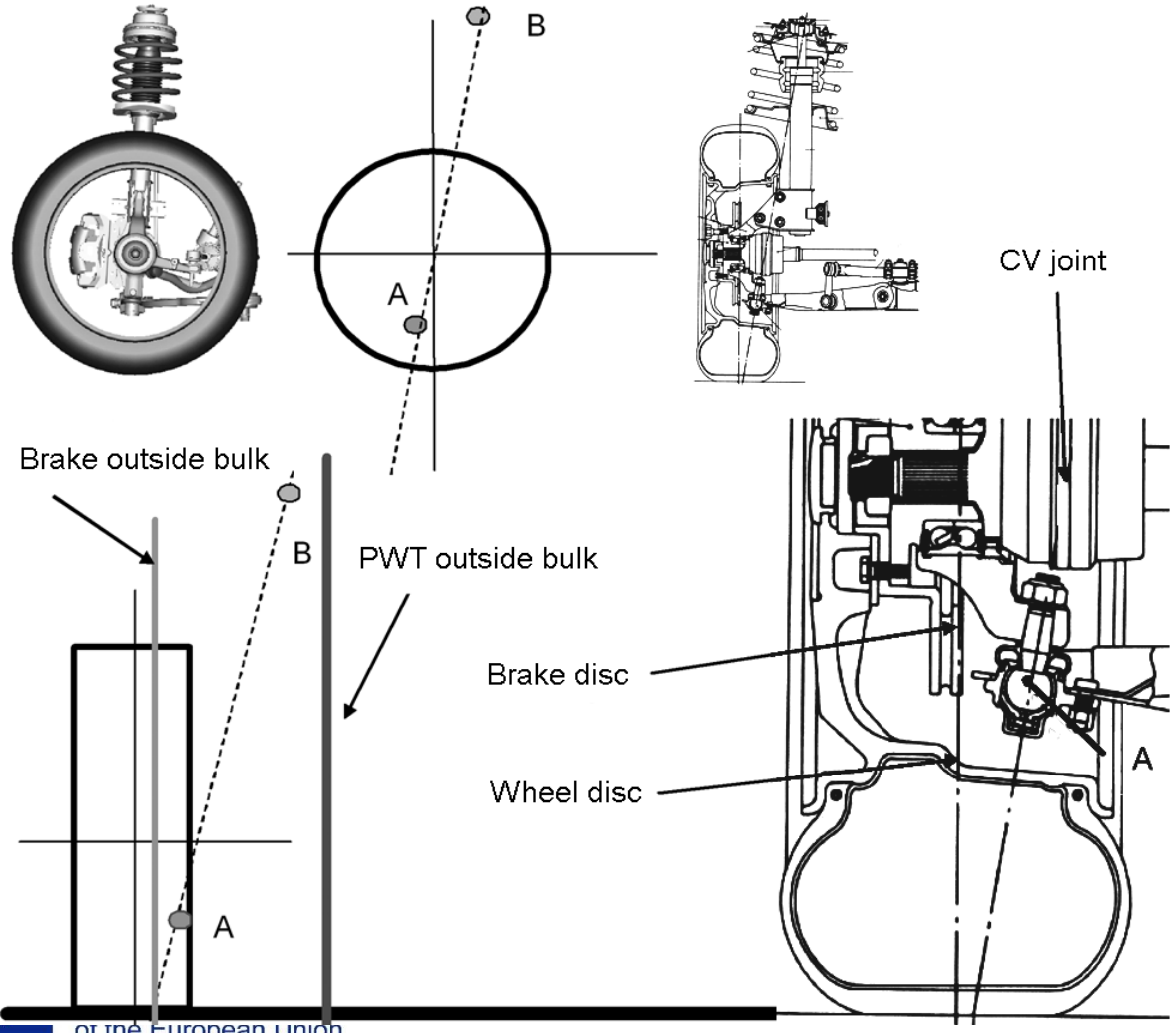

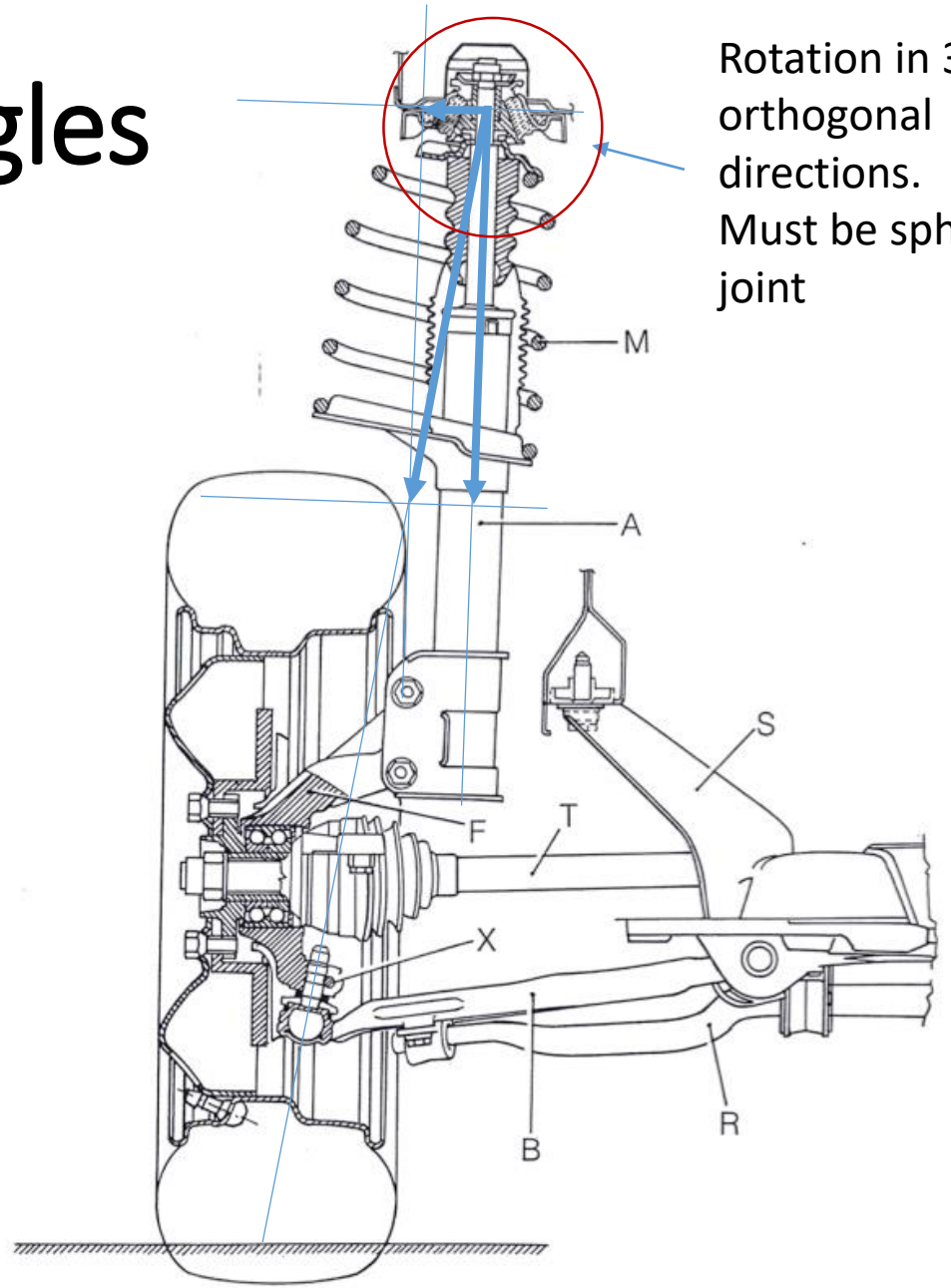

Rotation in 3 orthogonal directions.
Must be spherical joint

of the European Union

Mc Pherson spring offset

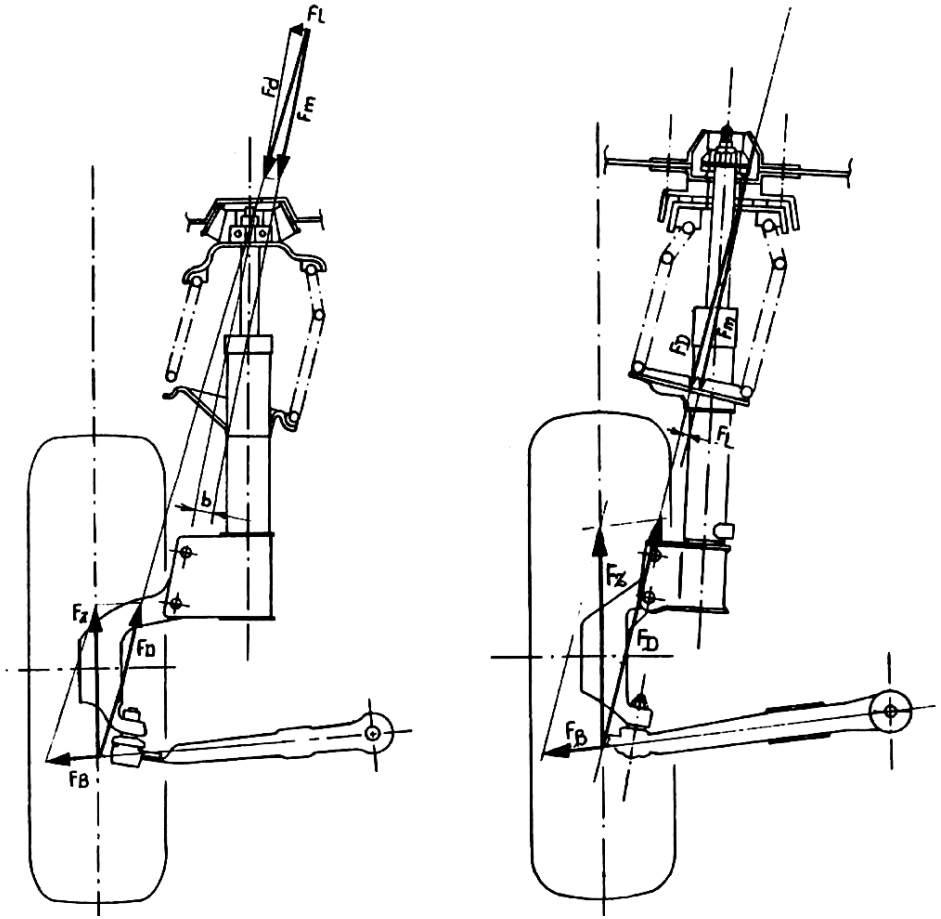

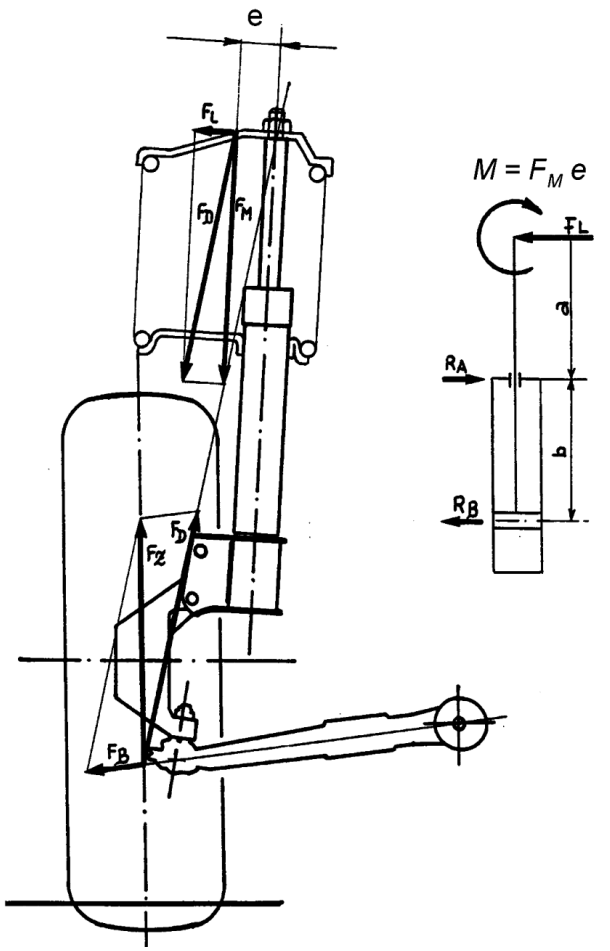

Co-funded by the
Erasmus+ Programme
of the European Union

SLOT 6: CONTROL SYSTEMS

- Height adjustment system control
- Regenerative Suspension control
- Active roll control

Co-funded by the
Erasmus+ Programme
of the European Union

Height Adjustment Suspension control

Co-funded by the
Erasmus+ Programme
of the European Union

Outline

- Why height adjustment systems in passenger cars?
- Industrial state of the art and possible new technologies/architectures.
- Key features of electromechanical height adjustment suspension systems.
- A case study.
- Conclusions.

Co-funded by the Erasmus+ Programme of the European Union

Motivations

FUEL CONSUMPTION AND gCO_2/km REDUCTION

C_x reduction only in extra urban - A Segment Car

- Improvements of vehicle accessibility
- Attitude modification according to vehicle load
- Off road attitude driving

2015 – 2020 → from 130 to 95 gCo2/km → -35 gCO2/km (NEDC)

Co-funded by the Erasmus+ Programme of the European Union

Pneumatic height adjustment system

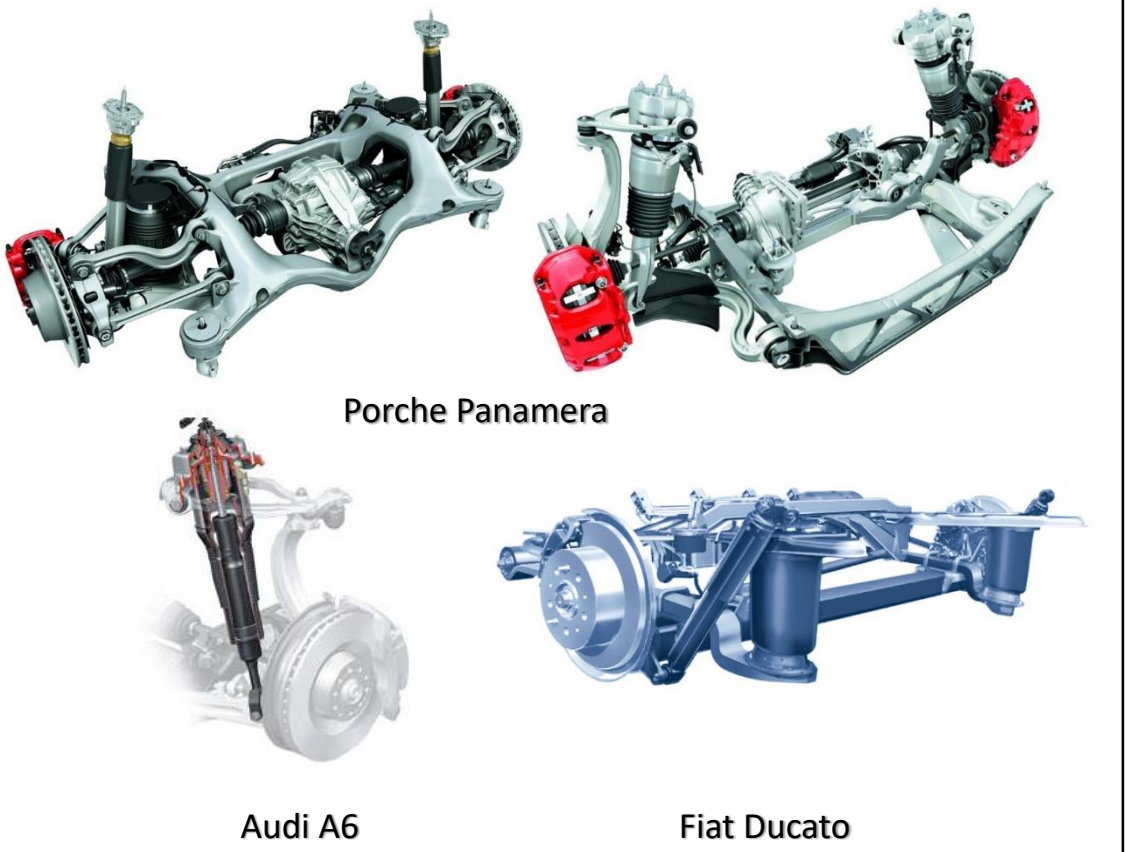

ZF Air suspension

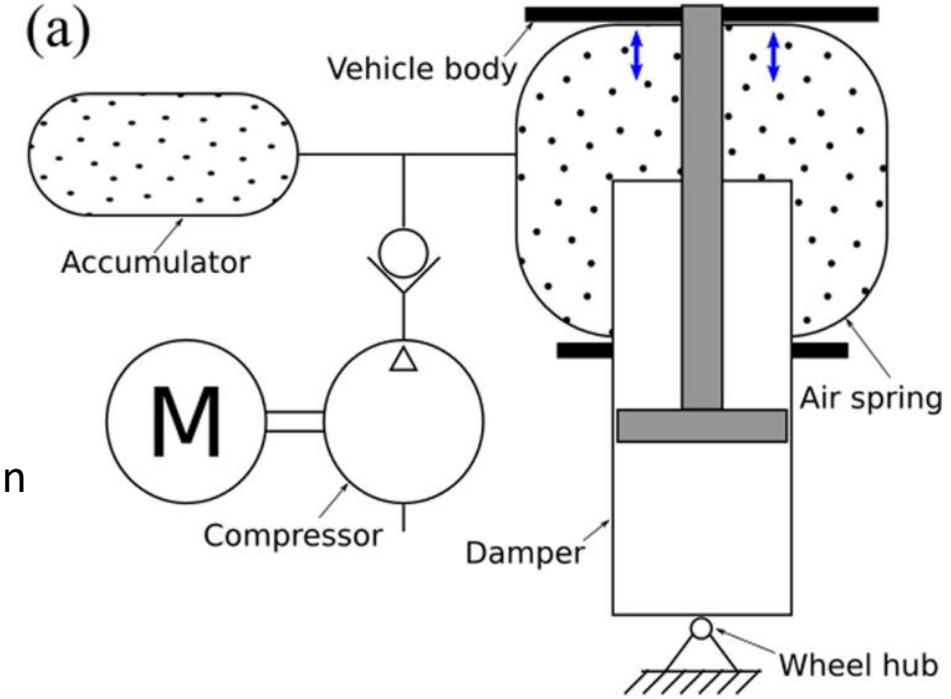

Co-funded by the Erasmus+ Programme of the European Union

Source: Porche, Audi, ZF and Amati

Hydraulic height adjustment system

Hydraulic Lower Plate Movimentation

Magneti Marelli S.P.A., US 2015/0028552 A1, **2015**

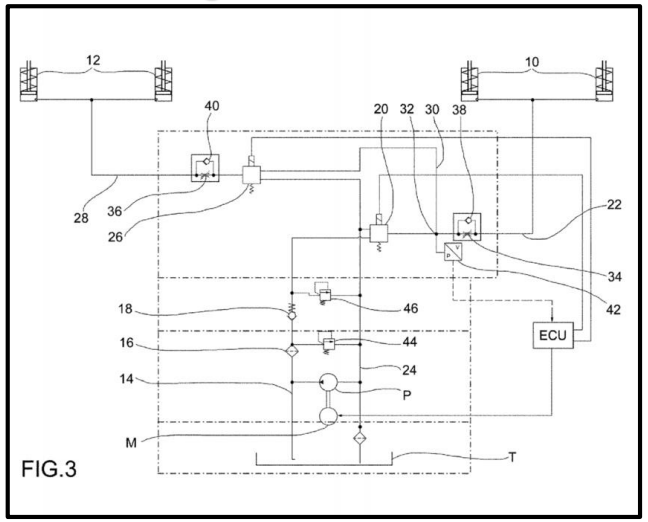

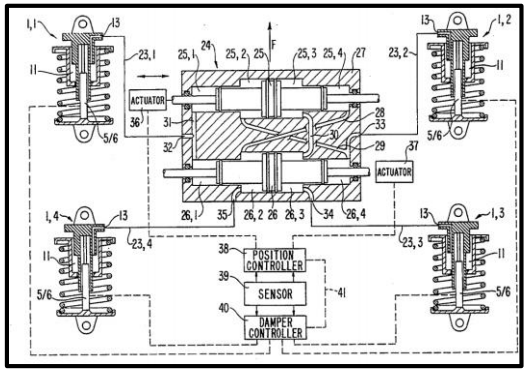

Hydraulic Upper Plate Movimentation

Mercedes, US 5401053A, **1995**

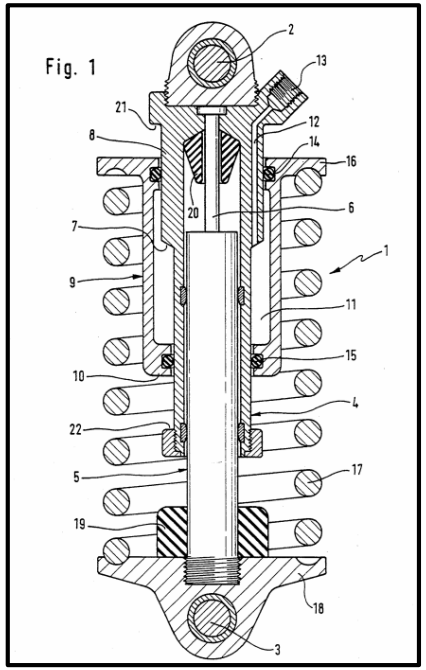

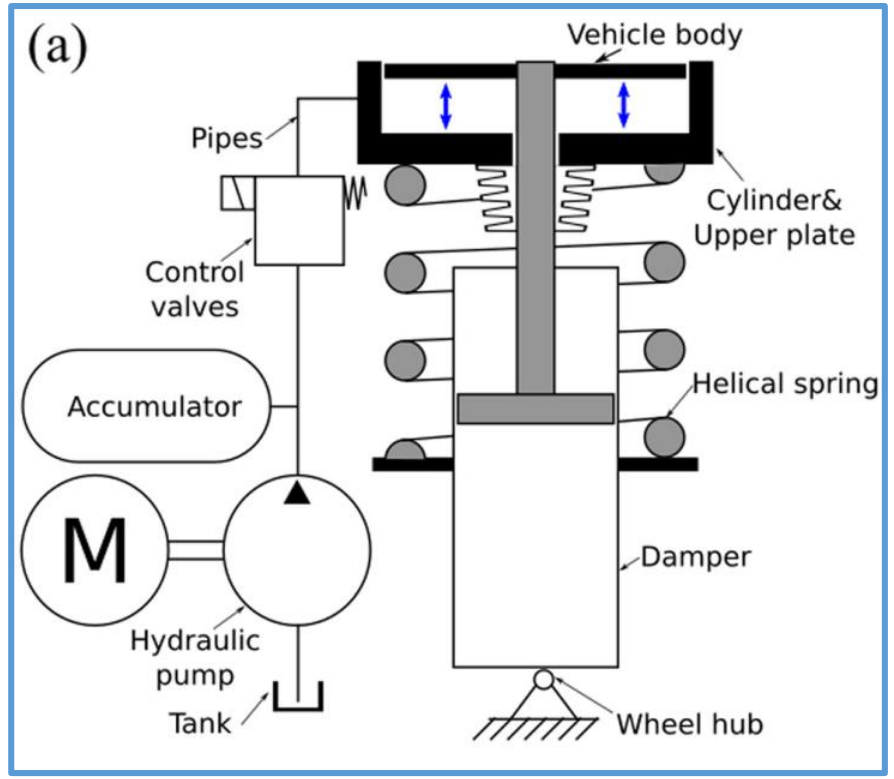

Co-funded by the
Erasmus+ Programme
of the European Union

Hydropneumatic height adjustment system

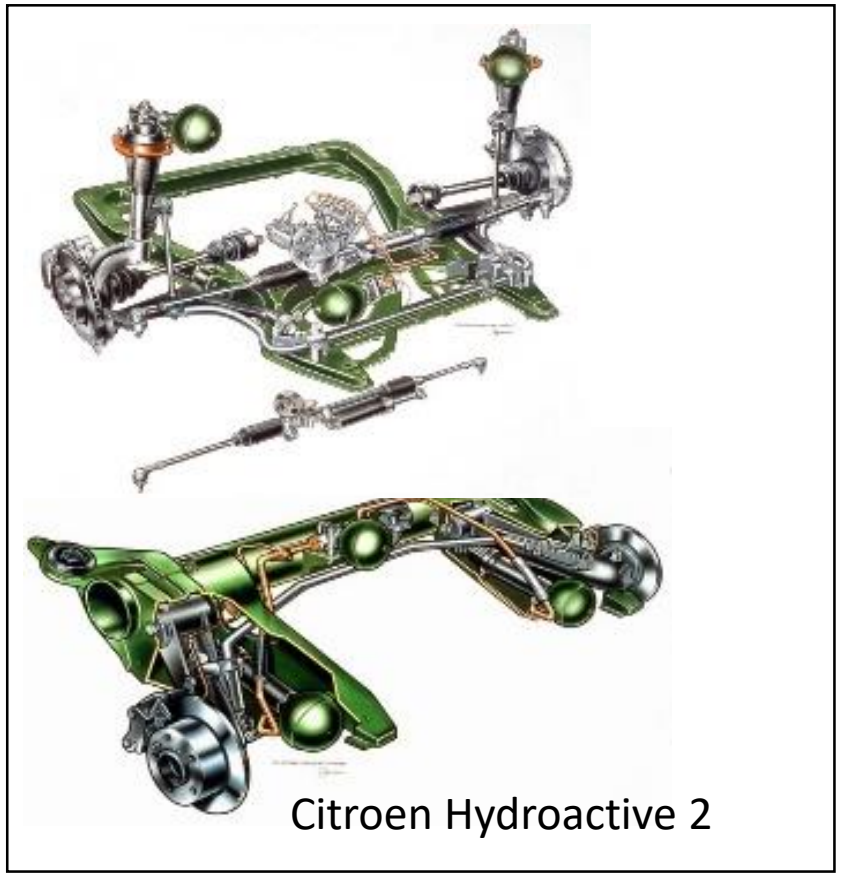
Citroen Hydroactive 2

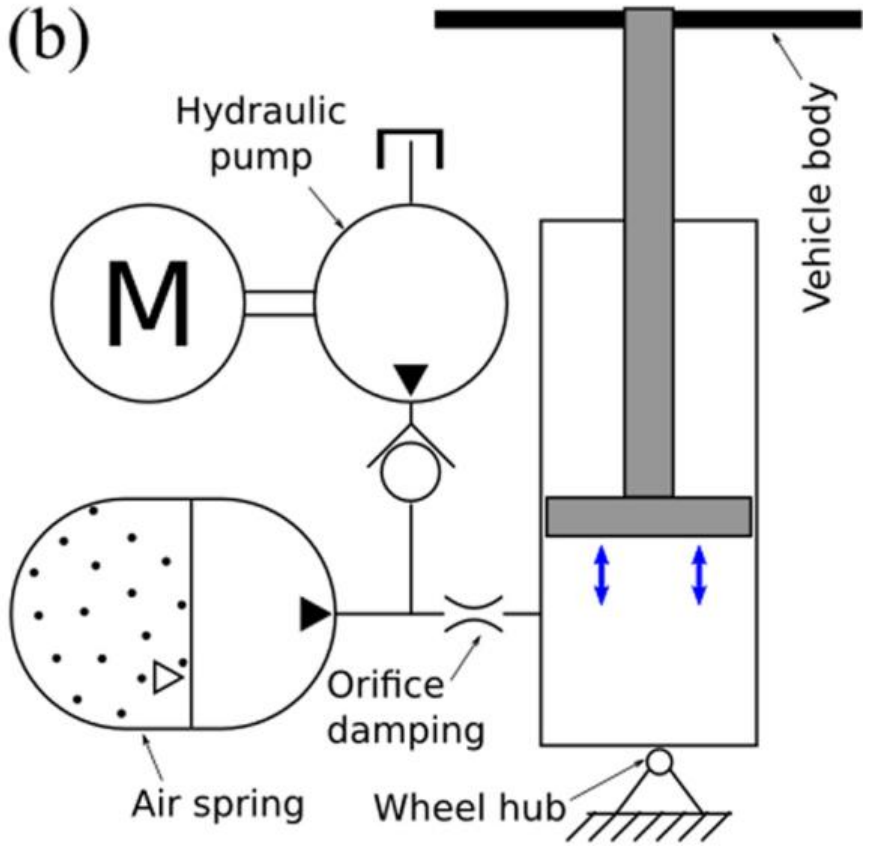

Co-funded by the Erasmus+ Programme of the European Union

Available Solutions on Market

HYDRAULIC SUSPENSIONS

AIR SUSPENSIONS

HYDROPNEUMATIC SUSPENSIONS

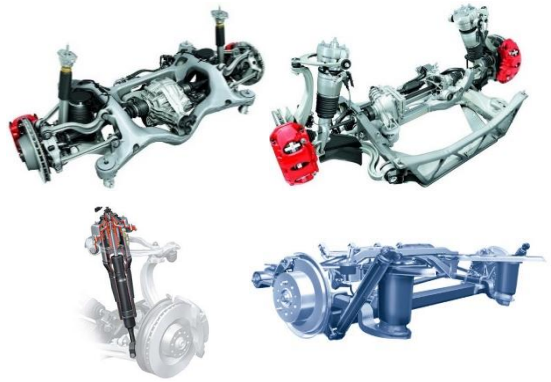

- **System complexity and high cost;**
- **Large space needed, not suitable for compact vehicles;**
- **Air spring works in parallel with shock absorber (defined travel);**
- **High segment cars.**

Co-funded by the Erasmus+ Programme of the European Union

Electromechanical height adjustment system

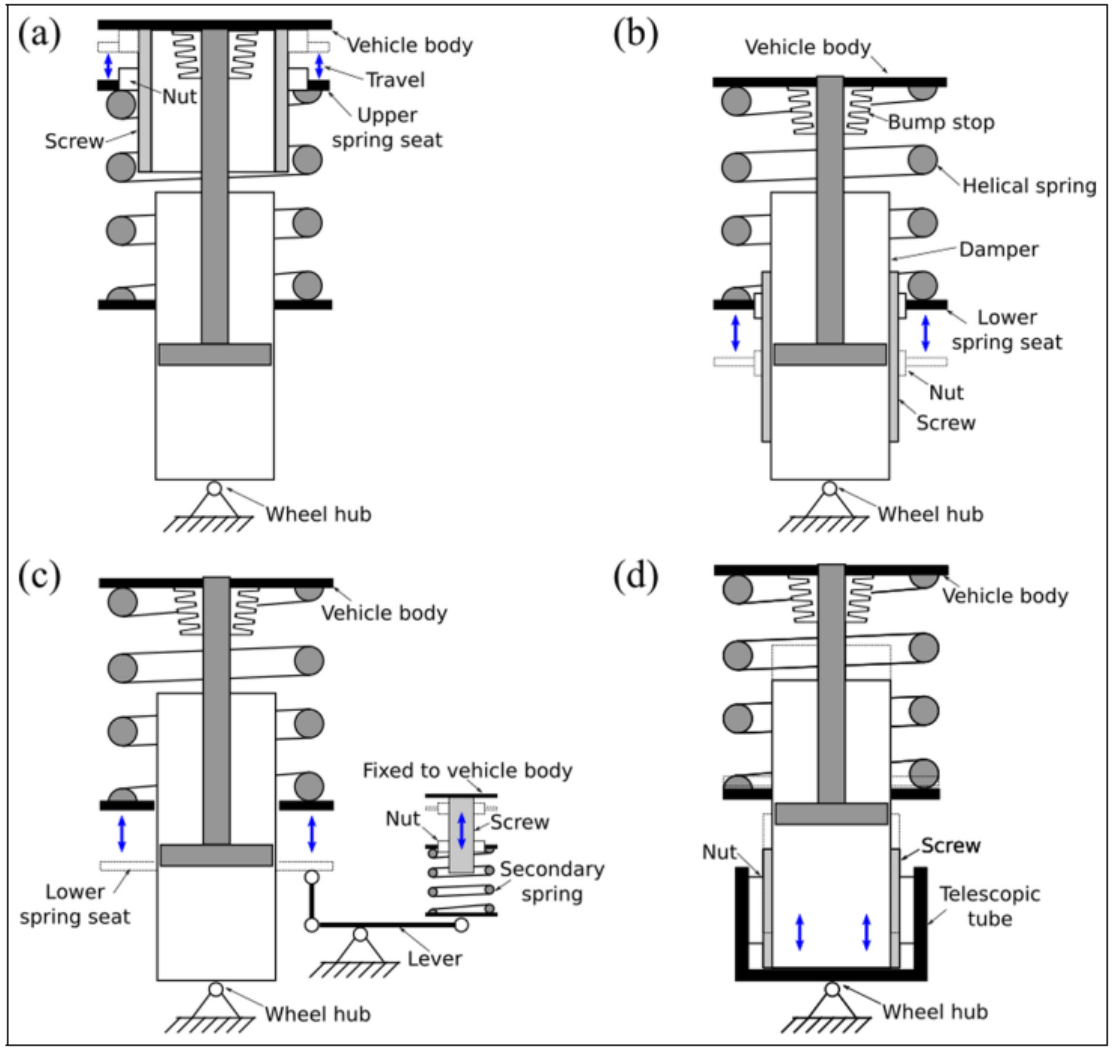

- **System simplicity;**
- **Relatively lower cost;**
- **Compact sizes;**
- **Modularity;**
- **High relaibility;**
- **Low segment cars.**

Co-funded by the Erasmus+ Programme of the European Union

Possible Configurations: Motion of lower plate

- **Mechanical Direct Lower Plate Movimentation**
  - Audi AG, US 2009/0146385A1, **2009**

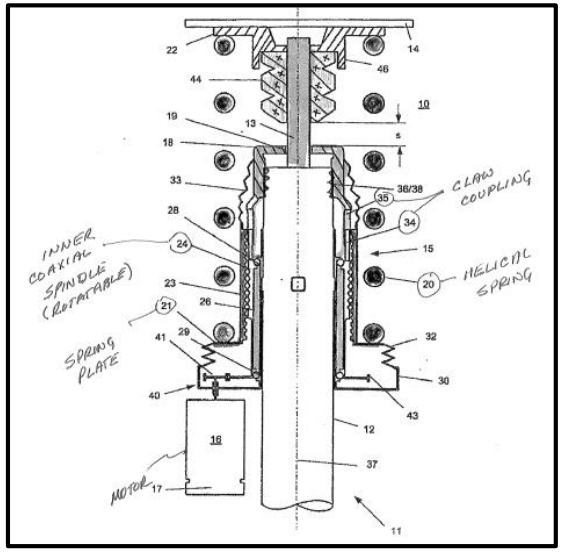

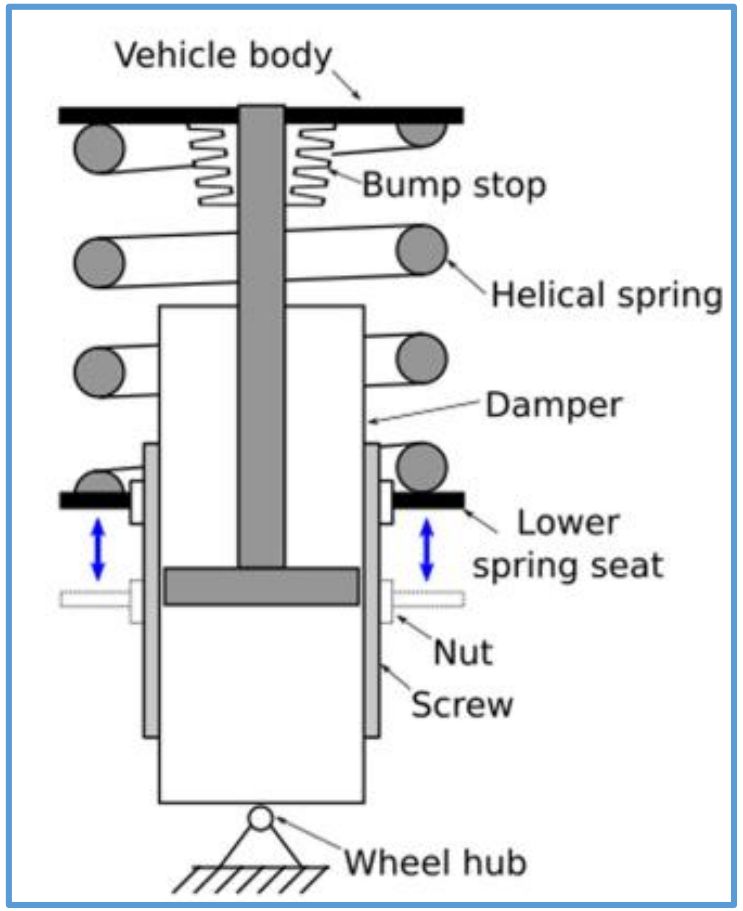

Co-funded by the Erasmus+ Programme of the European Union

Possible Configurations: Motion of lower plate

- **Lower Plate Movimentation with Leverages**
  - Audi AG, US 8317003B2, **2012**
  - Audi AG, EP 2199121B1, **2014**

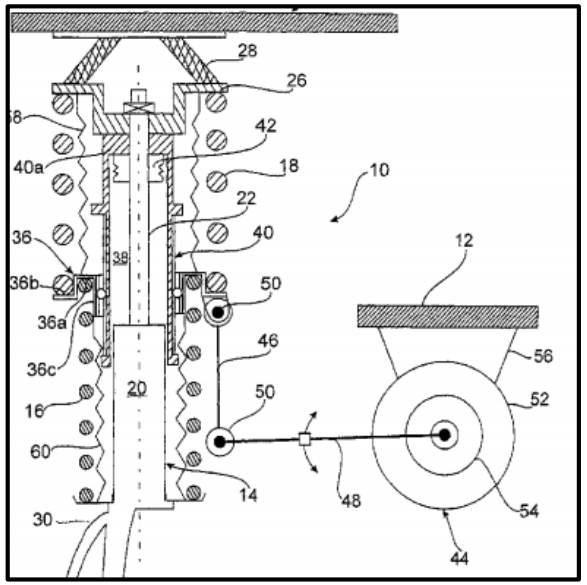

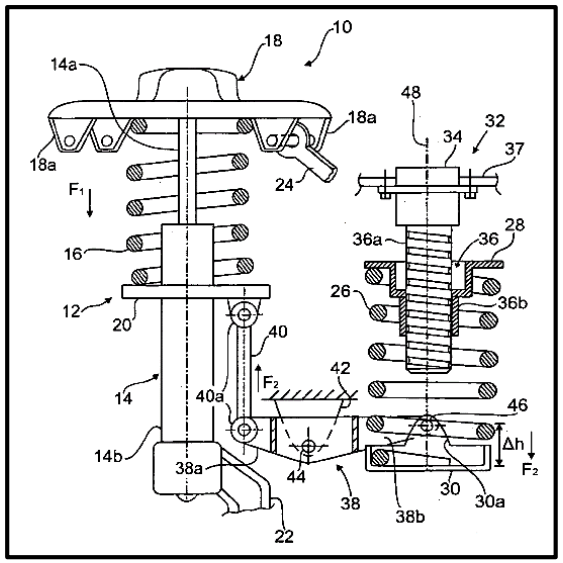

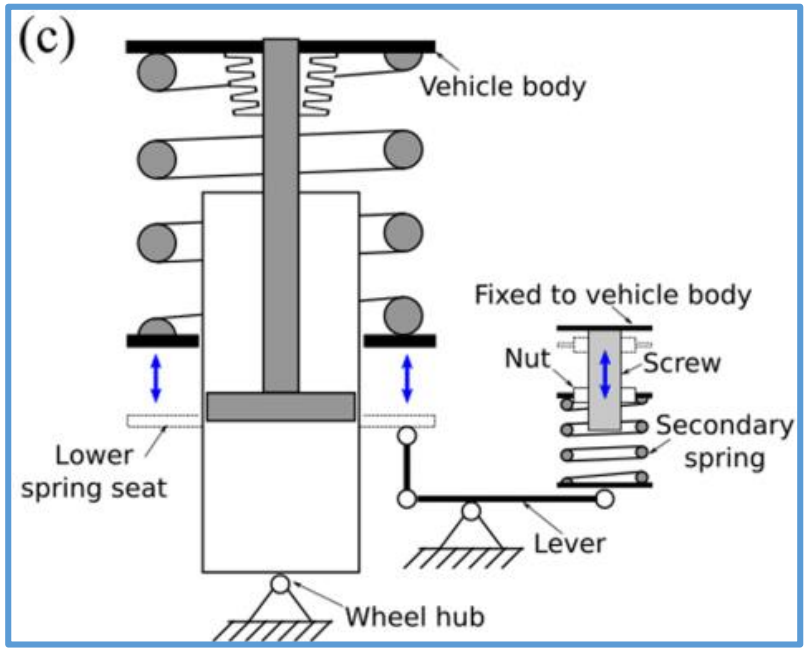

Co-funded by the Erasmus+ Programme of the European Union

Possible Configurations: Motion of the upper plate

- **Mechanical Upper Plate Movimentation**
  - Audi AG, EP 1970227A2, **2007**
  - Honda, US7922181B2, **2011**

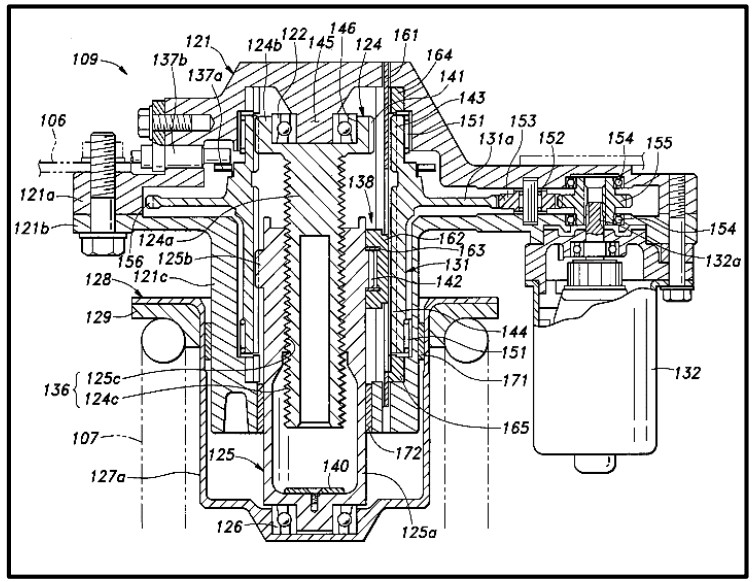

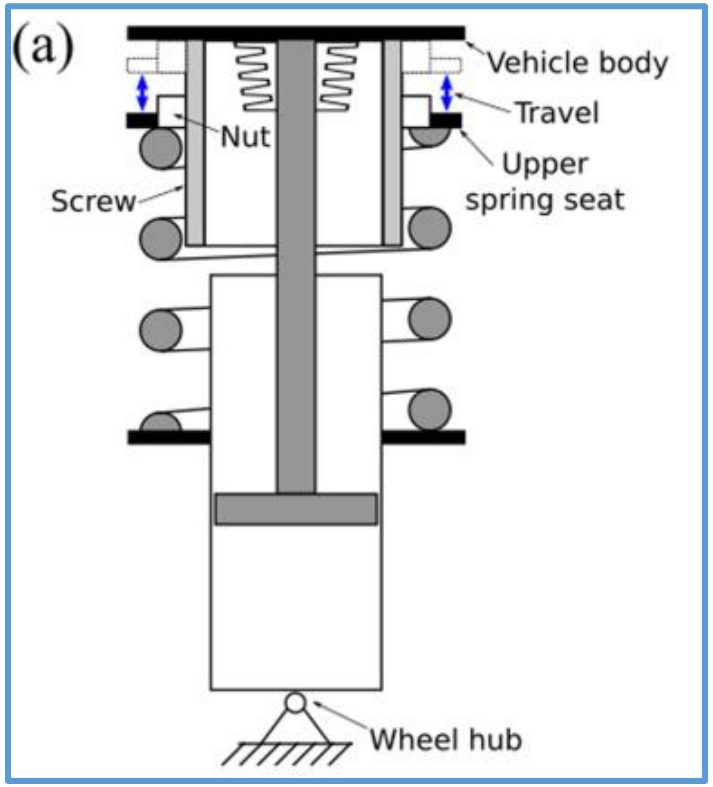

Co-funded by the
Erasmus+ Programme
of the European Union

Possible Configurations

- **Shock Absorber Tube Movimentation**
  - Hyundai, US 8833775B2, **2014**

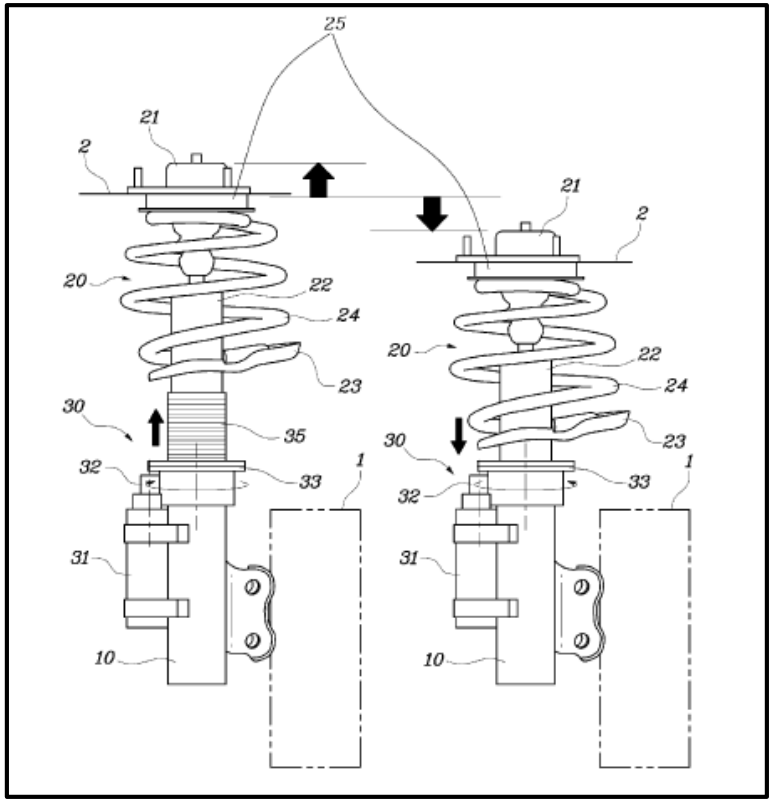

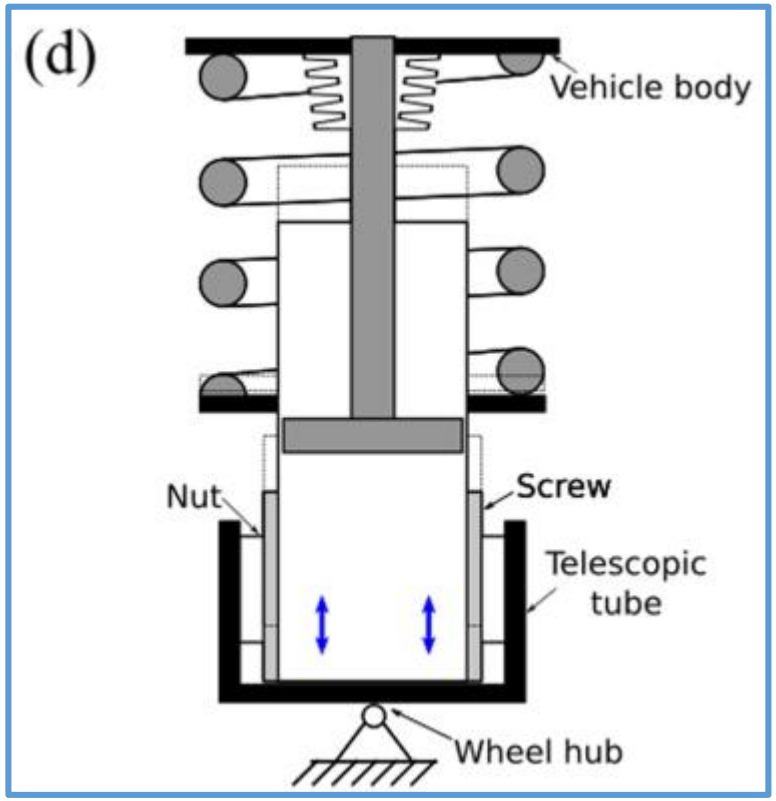

Co-funded by the Erasmus+ Programme of the European Union

Summary

Type / Features	Efficiency	Mechanical Complexity	Packaging	Additional Mass (S/US)	Modifications of suspension characteristics	Attitude for Slow active	Score
Spring holder, Mechanical	★	★★★	★ ★	US	★ ★	no	8
Lower Plate, Hydraulic	★ ★	★ ★	★	US	★ ★	yes	7
Spring holder, eccentric actuation	★ ★	★ ★	★	US	★ ★	no	7
Upper Plate, Mechanical	★ ★	★	★	S	★ ★	no	6
Upper Plate, Hydraulic	★ ★	★ ★	★	S	★ ★	yes	7
S.A. Tube	★	★	★ ★	US	★★★	no	7

Co-funded by the Erasmus+ Programme of the European Union

Proposed Solution: Front

- **Basic Idea:**
  - **Lower/rise the spring lower plate by an electromechanical actuator**
  - **The end stops location is not modified:**
    - **Global suspension stroke is not modified**
    - **No end stop loads on the mechanism**
    - **Comfort issues due to a different zero position with respect to the global stroke**

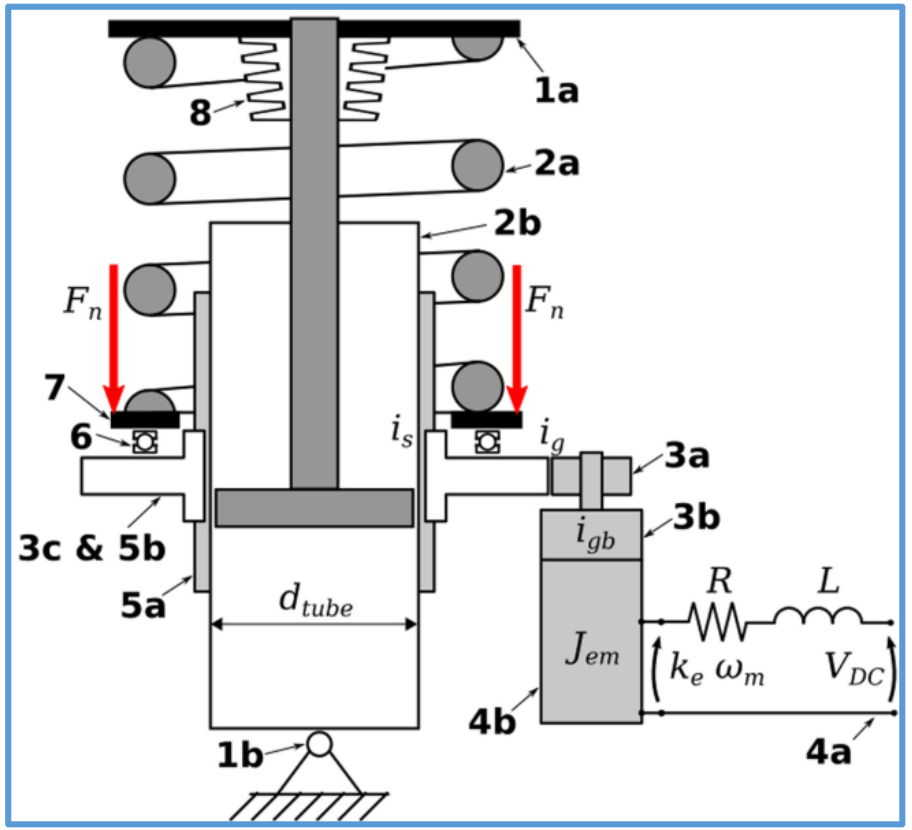

Co-funded by the Erasmus+ Programme of the European Union

Proposed Solution: Rear

- **Basic Idea:**
  - **Lower/rise the spring lower plate by an electromechanical actuator**
  - **The end stops location is not modified:**
    - **Global suspension stroke is not modified**
    - **No end stop loads on the mechanism**
    - **Comfort issues due to a different zero position with respect to the global stroke**

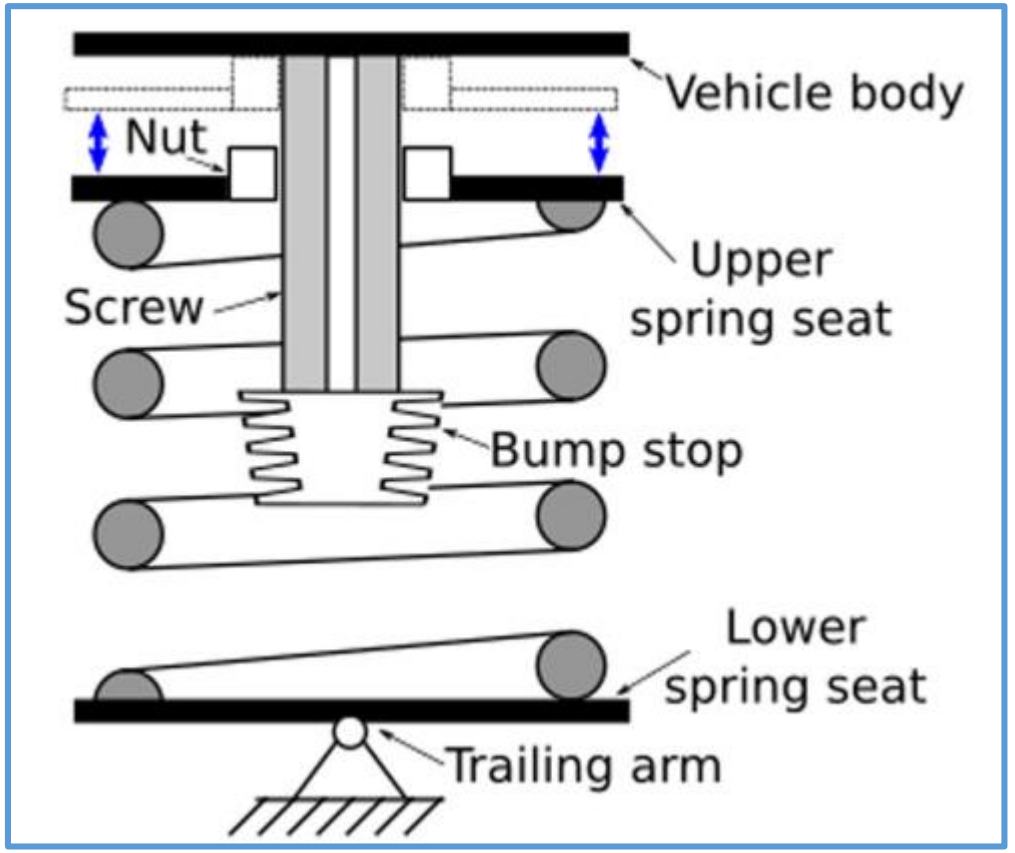

Co-funded by the Erasmus+ Programme of the European Union

Design Procedure

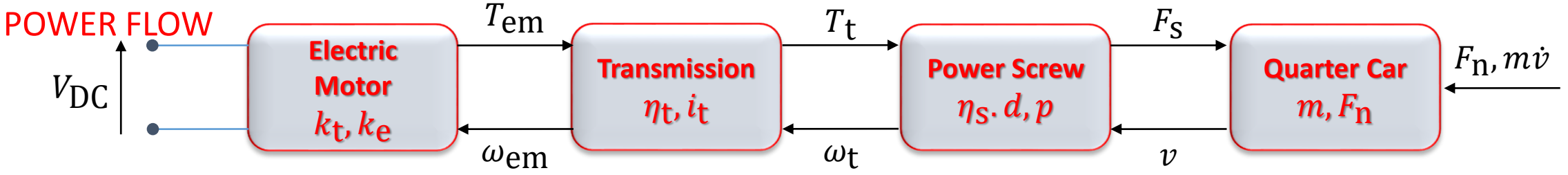

- Performance Definition
  - Stroke length - s [mm]
  - Actuation time - t [s]
  - Load - F_n [N]
  - Max total power - P_{max} [W]
- EM Power Computation

$$\begin{Bmatrix} \dot{\omega}_{em} \\ \omega_{em} \\ \dot{I} \end{Bmatrix} = \begin{bmatrix} 0 & 0 & \frac{k_t}{J_{eq}} \\ 1 & 0 & 0 \\ -\frac{k_e}{L} & 0 & -\frac{R}{L} \end{bmatrix} \begin{Bmatrix} \omega_{em} \\ \theta_{em} \\ I \end{Bmatrix} + \begin{bmatrix} 0 & -\frac{1}{J_{eq}} \\ 0 & 0 \\ \frac{1}{L} & 0 \end{bmatrix} \begin{Bmatrix} V_{DC} \\ T_r \end{Bmatrix}$$

$$P_{req,EM} = \frac{F_n}{\eta_{tot}} \cdot \frac{s}{t}$$

- Transmission efficiency can be estimated
- Screw efficiency can be computed as a function of different values of diameter and pitch

Co-funded by the Erasmus+ Programme of the European Union

Design Procedure

VARIABLES COMPUTATION

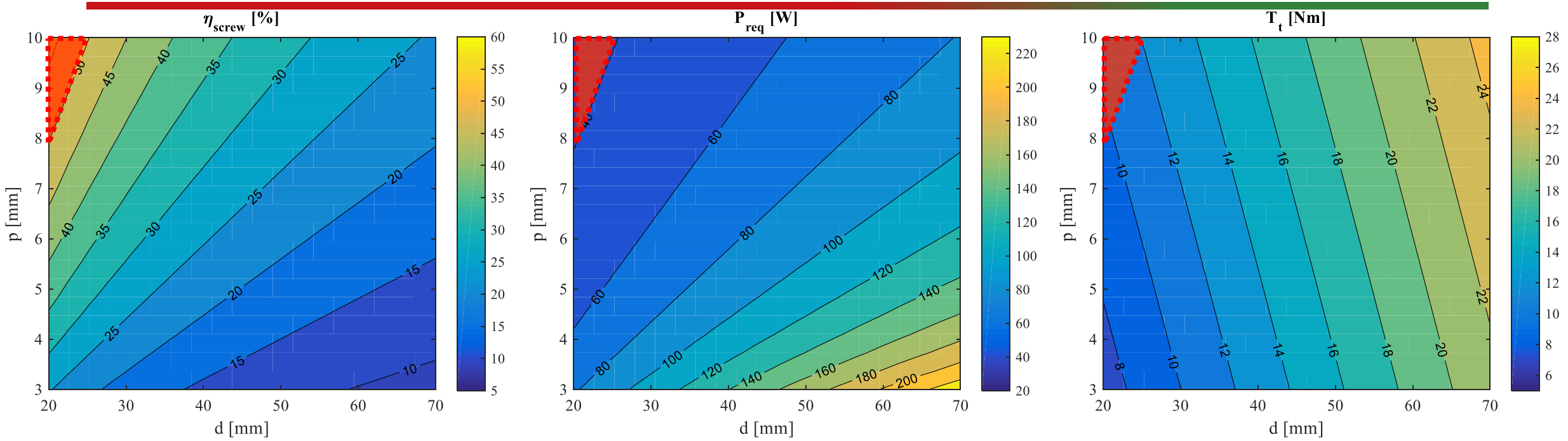

- The larger the diameter, the smaller is the efficiency. Power and required torque increase;
- Selection of the electric motor power;
- Selection of the transmission reduction ratio.

Irreversibility Constraint

Co-funded by the Erasmus+ Programme of the European Union

Design Procedure

OPTIMIZATION PROBLEM – Front Suspension (McPherson)

Constraints

$$\begin{cases} \eta_s < 50\% \\ d_{in,s} > d_{tube} \\ i < i_{th} \\ t_{50\,mm} < t_{max} \end{cases}$$

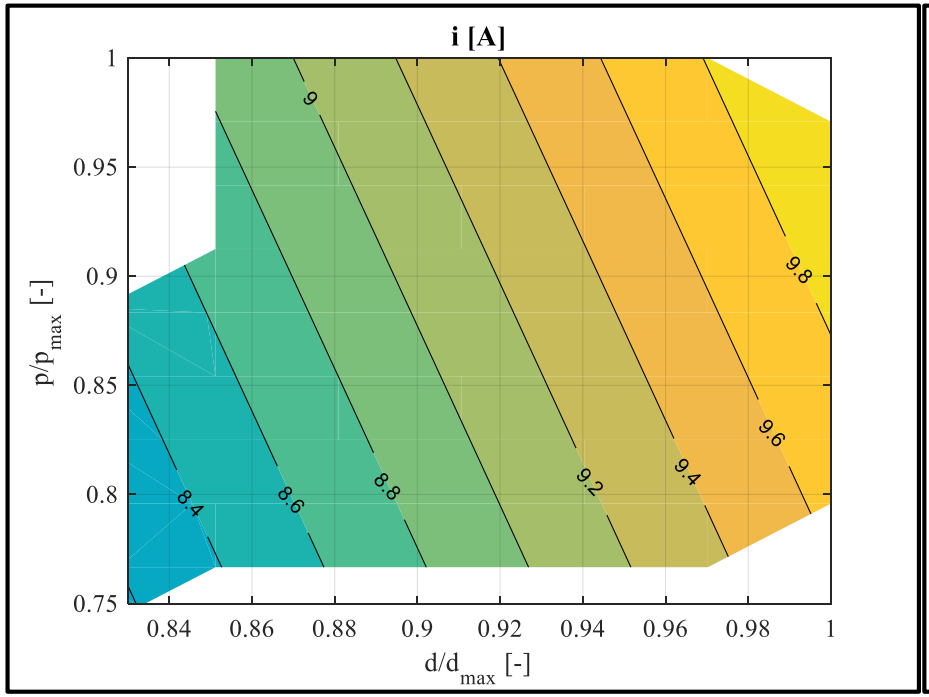

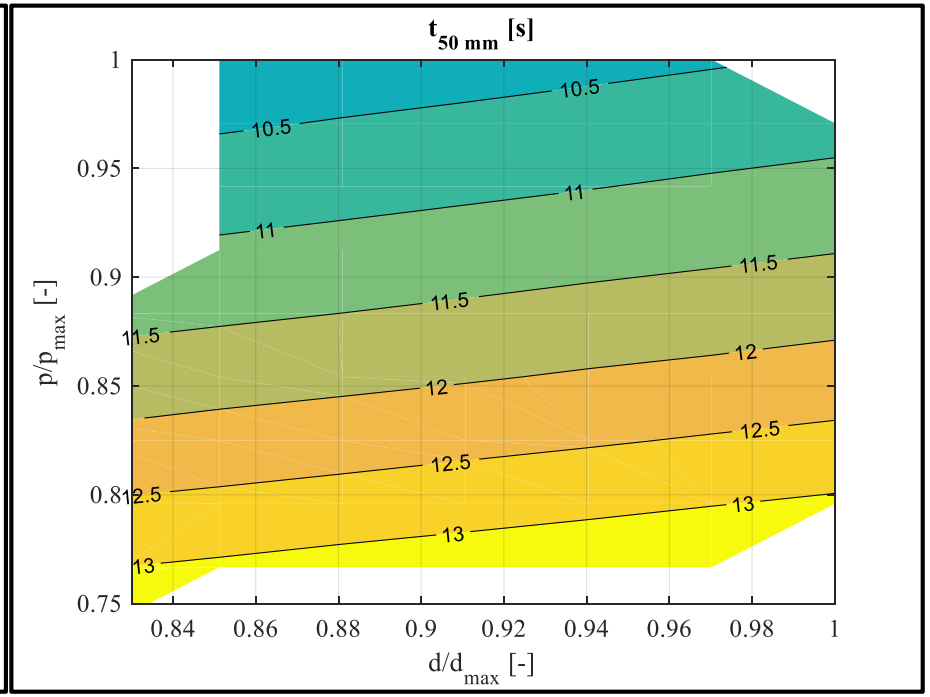

Co-funded by the Erasmus+ Programme of the European Union

Prototype Design

Front Suspension (McPherson)

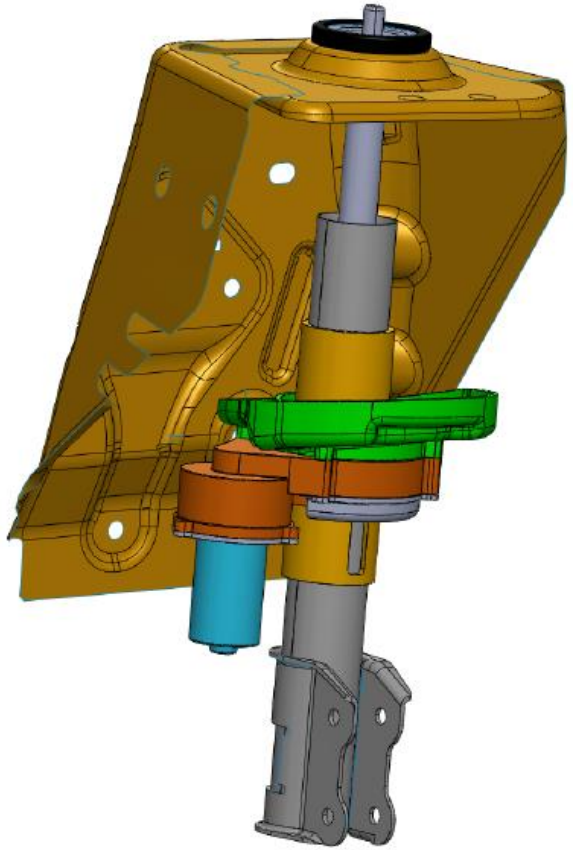

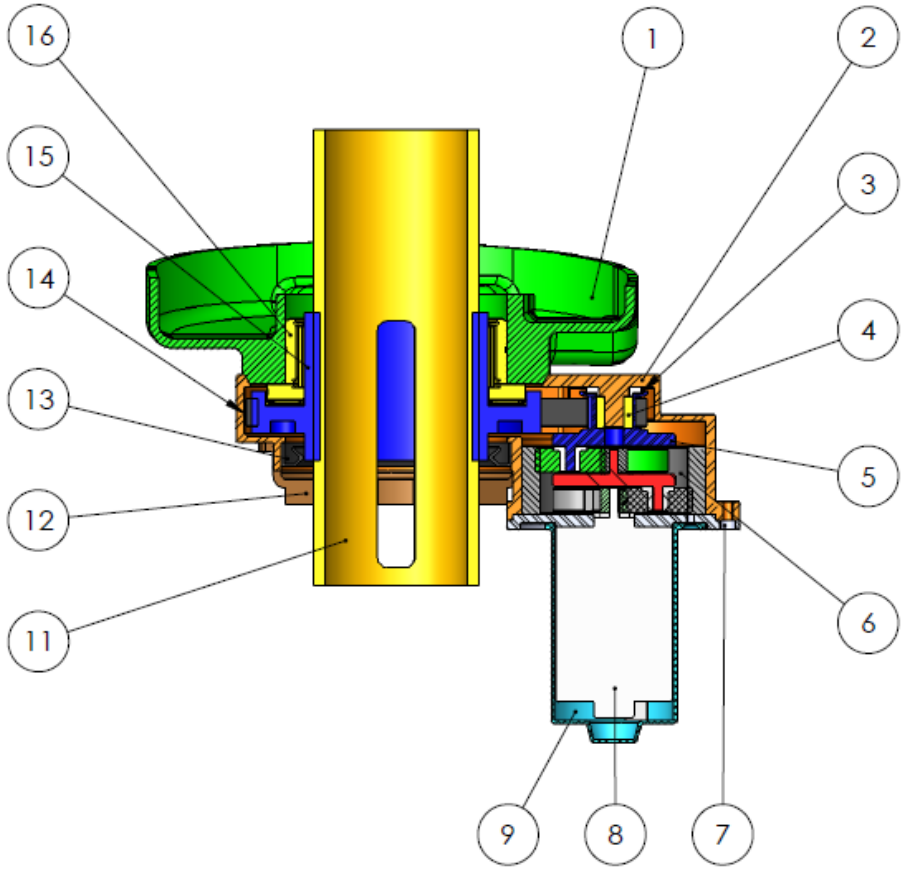

ITEM NO.	PART NUMBER	QTY.
1	Spring holder	1
2	Motor support	1
3	Pulley bushing	1
4	Needle bearing	1
5	Small pulley+carrier	1
6	Geartrain assembly	1
7	Motor support cover	1
8	DC electric motor	1
9	Motor cover	1
10	Shock absorber tube	1
11	Power screw	1
12	Anti rotation system	2
13	Sealing ring	1
14	Timing HTD Belt	1
15	Large pulley	1
16	Combined bearing	1

Co-funded by the Erasmus+ Programme of the European Union

Rear Suspension

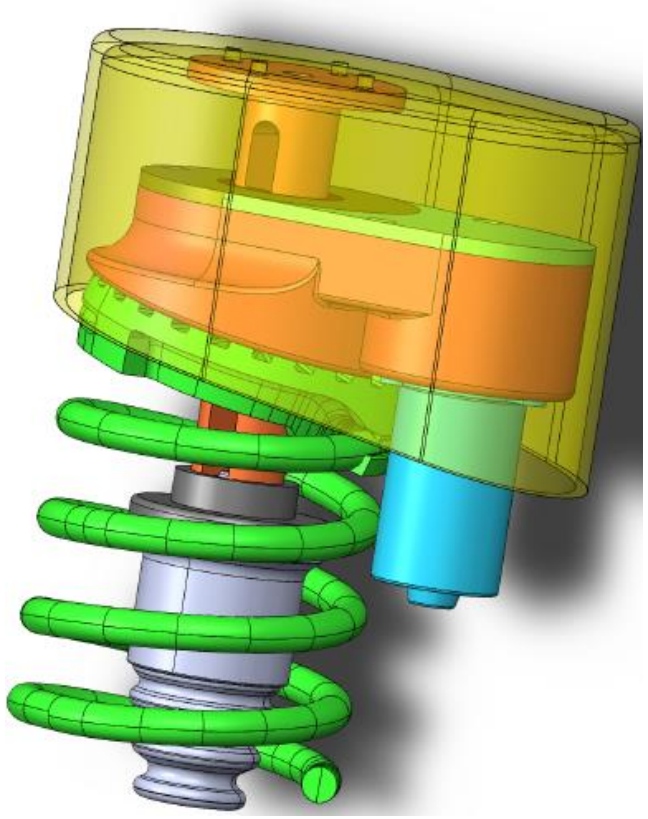

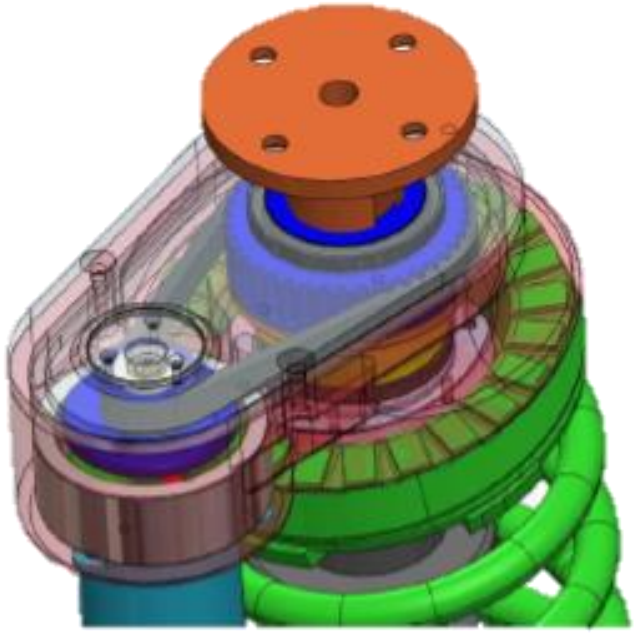

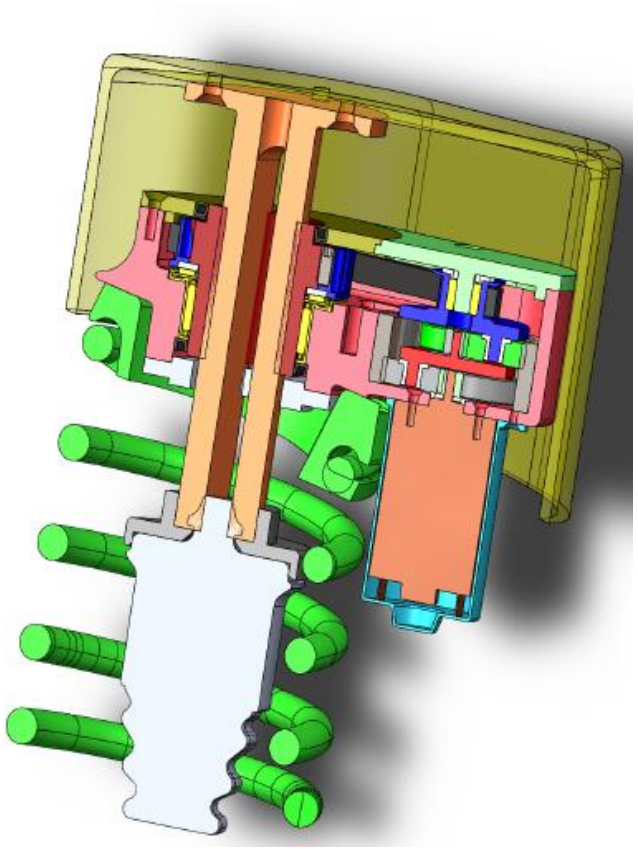

Co-funded by the
Erasmus+ Programme
of the European Union

Prototype Construction

Front Suspension Components

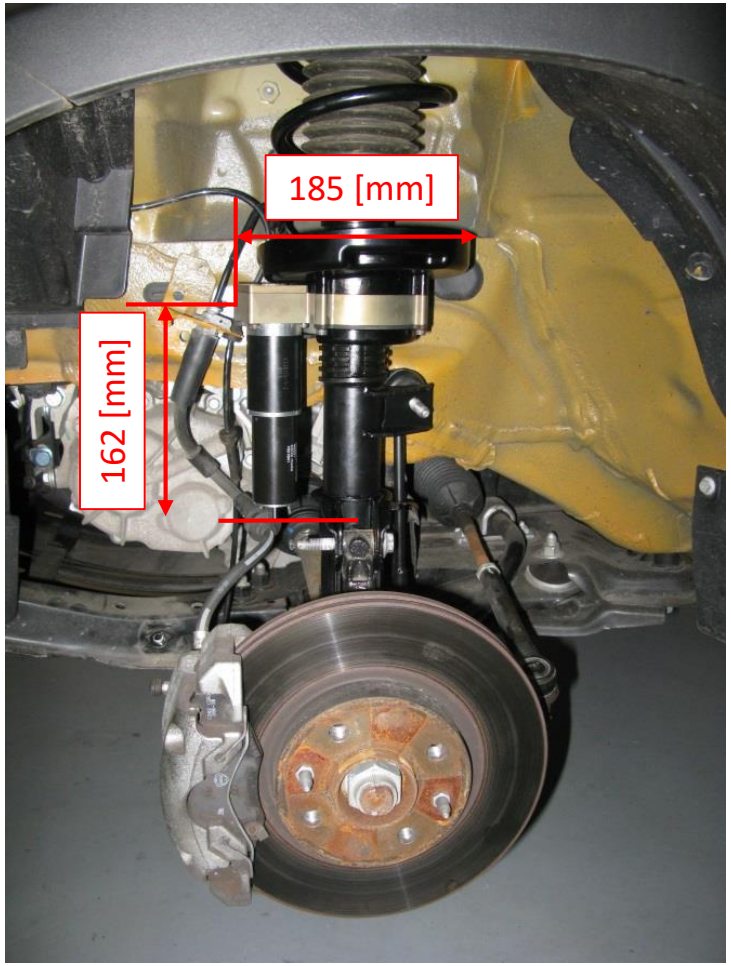

- Total added mass= 2.2 kg (unsprung mass)

Co-funded by the Erasmus+ Programme of the European Union

Prototype Construction

Rear Suspension Components

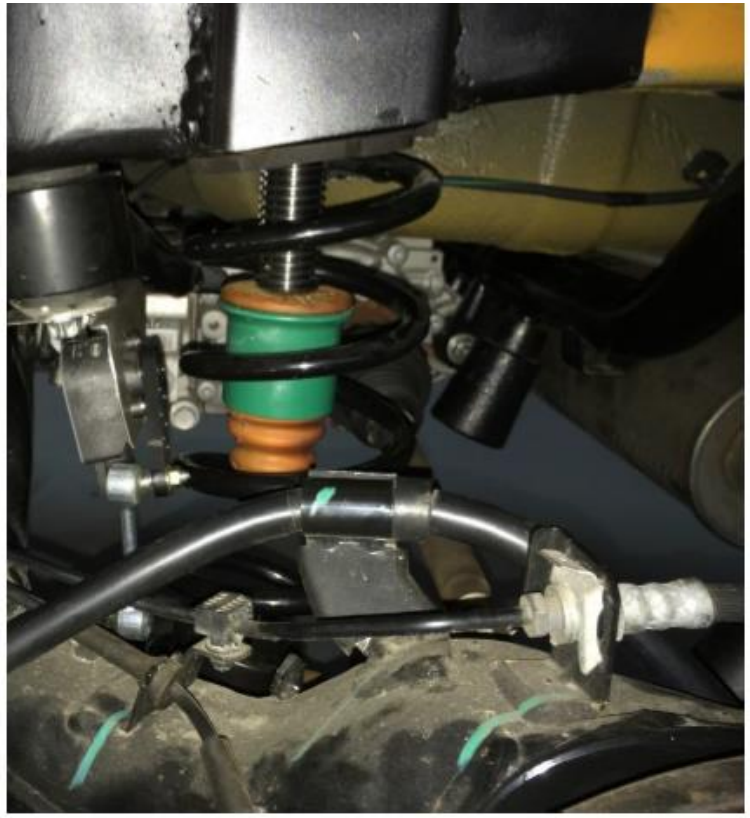

- Total added mass= 2.1 kg (sprung mass)

Co-funded by the
Erasmus+ Programme
of the European Union

Experimental Validations

Front Suspension Current Absorbtion

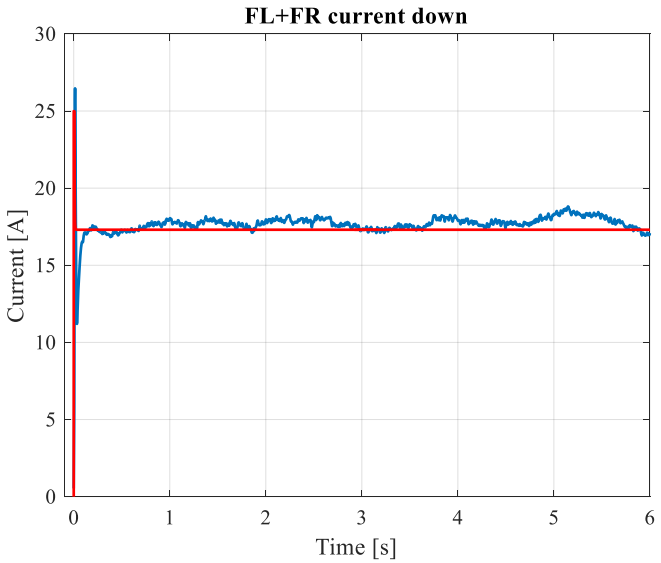

$$i_{mean} = 17\ A$$
$$P_{mean} = 200\ W$$

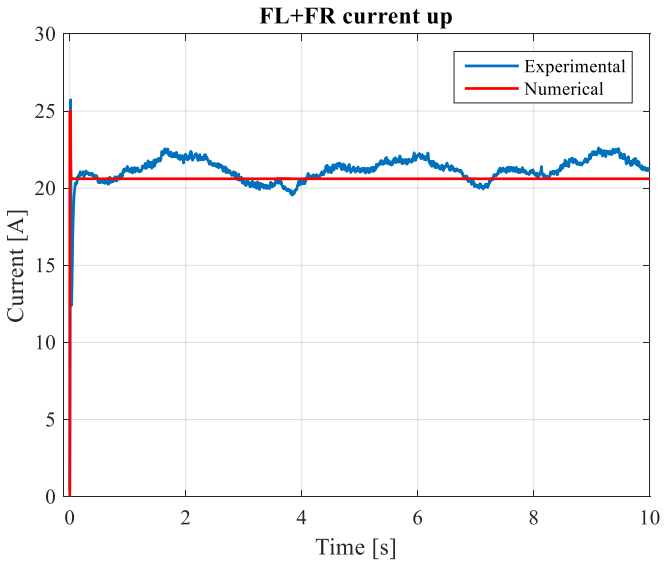

$$i_{mean} = 21\ A$$
$$P_{mean} = 250\ W$$

Co-funded by the Erasmus+ Programme of the European Union

Conclusions

- Height adjustment suspension systems seem to be promising technologies to reduce fuel consumptions and emissions, adding features like off road attitude and accessibility;
- Electromechanical actuation systems show the best compromise between benefits and cost in height adjustment devices;
- Integrated design is needed to achieve a compromise between size, weight and energy consumption;
- Experimental tests carried out on a prototype highlighted critical issues like screw efficiency, anti-rotation devices and packaging;
- Eccentric actuation seems a good compromise in terms of efficiency, robustness and packaging

Co-funded by the Erasmus+ Programme of the European Union

Improvements

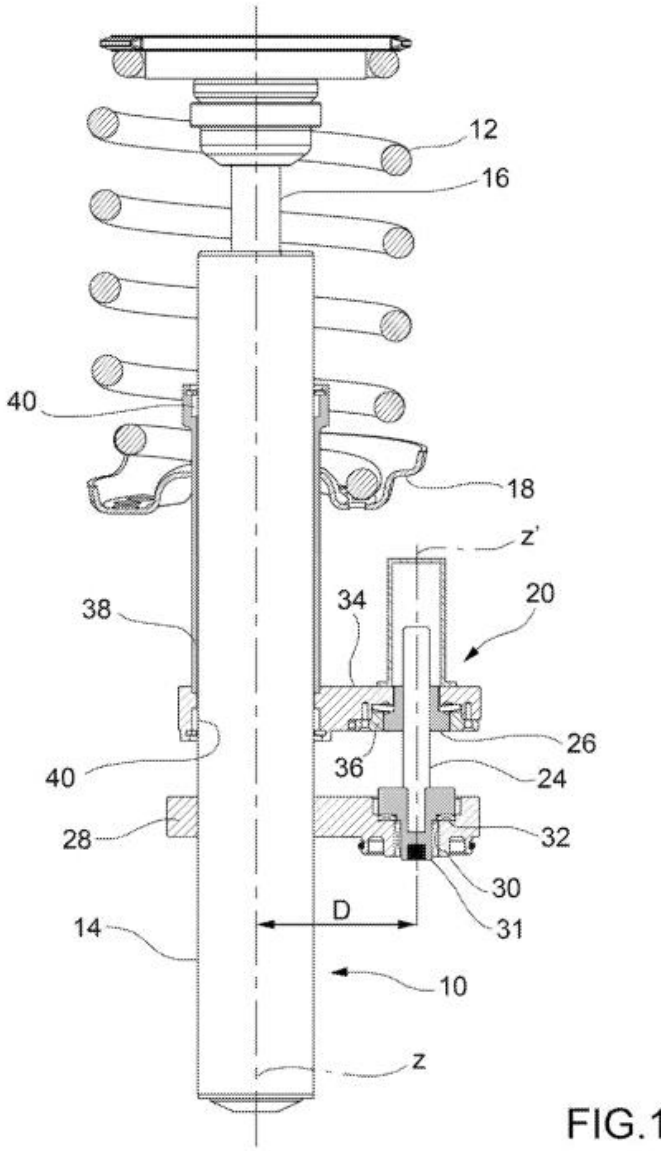

FIG.1

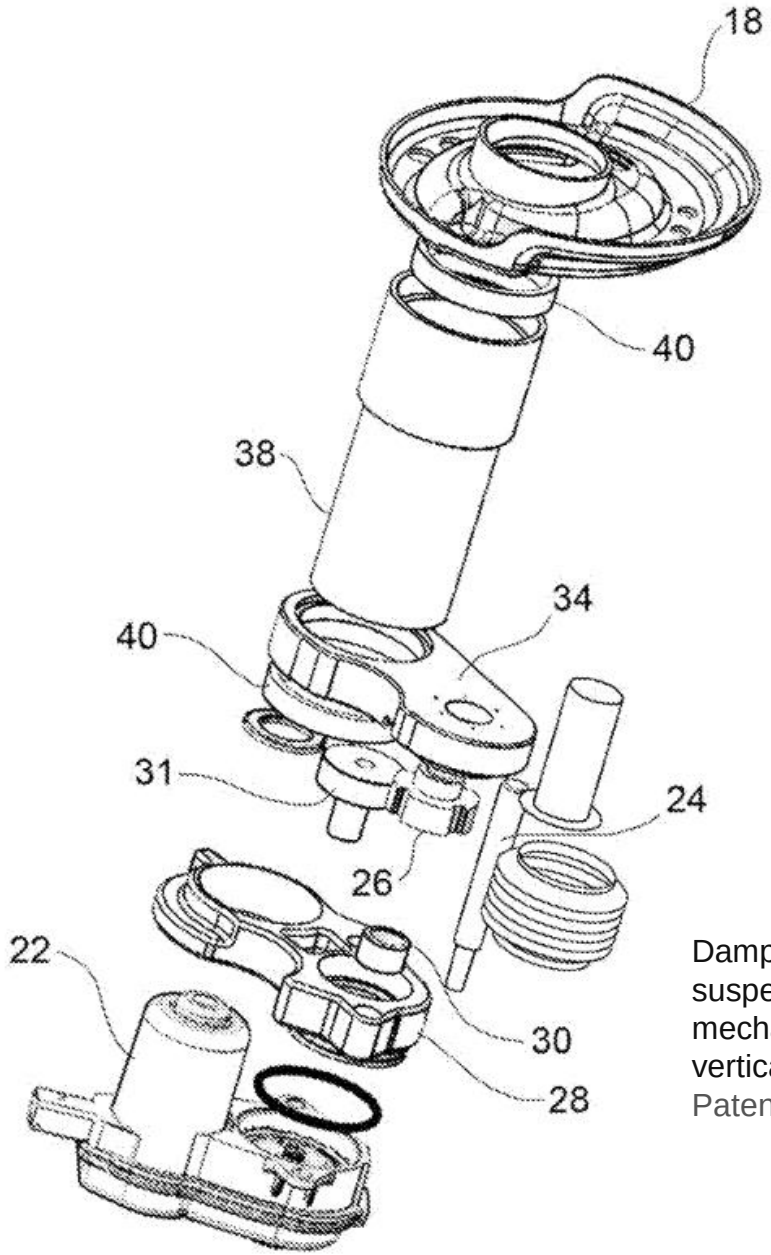

Damper and spring unit for a vehicle suspension provided with an electro-mechanical adjustment device for adjusting the vertical position of the spring

Patent: WO2019097461A1

Co-fun
Erasmus+ F
of the European Union

Regenerative Suspension control

Co-funded by the
Erasmus+ Programme
of the European Union

Classification of electromagnetic dampers

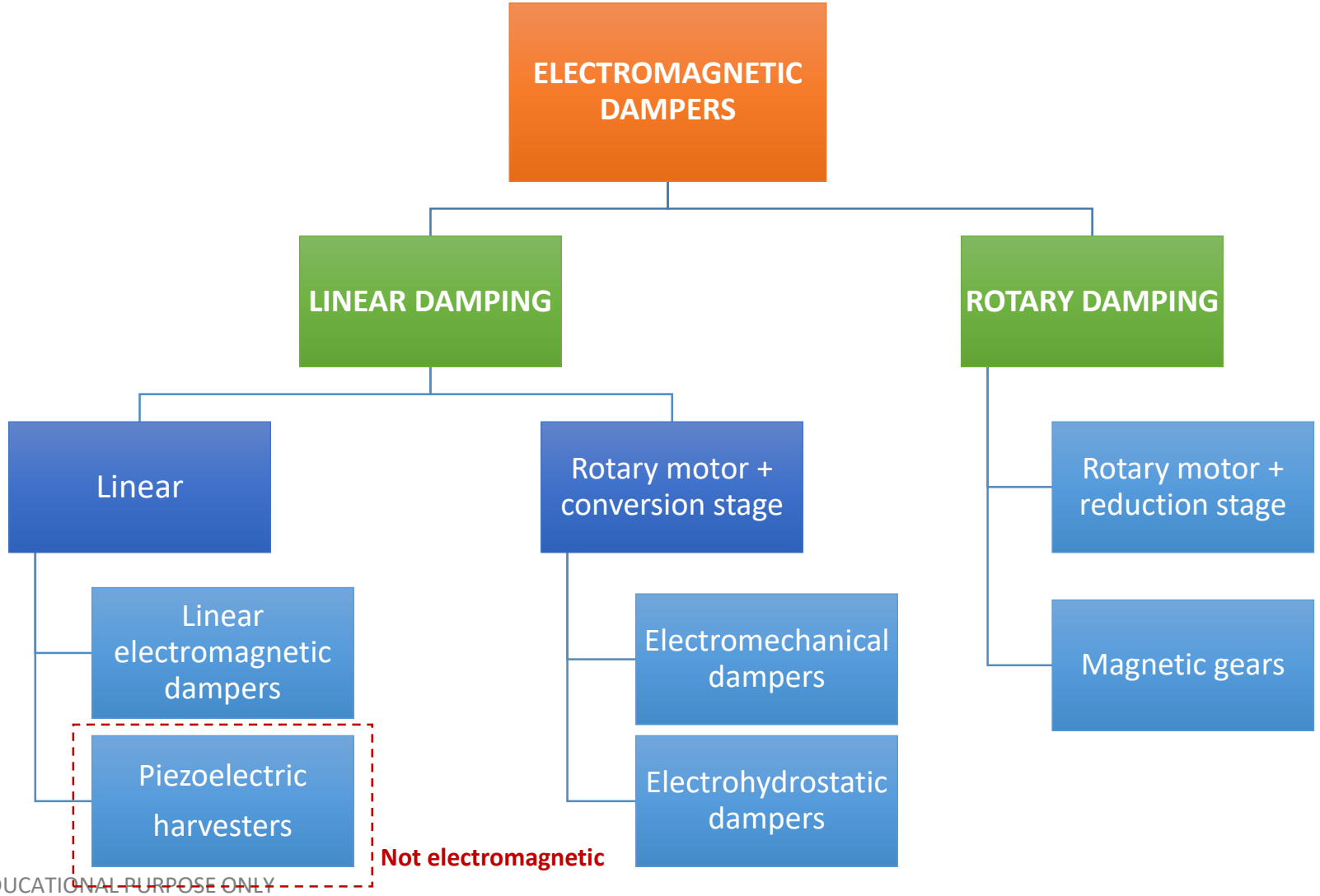

Co-funded by the Erasmus+ Programme of the European Union

Linear Electromagnetic Dampers

Ebrahimi et al. propose a linear damper with low power density, since 80% of the damping is attained through passive means, while the remaining 20% is active electromagnetic damping.

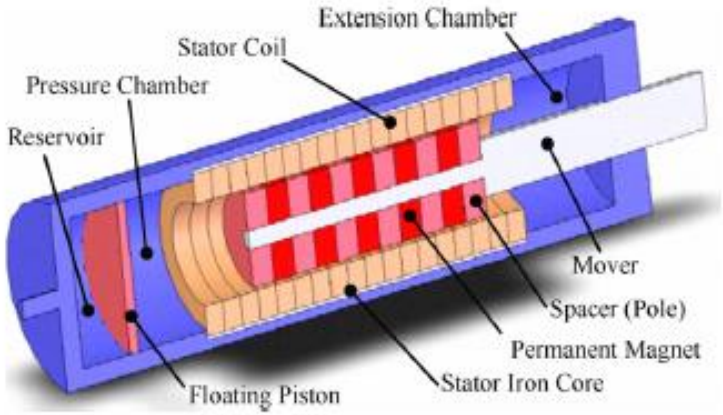

Paulides et al. propose a linear damper to use in parallel to a dissipative element. They are able to yield a RMS force of 1 kN and 2.5 kN of peak force. The device demands 40-50 W of electric power due to active control.

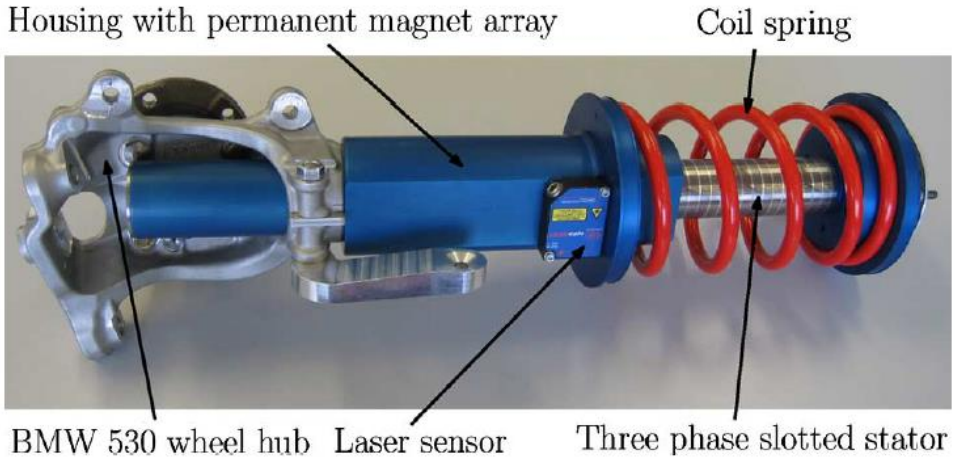

Co-funded by the Erasmus+ Programme of the European Union

Piezoelectric Harvesters

Hyundai patented a piezoelectric array solution to install on the spring coils and harvest power from their linear motion. They do not provide information on the harvested power

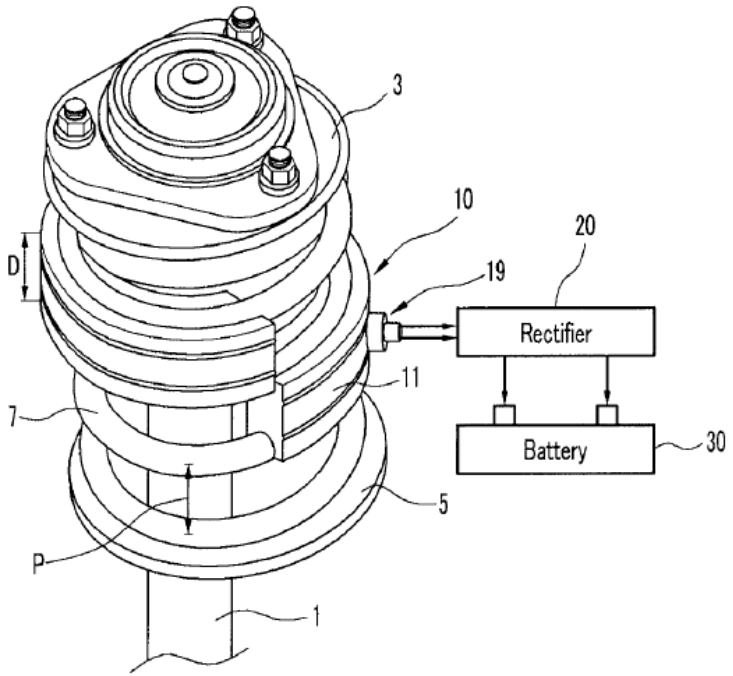

Xie and Wang suggest the introduction of a piezoelectric bar between the sprung mass and the suspension lower arm to harvest energy from suspension motion. With one bar of 15x15x100 mm, the device can harvest a RMS power of 738 W running through ISO D profile at 35 km/h.

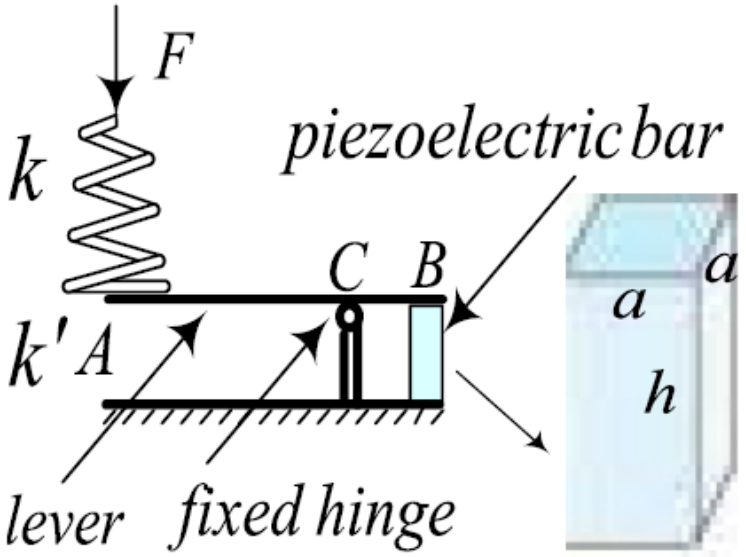

Co-funded by the Erasmus+ Programme of the European Union

Electromechanical Dampers

Ball screw solutions

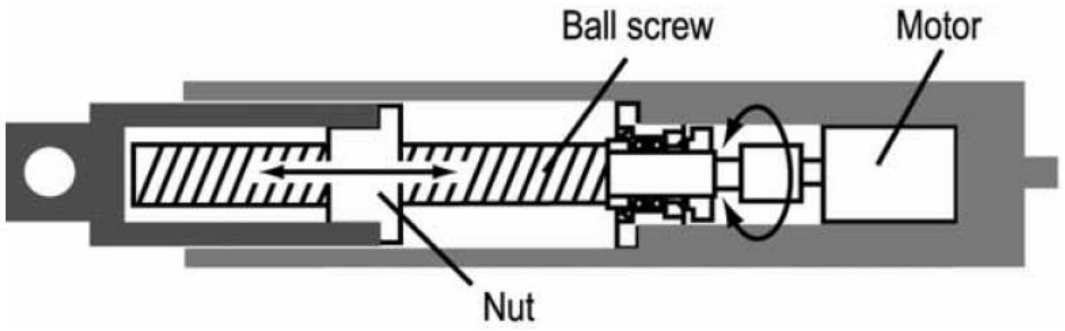

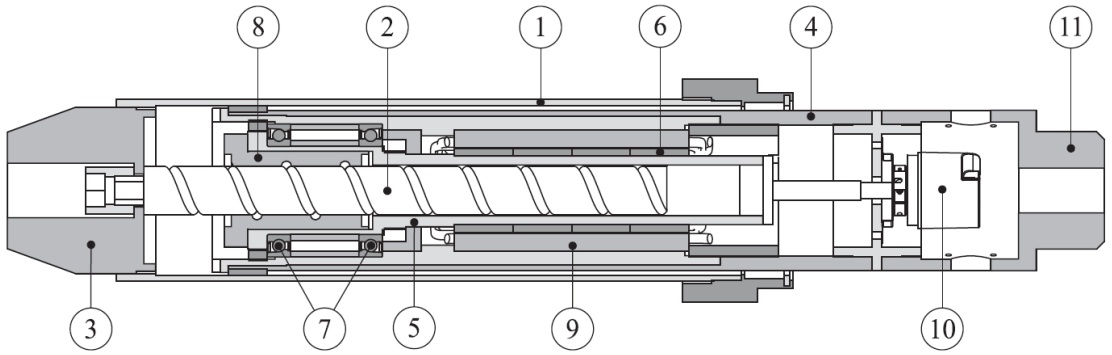

Figure 3. Shock absorber detailed section view. (1) Outer housing, (2) screw, (3) bottom cap, (4) inner housing, (5) rotor, (6) permanent magnets, (7) ball bearings, (8) nut, (9) stator, (10) encoder, (11) top cap.

Kawamoto et al. rotating screw solution for passenger cars.

Tonoli et al. rotating nut solution for off road vehicles.

Co-funded by the Erasmus+ Programme of the European Union

Electromechanical Dampers

Rack pinion solutions (Zuo et al.)

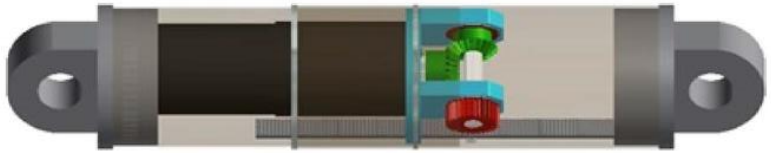

Non-rectified solution yields an average power of 19.2 W when running at 48 km/h on a “fairly smooth university campus road” (probably between ISO B and ISO C).

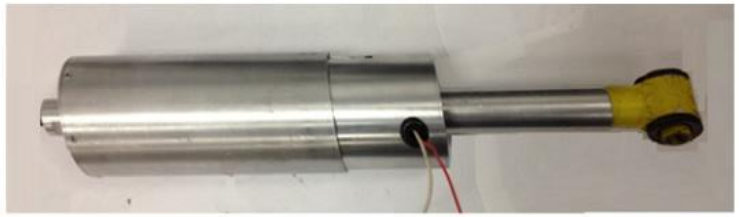

Rectified solution yields an average power of 15.2 W when running at 25 km/h on a “fairly smooth university campus road” (probably between ISO B and ISO C).

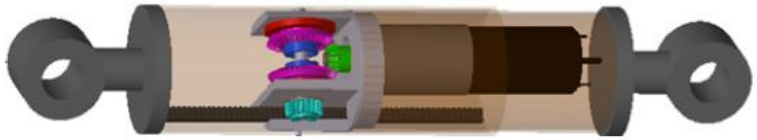

Co-funded by the Erasmus+ Programme of the European Union

Electromechanical Dampers

Two-leg mechanism

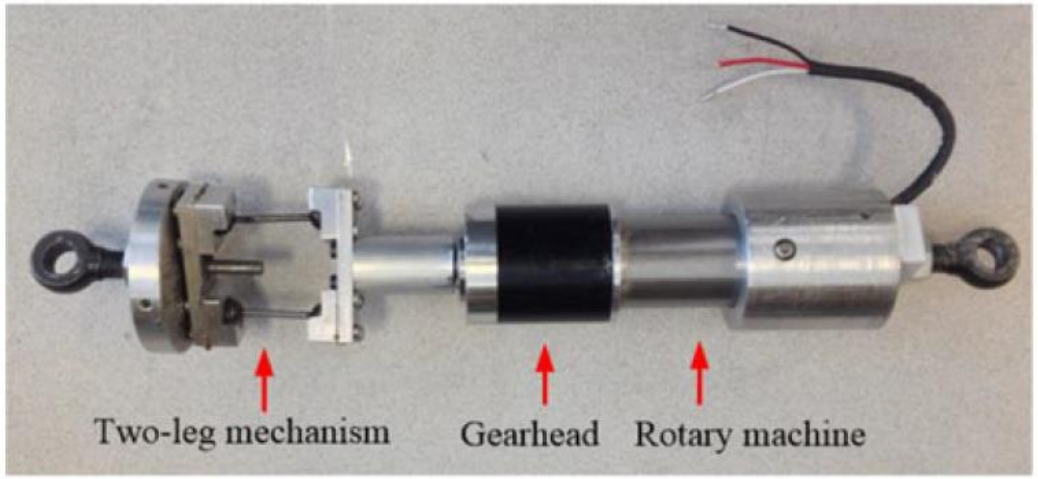

Maravandi et al. present a two-leg lever mechanism to convert linear into rotary motion.

Tests performed with a shaker demonstrate a total conversion efficiency of 0.59.

However, the device requires a gearbox to amplify the rotation and the stroke is limited by the inclination of the two legs.

Co-funded by the Erasmus+ Programme of the European Union

Electrohydrostatic Dampers

- **Levant Power** present numerous patents and some conference paper in the context of electrohydrostatic dampers.

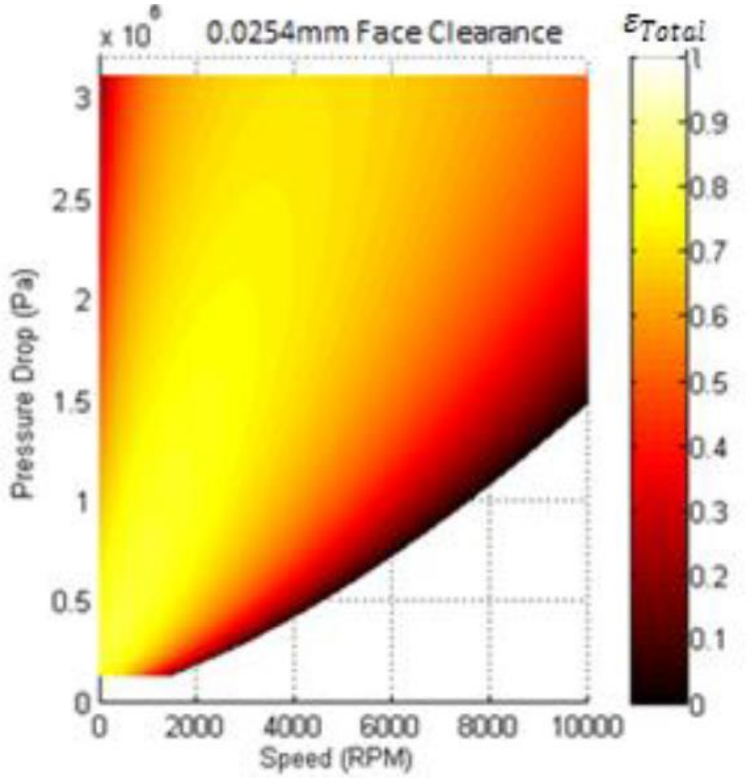

Their paper shows a high **pump** efficiency (0.8 max, mechanical + hydraulic) attained through simulations.
However, their website suggests the following **total** efficiency plot, where max. value is 0.5.

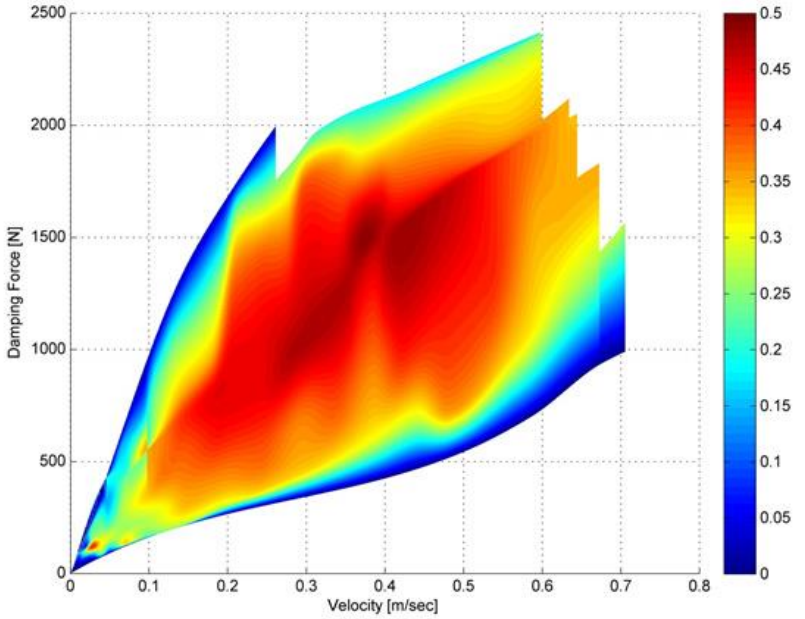

Co-funded by the Erasmus+ Programme of the European Union

Electrohydrostatic Dampers

Rectified solutions

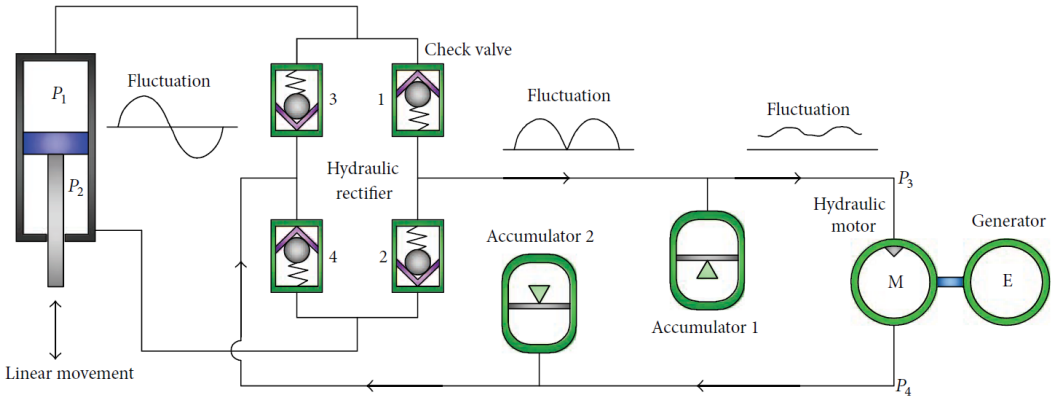

Fang et al. present a technology demonstrator able to yield a total conversion efficiency of 16.5%.

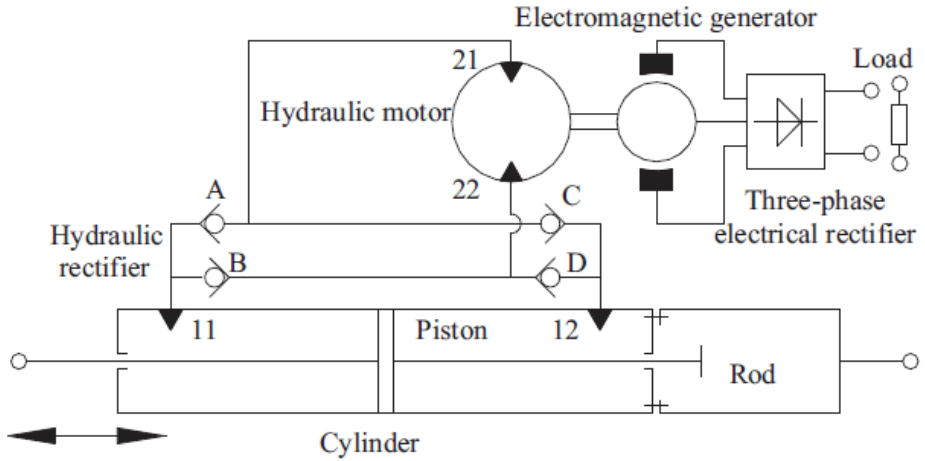

Li et al. present a prototype with total conversion efficiency of 39%

Co-funded by the Erasmus+ Programme of the European Union

Electrohydrostatic Dampers

Rectified solutions

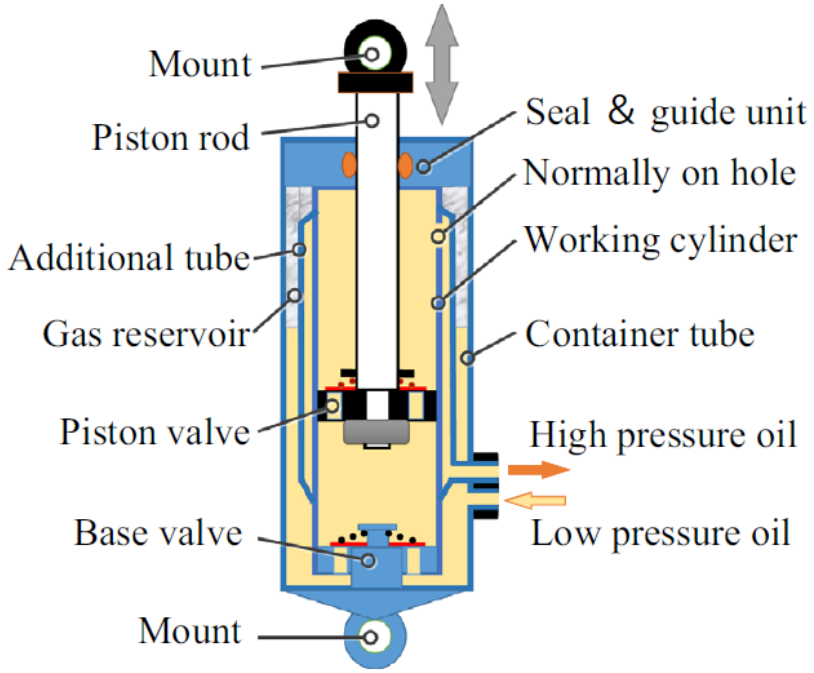

Zhang et al. determine the optimal hydraulic efficiency of a three-tube shock absorber (73%) through detailed modeling and simulation when employed on an electromagnetic damper layout.

Co-funded by the Erasmus+ Programme of the European Union

Electrohydrostatic Damper

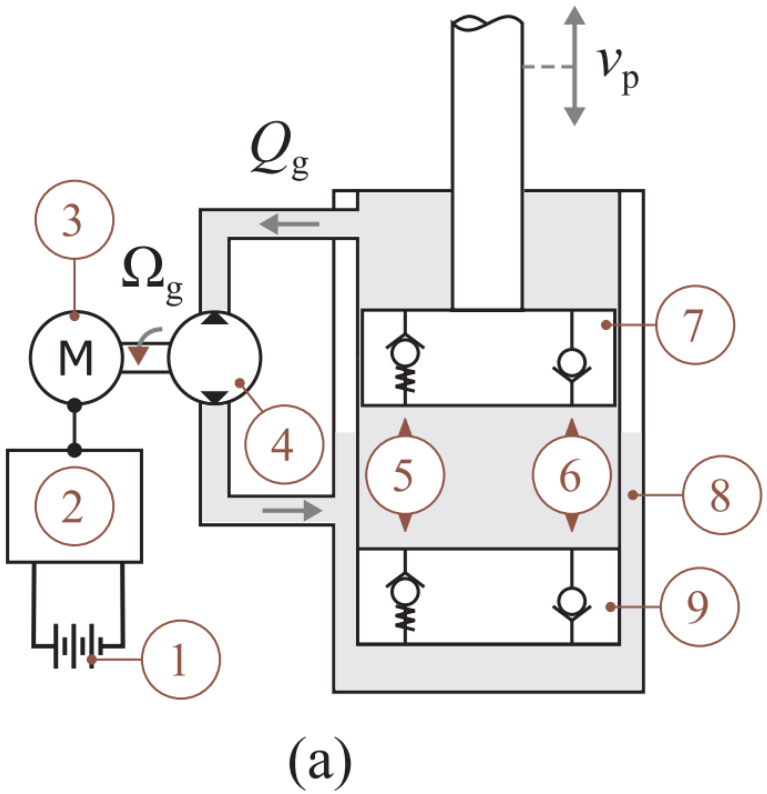

(a)

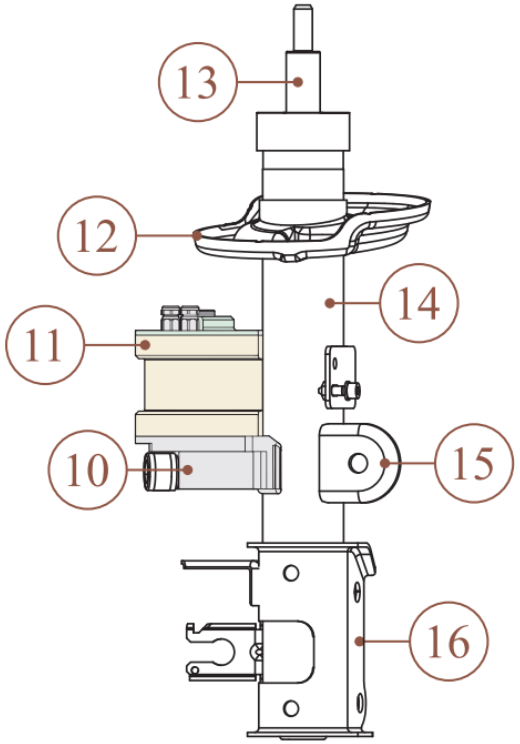

(b)

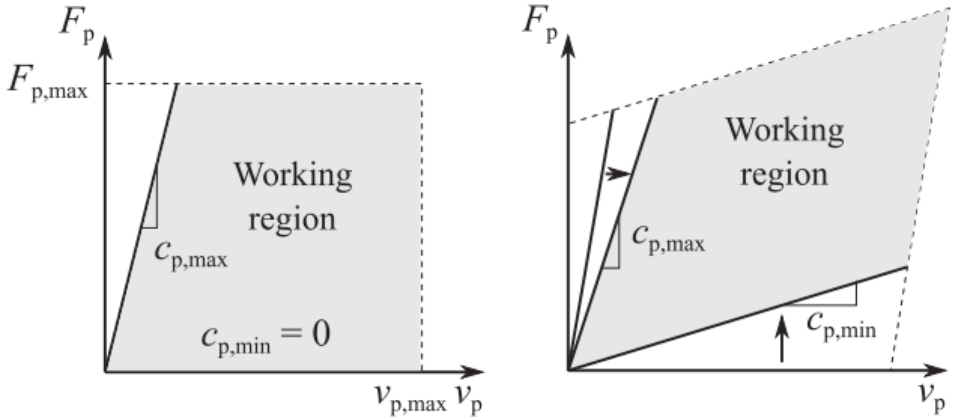

(a) ideal map (b) expected map

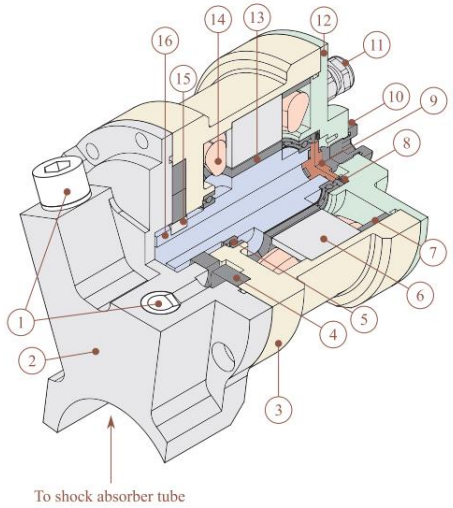

Optimized design and characterization of motor-pump unit for energyregenerative shock absorbers

Renato Galluzzi*, Yijun Xu, Nicola Amati, Andrea Tonoli

Co-funded by the Erasmus+ Programme of the European Union

Rotary Dampers

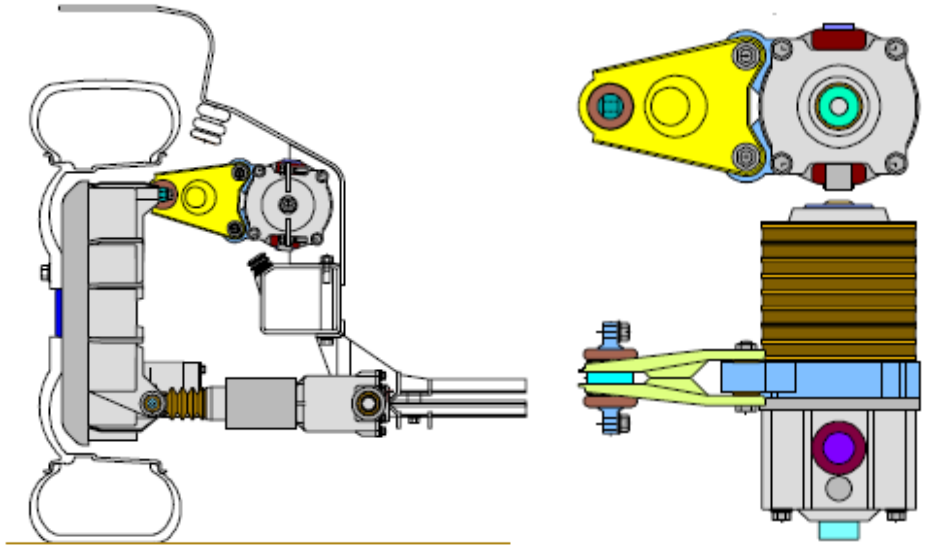

Volvo rotary spring-damper unit. Damping is **semi-active** (MR fluid). **One of the first rotary layouts.**

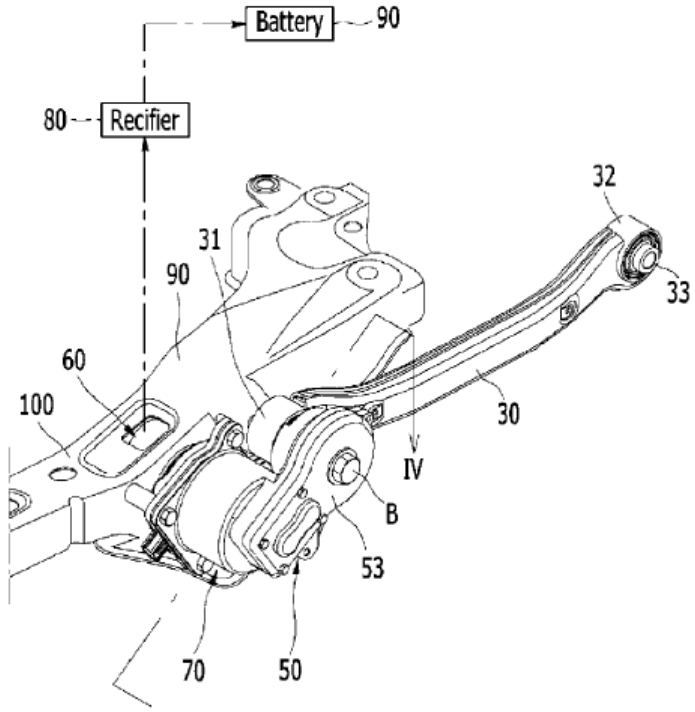

Hyundai rotary damper unit. **Motor + Reduction Stage.**

Co-funded by the Erasmus+ Programme of the European Union

State of Art – Electromechanical Rotary Damper

Hyundai [DE102013225356]

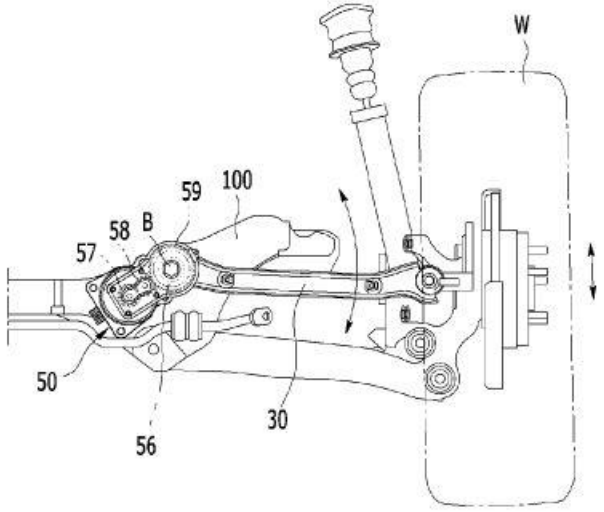

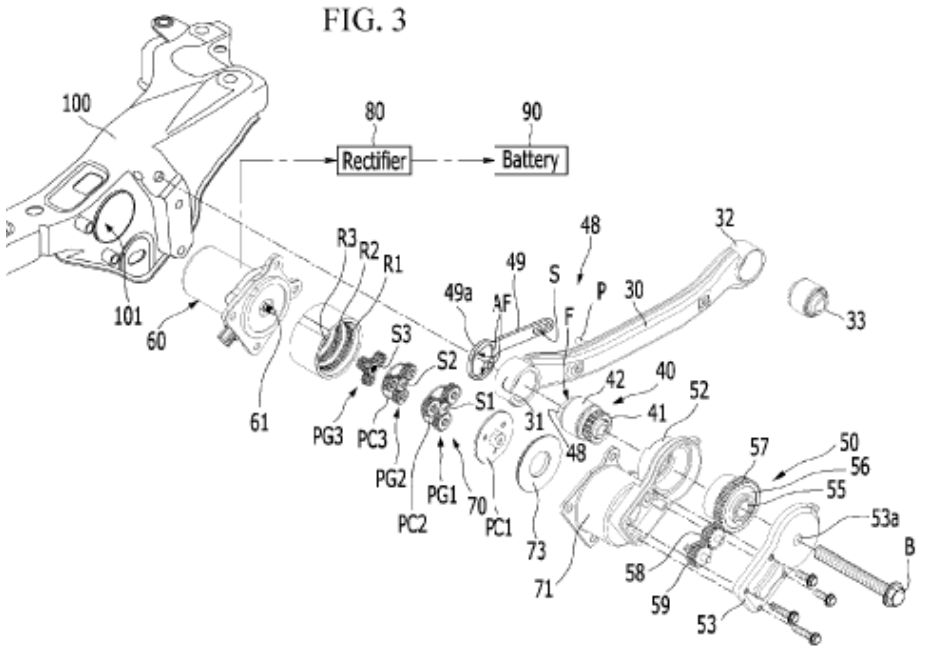

- One-way clutch 56. May be configured to transmit power in bumping or rebounding

- Gearbox:
  1 parallel axis stage (57, 59)
  +
  3 planetary set Stages (PC1-PG3)

Co-funded by the Erasmus+ Programme of the European Union

Rotary Dampers (Motor + Reduction Stage)

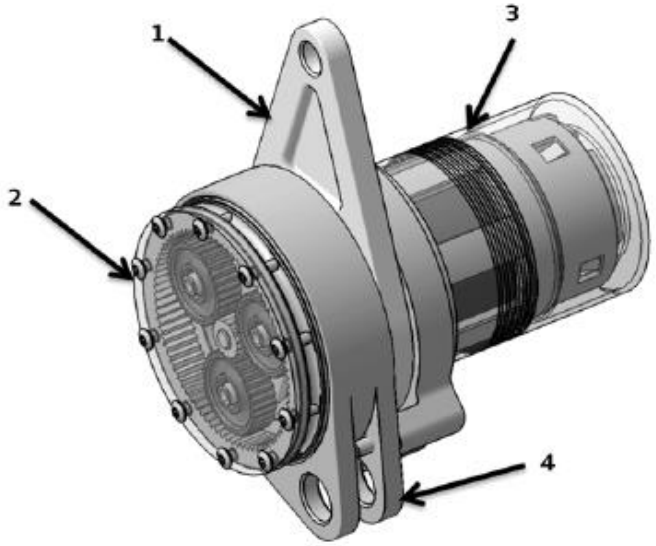

Audi eROT

1) Actuating lever
2) Two-stage planetary gearbox
3) Electric machine

AUDI claims 100-150 W of power from 4 corners running on German roads, with emission savings of 3 gCO2/km

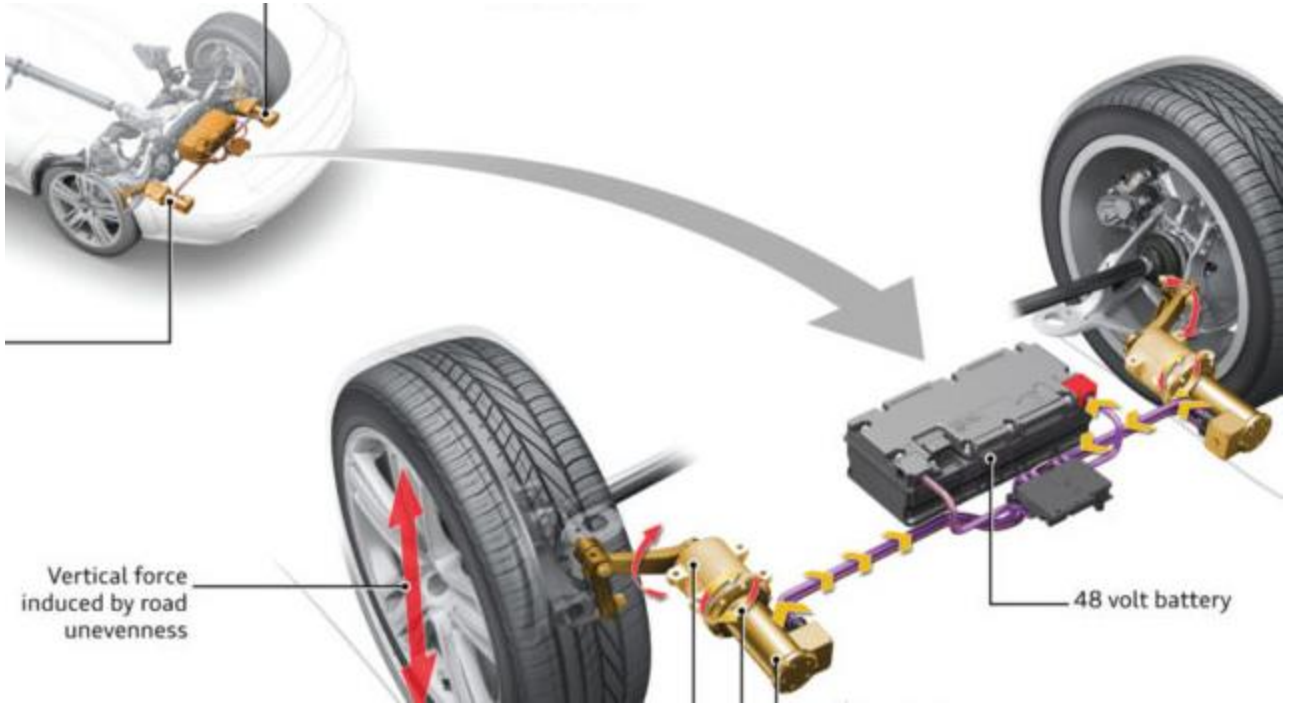

Co-funded by the Erasmus+ Programme of the European Union

Active Roll Control System

Co-funded by the
Erasmus+ Programme
of the European Union

ARC systems analysed

- Linear electro-hydrostatic actuators system
- Rotary electro-hydrostatic actuator system
- Rotary electro-mechanical actuator system
- Direct linear electro-mechanical actuators system
- Non direct linear electro-mechanical actuators system

Co-funded by the
Erasmus+ Programme
of the European Union

Electric Hydrostatic ARC systems

Land Rover Range Rover (2016 model) “Dynamic Response” system. Rotary Electric Hydrostatic ARC system by Delphi.

Max Pressure = 185 bar
Ramp rate = 400 bar/sec
Pump speed = 11250 RPM
260 mm Front wheel travel

https://youtu.be/XulkFsUnw64

Co-funded by the Erasmus+ Programme of the European Union

Hydraulic ARC systems

BMW X5 M and X6 M features the BMW Dynamic Drive system (older version), which consist of a rotary hydraulic actuator placed in the middle of stabilizer bar.

Source: BMW

Co-funded by the Erasmus+ Programme of the European Union

Rotary Electro mechanical ARC systems - Schaeffler

Schaeffler Design 1 – 12 V

BMW 7 series. Schaeffler ARC system (new BMW Dynamic Drive version) substitutes the rotary hydraulic ARC system of the previous version.

Also Rolls-Royce Phantom is equipped with the Schaeffler ARC system Design 1.

Source: BMW

Co-funded by the Erasmus+ Programme of the European Union

Rotary Electro mechanical ARC systems - Schaeffler

Schaeffler Design 2 – 48 V

The ARC system is equipped with the Audi SQ7, with the Bentley Bentayga and Bentley Mulsanne.

Source: Schaeffler

Co-funded by the Erasmus+ Programme of the European Union

Rotary Electro mechanical ARC systems - ZF

The ARC profile VI system is installed in Porsche Cayenne and Porsche Panamera and it is the core of the Porsche Dynamic Chassis Control (PDCC).

Source: ZF

Co-funded by the Erasmus+ Programme of the European Union

Linear electro-hydrostatic actuators system

Pendulum bars replaced by double acting hydraulic linear actuators that exert a torque on the anti roll bar, withstanding the roll moment of the vehicle body.

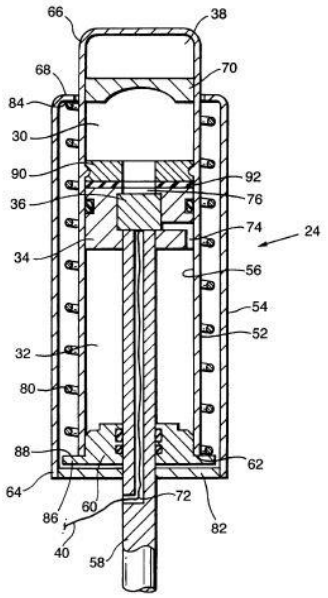

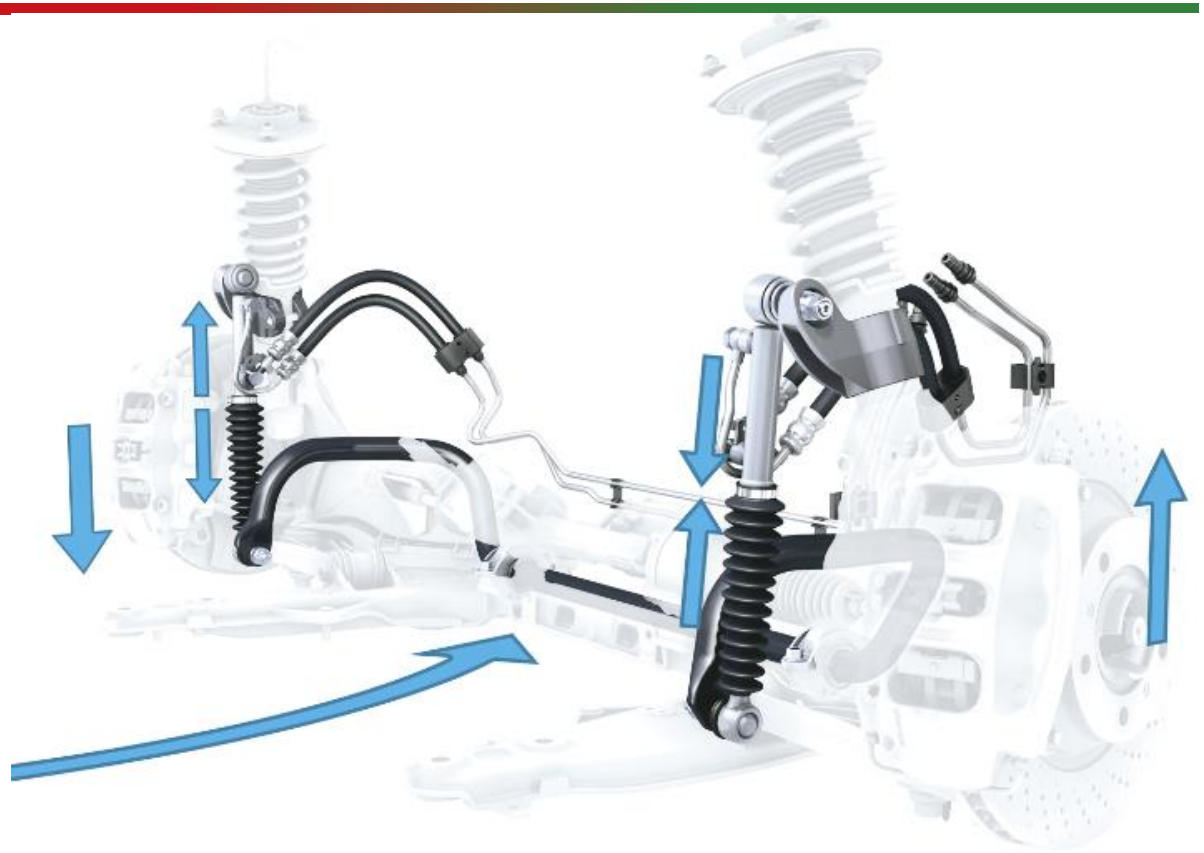

Delphi own actuator for ARC system, featuring a compressible gas chamber, a floating piston, a compressible spring, an electrically operated valve between the compression and rebound chamber and a bore along the piston rod.

Co-funded by the Erasmus+ Programme of the European Union

Rotary electro-hydrostatic actuator system

The double acting rotary actuator is placed in the middle of the anti roll bar. The actuator rotates the two halves of the torsion bar, adjusting the torque transmitted by the bar to compensate for the load transfer during a curve.

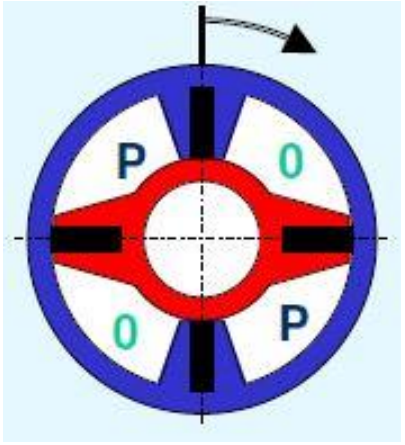

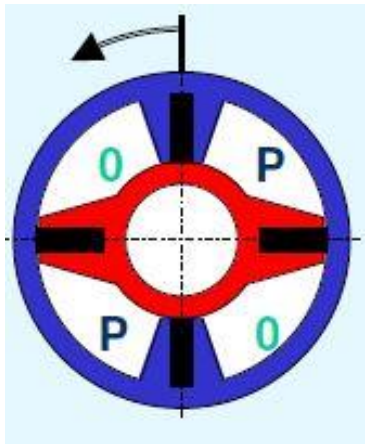

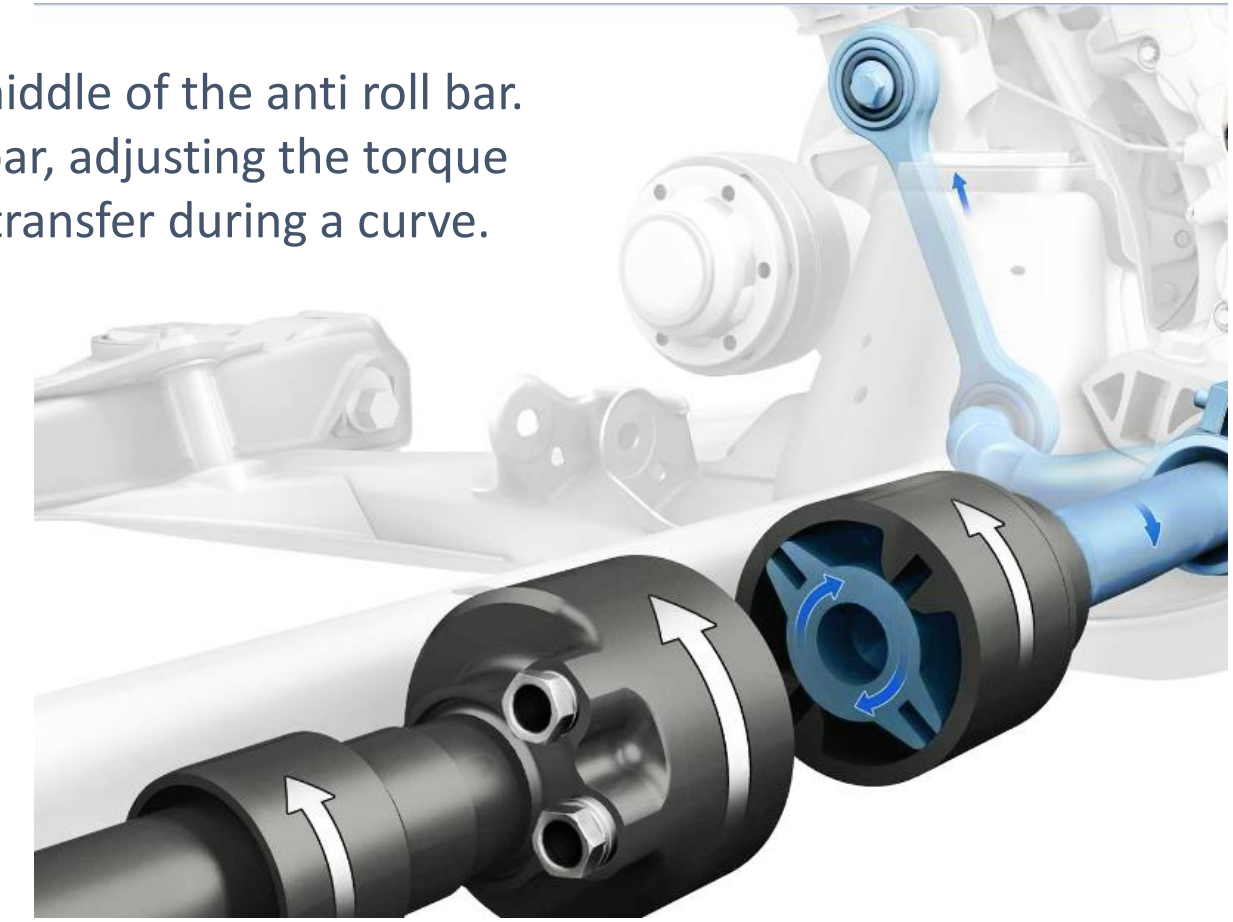

The anti roll moment exerted by the rotary actuator in the anti roll bar is function of pressure differential inside the actuator.

Co-funded by the Erasmus+ Programme of the European Union

Rotary electro mechanical actuator system

This ARC system features an electric motor connected with reduction gears, to counteract roll motion. The electric motor and the reduction gears together form the stabilizer actuator, positioned in the middle of the anti roll bar.
The most performing reduction gears mechanism is a multistage epycicloidal gear set, like a 3 stages planetary gear set.

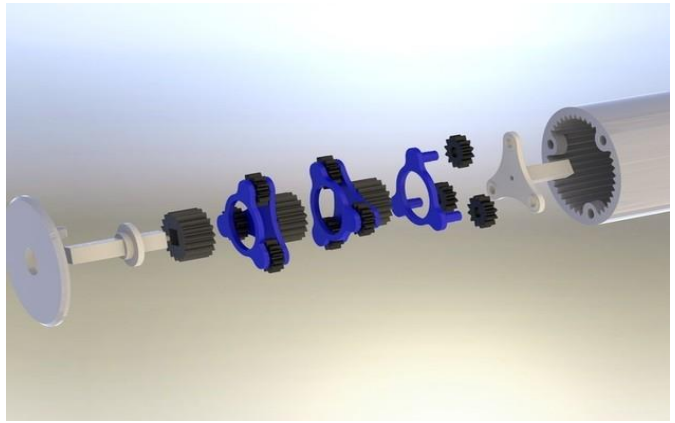

Co-funded by the
Erasmus+ Programme
of the European Union

Direct linear electro mechanical actuators system

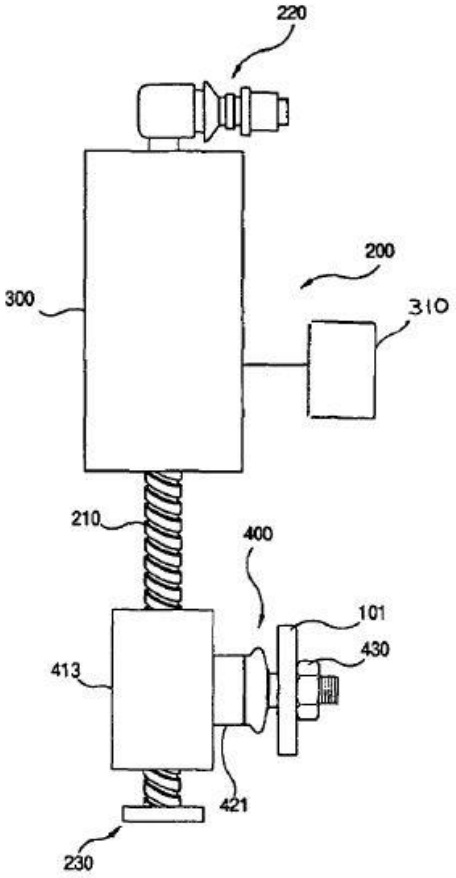

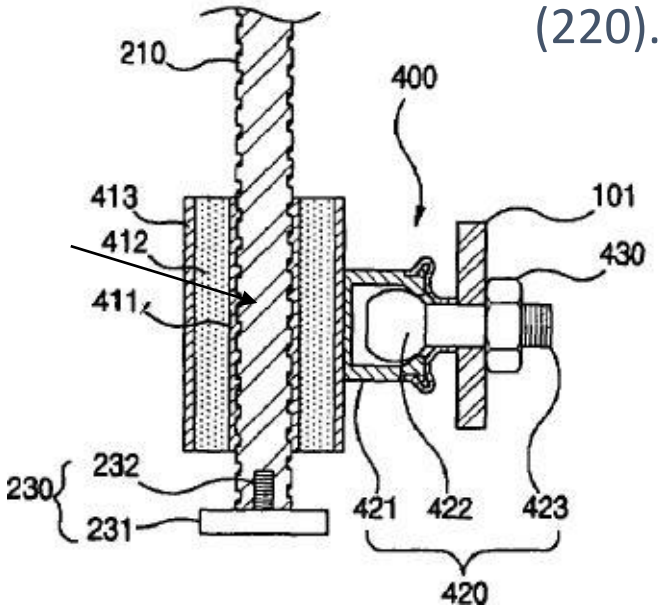

Hyundai own system.
The stabilizer bar (101) is connected trough a ball joint mechanism (420) to the linear electro mechanical actuator, which consists of screw rod (210) and an electric motor (300) , connected to the suspension strut trough a joint (220).

When the electric motor rotates, the rotative movement of the drive gear of the motor is converted in alternate movement of the screw rod, leading, so, to a deflection of the stabilizer bar end that creates an anti roll moment.

Co-funded by the Erasmus+ Programme of the European Union

Direct linear electro mechanical actuators system

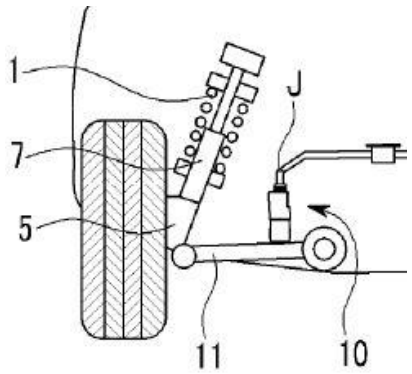

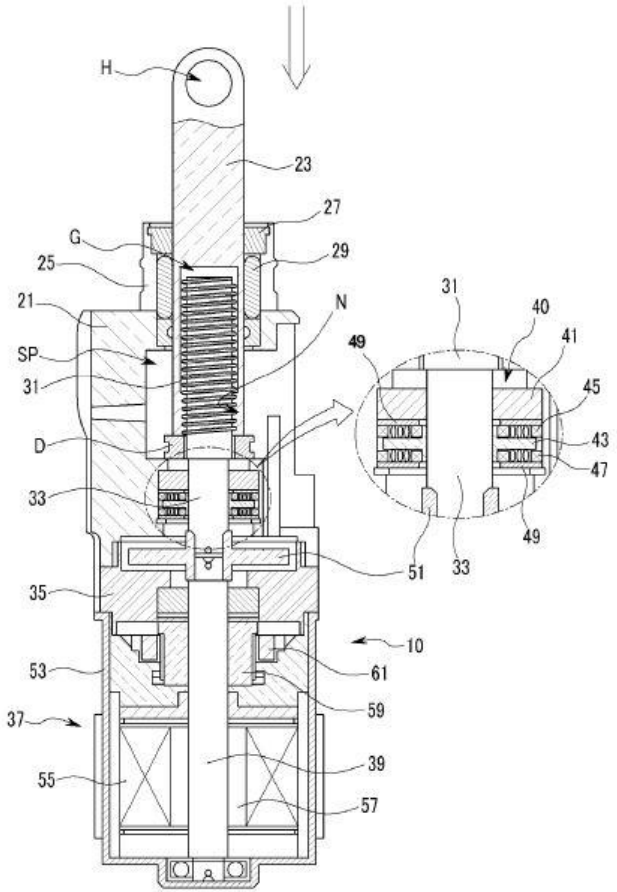

Hyundai own system.
The actuator consists of a drive electric motor (37) that puts in rotation a shaft (39) connected to the screw rotation shaft (33) through a coupling (51). The screw rotation shaft is integrally connected to the lower end of a lead screw (31) along the axial direction.
The lead screw rotates in the thread of a screw groove G formed in the lower interior surface of the power transmitter (23), which is connected to the anti roll bar end through a joint J placed in the engage hole H.

Co-funded by the Erasmus+ Programme of the European Union

Non direct linear electro mechanical actuators system

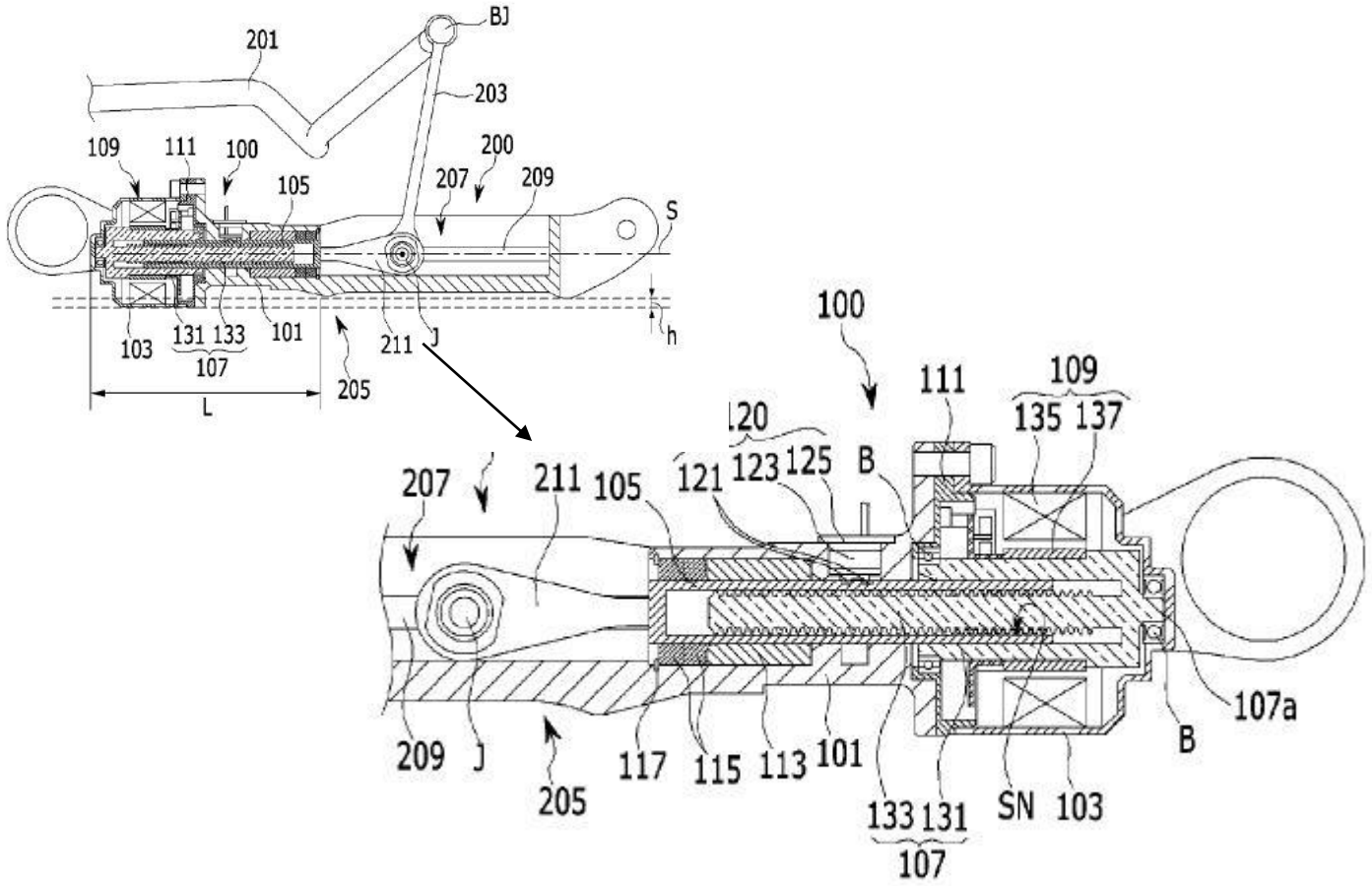

Hyundai own system.

The actuator is connected to the stabilizer bar (201) trough a ball joint connection with a stabilizer link (203). The actuator features a rail unit (200), in which a connector (211), linked to the lower end of stabilizer link, can slide. The connector is put in movement by the power transmission driving shaft (105) which translates due to the rotation of screw rotary body (107) induced by the electric motor (109).

The actuator is attached to the lower arm of suspension strut (205) and act transversally respect to vehicle own direction.

Co-funded by the Erasmus+ Programme of the European Union

Trade off of the actuators

ARC actuator typologies	Linear Hydrostatic	Rotary Hydrostatic	Rotary Electro-mech	Linear Electro-mech	Non Linear Electro-mech
Layout	In place of pendulum bars	In the middle of stabilizer bar	In the middle of stabilizer bar	In place of one pendulum bar	In place of one pendulum bar
Energy demand	+ < hydraulic systems	+ < hydraulic systems	++ possibility to recover energy	+	+
Working angle	Left/Right total free stroke function of suspension architecture 1 actuator - 2 actuators +	Left/Right total free stroke guaranteed. +/- 50° angles +	Left/Right total free stroke guaranteed. +	Left/Right total free stroke function of suspension architecture 1 actuator -	Left/Right total free stroke function of suspension architecture. System rigidly attached to lower frame -

Co-funded by the Erasmus+ Programme of the European Union

Trade off

ARC actuator typologies	Linear Hydrostatic	Rotary Hydrostatic	Rotary Electro-mech	Linear Electro-mech	Non Linear Electro-mech
Response time	-	-	+	+	+
Unsprung mass	-	+	+	++	++
Maintenance	- oil leakages, cavitation	- oil leakages, cavitation	+	+	+
Design and Installation	++	- big diameter	+	+	-
Performance	++	+++	+++	+	+
Fail safe characteristic	+ ≅ passive bar	+ ≅ passive bar	-	-	-
Cost	++	-	+	++	++

Co-funded by the Erasmus+ Programme of the European Union

Bibliography

1. Genta G, Morello L. The automotive chassis: volume 1: Component design. Springer Science & Business Media; 2008.
2. Genta G, Morello L. The automotive chassis: volume 2: System design. Springer Science & Business Media; 2008.
3. Onori S, Serrao L, Rizzoni G. Hybrid electric vehicles: Energy management strategies. London: Springer; 2016.
4. Guzzella L, Sciarretta A. Vehicle propulsion systems. Springer-Verlag Berlin Heidelberg; 2007 Jun.
5. Dietsche K, Klingebiel M. Bosch Automotive Handbook. 7th Edition, Robert Bosch GmbH. 2007.
6. Amati N, Tonoli A, Castellazzi L, Ruzimov S. Design of electromechanical height adjustable suspension. Proceedings of the Institution of Mechanical Engineers, Part D: Journal of Automobile Engineering. 2018 Aug;232(9):1253-69.
7. https://patents.google.com/patent/WO2019097461A1/en Patent: WO2019097461A1 Damper and spring unit for a vehicle suspension provided with an electro-mechanical adjustment device for adjusting the vertical position of the spring
8. https://patents.google.com/patent/WO2017202811A1
9. Gysen BL, Paulides JJ, Janssen JL, Lomonova EA. Active electromagnetic suspension system for improved vehicle dynamics. IEEE Transactions on Vehicular Technology. 2009 Dec 18;59(3):1156-63.
10. Ebrahimi B, Bolandhemmat H, Khamesee MB, Golnaraghi F. A hybrid electromagnetic shock absorber for active vehicle suspension systems. Vehicle System Dynamics. 2011 Feb 1;49(1-2):311-32.

Co-funded by the Erasmus+ Programme of the European Union

Engineering Knowledge Transfer Units to Increase Student´s Employability and Regional Development

https://www.facebook.com/unitederasmus/

Co-funded by the Erasmus+ Programme of the European Union